

# Continuous Monitoring and Automated Fault Detection and Diagnosis of Large Air-Handling Units

***Citation for published version (APA):***

Chitkara, S. (2022). *Continuous Monitoring and Automated Fault Detection and Diagnosis of Large Air-Handling Units*. Technische Universiteit Eindhoven.

***Document status and date:***

Published: 17/05/2022

***Document Version:***

Publisher's PDF, also known as Version of Record (includes final page, issue and volume numbers)

***Please check the document version of this publication:***

- A submitted manuscript is the version of the article upon submission and before peer-review. There can be important differences between the submitted version and the official published version of record. People interested in the research are advised to contact the author for the final version of the publication, or visit the DOI to the publisher's website.
- The final author version and the galley proof are versions of the publication after peer review.
- The final published version features the final layout of the paper including the volume, issue and page numbers.

[Link to publication](#)

***General rights***

Copyright and moral rights for the publications made accessible in the public portal are retained by the authors and/or other copyright owners and it is a condition of accessing publications that users recognise and abide by the legal requirements associated with these rights.

- Users may download and print one copy of any publication from the public portal for the purpose of private study or research.
- You may not further distribute the material or use it for any profit-making activity or commercial gain
- You may freely distribute the URL identifying the publication in the public portal.

If the publication is distributed under the terms of Article 25fa of the Dutch Copyright Act, indicated by the "Taverne" license above, please follow below link for the End User Agreement:

[www.tue.nl/taverne](http://www.tue.nl/taverne)

***Take down policy***

If you believe that this document breaches copyright please contact us at:

[openaccess@tue.nl](mailto:openaccess@tue.nl)

providing details and we will investigate your claim.

# **Continuous Monitoring and Automated Fault Detection and Diagnosis of Large Air-Handling Units**

Shobhit Chitkara  
May 17, 2022

EINDHOVEN UNIVERSITY OF TECHNOLOGY

Stan Ackermans Institute

SMART BUILDINGS & CITIES

# CONTINUOUS MONITORING AND AUTOMATED FAULT DETECTION AND DIAGNOSIS OF LARGE AIR-HANDLING UNITS

By

SHOBHIT CHITKARA

A thesis submitted in partial fulfillment of the requirements for the degree of  
Professional Doctorate of Engineering

The design described in this thesis has been carried out in accordance with the TU/e Code of  
Scientific Conduct

Prof. ir. Wim Zeiler, university coach

Dr. ir. Shalika Walker, university coach

ir. Alet van den Brink, company coach

Eindhoven, the Netherlands

May 17, 2022

This thesis has been established in collaboration with



## Project Partners:



TKI URBAN ENERGY  
Topsector Energy



ROC NIJMEGEN

Radboudumc



ISSO

A catalogue record is available from the Eindhoven University of Technology Library

SAI-report: 2022/022

# Executive Summary

Air-Handling Units (AHUs) are highly customized equipment. The regulations concerning AHUs are increasingly becoming strict to meet higher energy efficiency and ventilation goals, which adds to the complexity inherent with customised equipment. This upsurge in complexity increases the need for continuous maintenance and monitoring of AHUs. However, such programs are difficult to implement due to the shortage of skilled personnel. Therefore, continuous monitoring and Fault Detection and Diagnosis (FDD) processes need to be automated, referred as AFDD.

Despite the plethora of research on AFDD, there are limited real-life applications. Adding to this, the available solutions are either unreliable, unaffordable, and/or not scalable. Surveying through the literature on FDD tools that are commercially deployed or under development revealed that these tools rely on a combination of expert rules or first principles. Rules-based approaches are heavily reliant on sensed information and expert knowledge. This makes the maintenance of such tools unsustainable. Further, such tools carry very limited ability to prevent significant energy wastage.

It is estimated that up to 30% of energy could be saved through the effective use of data collected with continuous monitoring systems. To realise this, highly sensitive (ability to diagnose condition) diagnosis models can be trained with Artificial Intelligence (AI) based approaches that are scalable and have lesser reliance on expert knowledge and sensors. Through this project, an AFDD tool that incorporates these approaches has been developed. It is generally recommended to treat the fault detection and diagnosis processes separately as in this way, it is easier to overcome challenges associated with implementation. For example, supervised machine learning algorithms require annotated fault labels. In the designed tool, these practical limitations have been overcome and completely automated fault detection and diagnosis have been implemented.

For fault detection, a widely used machine learning algorithm called XGBoost is deployed, whilst for fault diagnosis, Bayesian network-based probabilistic models are deployed. Typically, these models are inhibitive due to the complexity associated with their development. For adding interpretability to these models, frameworks, such as (i) Shapley Additive Explanations (SHAP) for fault detection and (ii) 4-Symptoms and 3-Faults (4S3F) for fault diagnosis are included. The 4S3F framework is a generalizable framework that supports the development of diagnostic Bayesian networks using piping and instrumentation (P&I) diagrams prepared during HVAC design. Using these P&I schemes, the developed Bayesian networks have been discretised for cooling and heating mode operations of the AHU. This way the adopted diagnosis approach translates HVAC domain knowledge and remains in sync with building practitioner's approach toward fault diagnosis.

To understand the reliability and generalizability of the proposed FDD strategy, 5 case studies have been utilized with a diverse operational environment, weather conditions, and AHU configurations. Additionally, the developed diagnosis models are validated under multiple fault scenarios experimentally induced in two building environments. The specificity of the deployed diagnosis models exceeds 90% with samples collected through long-term test procedures exceeding 60 days. A fault condition diagnosed with a highly specific model imputes a very high likelihood of fault presence. Further, the developed diagnosis models not only distinguish between fault presence and absence conditions but can also accurately isolate root causes. The diagnosed outcomes are supported by visual evidence delivered through a web-based interactive user interface.

It's been noted that visualizations in the available continuous monitoring tools are not sufficient to aid visual diagnostic procedures. Therefore, a lot more time is consumed in preparing data than using it for preventing energy wastage. In the developed AFDD tool, this aspect has been taken care of through visualisations that promise to support building practitioners and take a step forward toward human-in-the-loop diagnostics. Further, a fault library is also realized using a lightweight database structure to manage taxonomy, prior fault probabilities and recommendations for fault correction. The developed scheme is useful for building practitioners to manage information on faults easily and consistently. Upon deployment, it is estimated that nearly 33% chiller of energy waste can be prevented using the AFDD tool. A financial plan to roll out the tool commercially for non-residential buildings in the Netherlands carrying large HVAC installations has been developed. It's projected that a SaaS business providing such a tool is financially viable. Under all forecasted revenue scenarios profitability can be realised in a window of 5 years from inception.

# Acknowledgements

The research work is funded by the TKI Urban Energy project 'Continuous commissioning of lowdT'; and the Eindhoven Engine project 'CM-HVAC-FDD'.

I feel privileged to have worked alongside and under the guidance of several team members from Kropman Installatietechniek. I would like to thank Joris de Ruiter and Jan-Willem Dubbeldam at TCC, Kropman for facilitating the data collection and software integration processes. I consider myself fortunate for the incredible support and help I have received from John Verlaan, Roel Vos, Martijn Verduijn, and Marco van As for the experimental work. A special note of thanks to Joep van der Velden for his constant mentorship through this process.

Coming back to academia would otherwise have been very difficult albeit for the mentorship and guidance I received from Prof. Wim Zeiler, chair, the Building Services group. I would like to express my sincere gratitude to my company supervisor, Alet van den Brink for helping me grasp the nuances of building installations. I cannot thank my co-supervisor, Dr. Shalika Walker enough for believing in my ability and setting me on the right path.

Throughout the writing of this dissertation, I have received a great deal of support and assistance from my colleagues and coaches at the Department of Built Environment at TU/e and the SBC Program. I would like to acknowledge my colleagues Waqas Khan, Julien Le Prince, and Karthik Gunderi, who lent their never-ending support throughout the process. I would like to particularly single out Anand Thamban for helping me design the tool and further my research.

Last but not the least, I feel indebted to my family and especially my wife Chetna Palaniappan for the incredible support she has offered through this process. Thank you for being my friend, companion, wife, and guide all at the same time and for motivating me to pursue this. I would like to dedicate this thesis to you.

# Abstract

The built environment is responsible for 37% of energy consumption. Up to 30% of this energy is consumed inefficiently due to inadequate Fault Detection and Diagnosis (FDD). The unavailability of trained technical personnel and the growing complexity of HVAC design add to further inefficiency. A reliable and automated FDD (AFDD) strategy for air handling units is key to addressing these issues. Even though numerous AI-based AFDD approaches have been published, real-world applications are more complex and rarely discussed. In this project, a Python-based AFDD tool is prototyped. The business logics contained in this tool have been verified and validated using data collected from five case studies.

For designing the FDD business logics, a structured three-step process is proposed. Firstly, the design space is narrowed down using a system analysis (Pareto-Lean approach) step and use cases are identified for developing fault detection models. More specifically, faults causing the largest energy performance gap and sensors relevant for FDD have been identified. Secondly, the use cases are handled utilizing a data-driven strategy to generate fault symptoms using a machine learning algorithm (XGBoost). Thirdly, the detected faults are isolated using a generic fault diagnosis framework known as 4S3F – Four Symptoms and Three Faults. This way the fault detection and diagnosis aspects are separately handled using AI-based approaches. Upon experimental validation of the developed diagnosis models, a diagnosis specificity exceeding 90% is realized.

The results obtained from the FDD process are visualized using a web development framework. Design sprints are utilized to collate requirements for a user-friendly interface that would support human-in-the-loop diagnostics. The prototyped tool is integrated with a commercially operated continuous monitoring system, currently being utilized to monitor 400 buildings. It is observed that the prototyped AFDD tool could prevent up to 33% of the energy consumed by the chiller. Moreover, the results presented will contribute to the development, adoption, and deployment of AI-based FDD strategies in commercial applications.

# Abbreviations

AFT	Accelerated Failure Time Model
AHU	Air-Handling Units
AI	Artificial Intelligence
ANN	Artificial Neural Networks
AFDD	Automated Fault Detection and Diagnosis
ARMAX	Autoregressive Moving Average with Extra Input
BAS	Building Automation System
CART	Classification And Regression Trees
CMS	Continuous Monitoring System
CNN	Convolutional Neural Networks
DBN	Diagnostic Bayesian Network
EATR	Exhaust Air Transfer Ratio
ERP	Enterprise Resource Planning
FDA	Fischer Discriminant Analysis
FDD	Fault Detection and Diagnosis
GRNN	General Regression Neural Network
HMM	Hidden Markov Models
HRW	Heat Recovery Wheel
HVAC	Heating, Ventilation and Air Conditioning
IoT	Internet of Things
ML	Machine Learning
UI	User Interface
OACF	Outdoor Air Correction Factor
PCA	Principal Component Analysis
P&ID	Piping and Instrumentation Diagram
PID	Proportional-Integral-Derivative Controller
SAX	Symbolic Aggregate Approximation
SVM	Support Vector Machine
SVR	Support Vector Regression
TS	Time series
XGBoost	Extreme Gradient Boosting
4S3F	Four Symptoms and Three Faults

# Contents

1	Introduction .....	1
1.1	Definitions.....	2
1.2	Related Work.....	3
1.2.1	FDD Approaches.....	3
1.2.2	FDD Applications.....	5
1.3	Project plan and Work packages .....	5
1.4	Outline of the report.....	6
2	Design approach and methodology .....	8
2.1	Requirements.....	8
2.1.1	Stakeholder analysis and their interests.....	8
2.1.2	AFDD tool requirements from literature .....	11
2.1.3	Requirements Summary .....	11
2.2	Design Methodology.....	13
2.2.1	AFDD Tool Overview .....	13
2.2.2	FDD business layer .....	14
2.2.3	Data visualization layer.....	15
2.2.4	AFDD tool integration .....	16
2.3	Case Studies .....	17
2.3.1	Air-Handling Unit description.....	17
2.3.2	Case study description.....	17
3	FDD Business Layer .....	22
3.1	Fault impact analysis .....	22
3.1.1	Methodology.....	23
3.1.2	Results and Discussion .....	23
3.2	Sensor impact analysis.....	24
3.2.1	Methodology.....	25
3.2.2	Results and Discussion .....	25
3.3	Conclusion – Fault and Sensor impact analysis.....	26
3.4	Fault Detection.....	26
3.4.1	Valve position prediction model .....	28
3.4.2	HRW supply temperature and relative humidity prediction models .....	31
3.5	Fault Diagnosis .....	34
3.5.1	Cooling mode operation.....	35
3.5.2	Heating mode operation .....	38
3.5.3	Heat Recovery Wheel .....	41
3.6	Conclusion.....	42
4	Automated Fault Detection and Diagnosis - Tool .....	43
4.1	AFDD Tool Backend.....	43

4.1.1	Fault Library .....	44
4.1.2	AFDD inference .....	45
4.2	AFDD Tool Frontend .....	45
4.2.1	Key Performance Indicators (KPIs) .....	46
4.2.2	Virtual Sensors .....	48
4.2.3	Data Dashboarding.....	48
5	Discussion .....	54
5.1	Assessment of technical viability .....	54
5.2	Assessment of financial viability .....	55
5.3	Deployment Risk Assessment.....	55
6	Conclusions and recommendations for future development.....	56
7	References.....	57
8	APPENDIX.....	65
APPENDIX A.	Design and Methodology.....	65
APPENDIX B.	Systems Description, Case Studies, .....	66
APPENDIX C.	Fault Impact Analysis and Sensor Impact Analysis .....	73
APPENDIX D.	FDD Business Layer – Fault Detection and Fault Diagnosis .....	84
APPENDIX E.	FDD APPLICATION.....	109
APPENDIX F.	Discussion .....	110

# 1 INTRODUCTION

The direct and indirect CO<sub>2</sub> emissions from energy use in buildings surpassed 10GTCO<sub>2</sub> in 2019, the highest recorded level [1]. Space cooling and heating applications are key drivers of this demand [1]. Further, the space cooling and heating requirements need to tackle extraneous headwinds due to rising global temperatures and the ongoing gas crisis [1,2].

In the Built Environment, the Heating, Ventilation, and Air Conditioning (HVAC) accounts for over 50% of the emissions. Research indicates that energetic performance of HVAC systems is significantly (~10-30%) higher energy than design. This energy gap is attributable to inadequate monitoring, ageing, failures, faults, or inadequate maintenance [3,4]. Within HVAC systems, Air-Handling Units (AHU) are an important and widely studied sub-system, as it combines cooling and heating sub-systems with ventilation [5,6]. AHUs are highly customized equipment [7]. These customizations are tailored to meet end-use requirements such as compactness, ventilation, and thermal load requirements. Poor system integration of AHUs can lead to hardware failures and controller errors [8]. In addition, regulations concerning AHUs are increasingly becoming stricter to meet energy efficiency and while ventilation goals are increased [9], which adds to the complexity inherent with customizations. This has amplified the need for continuous maintenance and monitoring of such equipment.

There is a lack of experienced facility managers which combined with increasing cost pressures in facility management leads to an inadequate resource allocation [10]. To this end, Bruton et al. in [5] reported that ratio of staff allocated for supervising and maintenance of an Air-Handling Unit (AHU) is typically 1:20. To address this widening gap, automation of processes is highly desirable. This is legislatively endorsed by European Union's recommendations published in June 2019 that recommended HVAC systems with a rated output of more than 290kW to be equipped with Building Automation Systems (BAS) [11]

Although, operation of buildings is being increasingly automated, efficiency gains realized are not sufficient to meet decarbonization targets [1]. It is estimated that up to 30% energy could be saved through the effective use of data collected through deployed continuous monitoring systems (CMS) [6]. An umbrella of processes such as continuous commissioning, monitoring or model-based commissioning (MBCC) labelled as Cx are deployed in combination with CMS systems to realize low energy use and higher comfort levels [12]. Fault Detection and Diagnosis (FDD) is an important subdomain of Monitoring based commissioning and can be utilized for achieving energy efficiency goals as highlighted in Figure 1. For instance, continuous gains (indicated in yellow and beneath) can be realized in a programmatic way through a building's lifecycle.

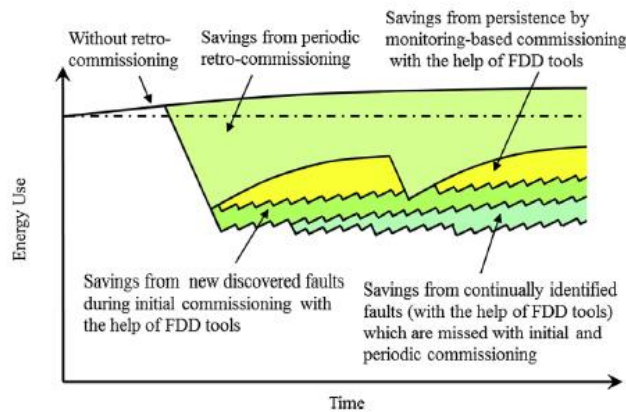


Figure 1: The role of FDD tools in monitoring-based commissioning to avoid the loss of energy efficiency [4]

Automated FDD (AFDD) tools are being developed since the 1980s complimented by development of direct digital controllers (DDC) and micro-computers [13]. Despite prior research, there remain limited real-life applications [6]. Adding to this, the available solutions are either unreliable, unaffordable, and/or not scalable (Zhao et al., 2019). Further, the current acceptance of the available state-of-the-art is limited to early adopters or innovators on the technology adoption curve [14]. Furthermore, application of the available techniques to AHUs operating in the Netherlands is understudied. For example, research contribution from the Netherlands towards application of artificial intelligence (AI) methods for HVAC systems is a less than 3% [15].

Considering the discussed aspects, the direct contribution of this project is to add to the limited real-life demonstrations of FDD and inspire its widespread adoption. More specifically, the design, development, and validation of an AFDD tool that utilizes AI methods is discussed. Further, the tool is integrated with the commercially operated CMS application developed by Kropman called InsiteSuite. This CMS is being utilized to monitor over 400 buildings in the Netherlands.

## 1.1 DEFINITIONS

In this section some the key terminologies concerning continuous monitoring and FDD process are defined.

**Continuous Monitoring (CM):** CM finds its origins in the auditing domain and is a widely accepted process used for continuous auditing [16]. In buildings, IT tools such as Building Automation Systems (BAS), Building Management Systems (BMS), Energy Management Systems (EMS) are often deployed for continuous monitoring and control [17].

**Faults:** Faults are unpermitted deviation of at least one characteristic property (feature) of the system from acceptable, usual, standard condition [18]. In another definition, Li et al. in [19] described fault as an instance where either a system or an equipment or a component performs in a way that is detrimental to either thermal comfort or energy efficiency of a building. The development of faults in a system can be either abrupt (stepwise), incipient (drift like) or intermittent [13].

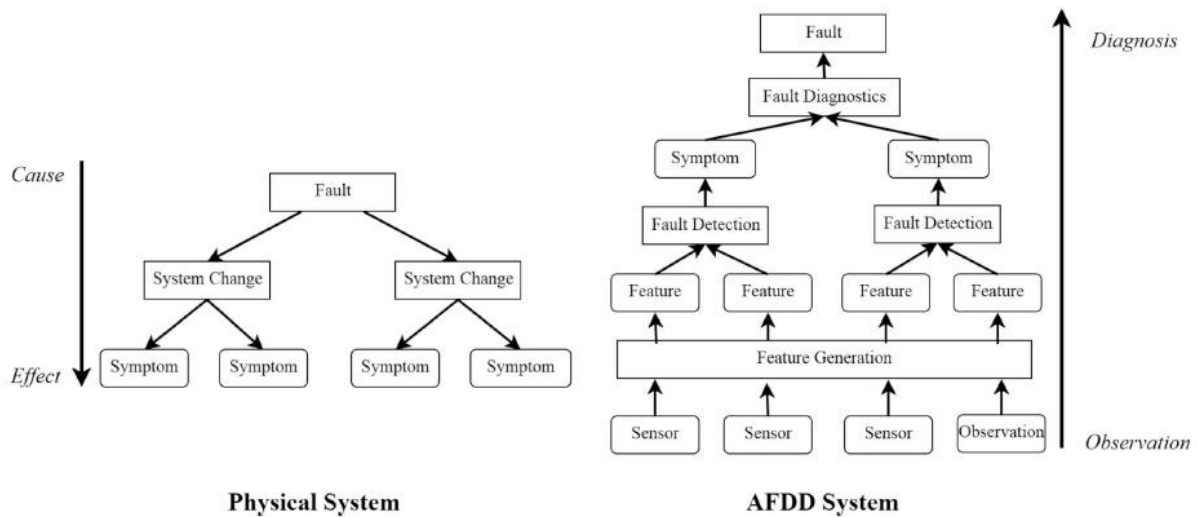


Fig. 1. Overview of an AFDD system – from observation to diagnosis.

Figure 2: AFDD system overview - cause to effect and observation to diagnosis [13]

**Fault Detection:** Quoting Ding in [20], fault detection is “the detection of occurrence of faults in functional units of the process, which lead to undesired or intolerable behaviour of the whole system”. In an automated process this implies change detection on features (see Figure 2) and/or measured variables referencing nominal values [13]. Therefore, this process is also alternatively referred to as ‘Anomaly Detection’ or ‘Symptom Detection’ [21].

**Symptoms:** The detected faults provide valuable information that can be utilized in the diagnosis process and is generally referred to symptoms (see Figure 2, left). Symptoms can either be analytical or heuristic, wherein the former is obtained from automated detection algorithms and the latter is generated through human observation [13].

**Fault Diagnosis:** Fault diagnosis is a logical step following fault detection (see Figure 2, right) and is the process that involves fault identification or classification or isolation or disease diagnosis or root cause determination [13,21] In some circumstances, fault detected or diagnosed may yield same outcomes but in general a two stepped approach is required to determine root cause as the same symptoms can be observed with different faults.

## 1.2 RELATED WORK

The related work carried out in the field of FDD for HVAC systems is discussed in this section. In section 1.2.1, various approaches proposed for AFDD are identified through a systematic literature review process and are introduced. In section 1.2.2, first the application of FDD and the progress made towards its application is discussed. Thereafter, the challenges impeding its adoption are summarized.

### 1.2.1 FDD Approaches

Over the previous decade, a noticeable increased has been observed in the number of articles published on AFDD approaches focusing on black-box models [13]. Zhao et al. in [4] classified the published methods for fault detection and diagnosis (see Figure 3 and Figure 4). Using this classification, FDD methods can be identified as Data driven-based or Knowledge driven-based. Data driven-based methods use process data collected at buildings, whilst Knowledge driven-based based methods rely on domain experts. For example, Rule-based methods use rule sets written using prior knowledge of the system. Further, for fault detection only data driven-based techniques are sub-classified as AI-based methods, whilst for fault diagnosis both data driven-based and inference-based techniques such as Bayesian inference are also sub-classified as AI-based methods.

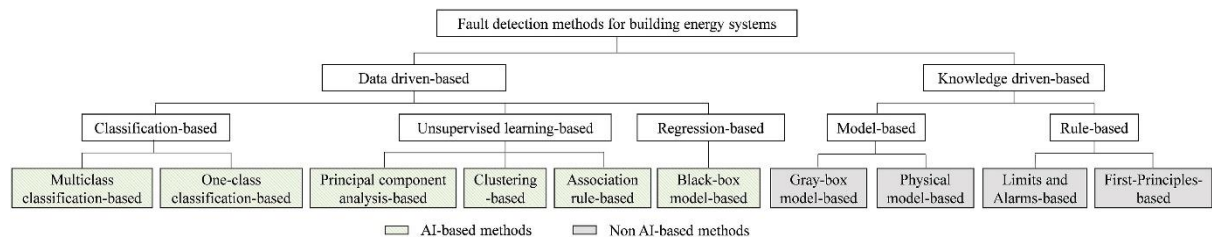


Figure 3: Classification of Fault Detection methods for building energy systems [4]

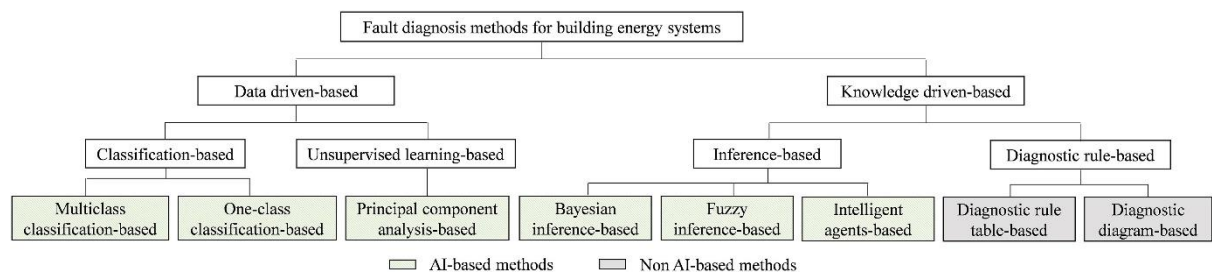


Figure 4: Classification of Fault Diagnosis methods for building energy systems [4]

Through a literature review 193 published journal and conference articles on FDD methods for HVAC systems are identified. The FDD techniques for AHUs in these articles is summarized in Figure 5. It can be observed that unsupervised or semi-supervised techniques such as principal component analysis (PCA), Clustering, Association Rules, Symbolic Aggregate Approximation (SAX) based techniques are quite popular given annotated fault labels required for supervised learning techniques such as artificial neural networks (ANN) are unavailable. However, it should be noted that supervised learning techniques outperform unsupervised learning techniques [22].

Labelling data for faulty operation is difficult due to four reasons cited below:

1. Chances of HVAC system operating in normal state are much higher than faulty state [23].
2. It is very expensive and impractical to get sufficient training data for every fault [24]. For example, in the RP-1312A project of ASHRAE it took nearly a year to generate labeled data for 19 different AHU faults, however, still could not cover the wide range of possible operation conditions [4].
3. There is no established or set process for annotation in building operations. Typically, maintenance records or work orders are maintained in Enterprise Resource Planning (ERP) systems and can be read using text mining techniques [25]. However, there is limited interoperability between such systems and FDD or BAS systems. Further, using this approach it is very difficult to precisely label a particular data point as faulty or normal.
4. Using available measurements at a buildings only certain faults can be detected, which makes it difficult to develop models for new or unobserved faults [24].

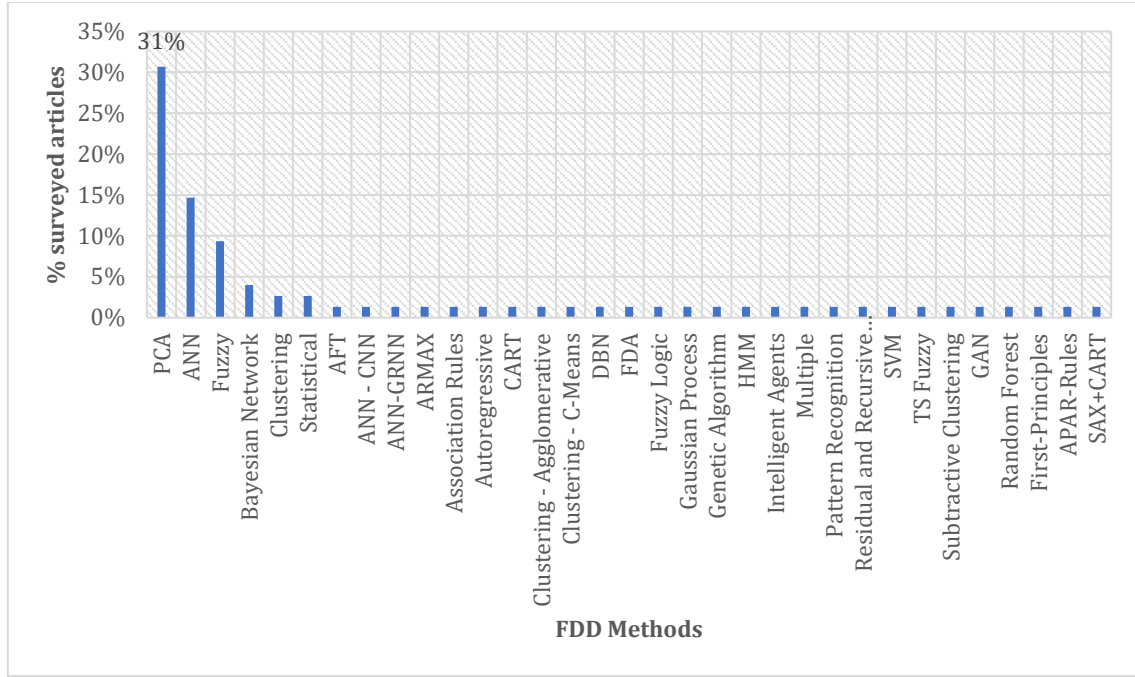


Figure 5: AFDD Techniques for AHU - Ranked in order of popularity

Simulation models are helpful for studying fault behaviour inexpensively [19]. The process of generating bulk data containing a variety of faults is referred to as 'Fault Modelling' [19]. Fault models prepared using this process have been utilized for: a) testing FDD methods, b) facilitate fault impact analysis [19]. Fault impact on energy and comfort indicators can be understood using this approach [26]. Quantifiable indicator such as fault impact is helpful towards commissioning and prioritization activities [26]. This is discussed further in Chapter 3.

For fault detection, regression-based (see Figure 3) or residual generation approaches offer an alternative to working with labelled data. In separate reviews by [27] and [4] regression-based approaches constitute 27% and 26% of published research articles respectively. Here, a black-box model is prepared to model relationship between inputs (or 'features') and outputs (or 'targets'). Amongst, the studied regression-based methods artificial neural networks (ANN) based, and support vector regression (SVR) based approaches are quite popular. Despite this popularity, a comparison between advanced ML techniques made by Chakraborty et al. in [28] and Walker et al. in [29], revealed that gradient boosting ML algorithms perform better than competing algorithms such as Artificial Neural Networks (ANN), Linear Regression, Random Forest, Support Vector Machine (SVM).

For fault diagnosis, knowledge or expert based methods (see Figure 4) are more reliable than data driven-based classifiers due to two reasons: a) uncertainty or incompleteness of information, b) unavailability of fault labels to train AI models that can learn the causality between faults and symptoms (see Figure 2). In their review, Zhao et al. in [4] identified that Bayesian network-based and Fuzzy logic-based approaches are equally popular. Bayesian network-based approaches have been successfully applied by [30–36] for AHUs. In general, these models can handle circumstances when incomplete, uncertain, or conflicting information is presented as their outputs are fault probabilities instead of Boolean fault outcomes [35].

In the context of diagnosis, Bayesian networks are also referred to as Diagnostic Bayesian Networks (DBNs). DBNs are directed acyclic graph models that explain the causal relationships between faults and symptoms. The DBN structure is further explained by initial beliefs mapped as prior and conditional probability tables [33]. These beliefs are updated as new evidence is received using Bayesian inference to compute posterior probabilities. Despite, the discussed advantages construction of such networks is often tedious and developed diagnosis models lack interpretability required for their widespread adoption. Taal et al. in [21], proposed DBNs based 4S3F framework. Here, the 4S implies four generic symptom types, namely energy performance, balance symptoms, operational state, and additional symptoms, and the 3F refers to three different fault categories: model, control, and component faults. Further, this framework draws a clear connection between the developed DBN and the piping and instrumentation (P&I) diagram. Further, its architecture is based on systems engineering theory and how the system can be redistributed across multiple P&I schemes [21]. Moreover, the framework proposes a generalizable and automatable approach to creating Bayesian networks for diagnosing

faults in HVAC systems. Importantly, the approach has been successfully demonstrated at AHU installations in the Dutch built environment.

### 1.2.2 FDD Applications

Energy conservation for building and community systems (ECBCS) is a global program piloted by International Energy Agency (IEA). Annex 47 is sub-track of this program that concerns cost-effective commissioning for existing and low energy buildings[37]. Within Annex 47, a total of 18 FDD tools were surveyed, and it was identified that a) automation and robust application is highly desirable, b) the developed interfaces of the tool need improvement, c) require better integration with the commissioning process [38].

Granderson et al. in [39] surveyed commercially deployed and under development FDD tools. It can be observed from their survey that FDD tools being utilized by the industry typically rely on a combination of expert rules or first principles. For example, [40] proposed a cloud based AFDD tool for AHUs. Their tool utilizes AHU performance assessment rules (APAR) [41]. Granderson et al. in [42] surveyed 14 commercially deployed tools and noted that whilst their software stack was proprietary several vendors offer application programming interface (API) to support integration.

Prouzeau et al. in [43], pointed out that despite there being availability of large sets of data collected through BMS or Internet of Things (IoT) sensors, its visualization is not effective enough to support building managers for Cx or FDD processes. For applying AFDD for AHUs effectively, identifying operation modes of AHUs is key [40]. Bespoke nature of AHU design and its logical operation determined by the control system vendor makes this process quite complicated [5].

Nine key issues preventing widespread deployment of AFDD systems are listed below:

1. Rules-based systems heavily rely on the sensed information. Due to the sensitivity of building owners to initial project costs, most building installations only have sensors limited to their control functionality [4]. For example, a space involving transfer of heat, mass, light with its outdoor environment, occupants, neighboring spaces, and various building installations is often monitored through just a thermostat [13]. Due to the lack of this additional information, it is difficult to develop reliable AFDD models.
2. The lack of standards regarding quality and positioning of deployed sensors further complicates the FDD process. Machine Learning (ML) models that rely on data collected through these sensors typically grapple with two kinds of uncertainty: a) epistemic and b) aleatory [44]. It is desirable to carefully handle the epistemic (or reducible) uncertainty to successfully apply model-based approaches [12]
3. There is a lack of a unified framework for developing generic key-performance indicators (KPIs) and associated rules for automated fault diagnosis [45].
4. The limits utilized for generating alarms using the rule-based approaches are typically set at a higher threshold than desired to minimize the number of false positives [6]. This reduces the ability of an FDD system to detect faults with lower severity and prevent energy waste significantly.
5. Typically, the alarms configured in CM systems are configured once and are not updated continuously. Hence, they fail to detect symptoms that do not breach obvious thresholds [5].
6. Approaches that utilize black-box models do not inspire a lot of confidence with building practitioners as they are not very interpretable [6].
7. Approaches that rely on experts for faults are difficult to maintain and scale. This is since building occupancy pattern or service personnel evolve with time, and knowledge transfer is often difficult.
8. Published research methods on novel FDD techniques start with utilizing a prepared dataset. However, the practical application of these methods with operational CMS is rarely discussed.
9. Analytical functions in the facility management aren't widespread yet [46]. Commercial alternatives such as Analytics or Software as-a-service models need to be explored for software procurement that can guarantee value delivery.

## 1.3 PROJECT PLAN AND WORK PACKAGES

The goal of the project is to design and prototype an automated tool that can robustly detect and diagnose faults within AHUs, and support maintenance to decrease energy use and to increase human comfort. To meet the identified this goal key objectives are detailed hereafter:

1. Identify and overcome problems associated with implementation of Automated Fault Detection and Diagnosis methods for AHUs
2. Identify most important causes that lead to inefficient energy performance of AHUs.

3. Evaluate, design, and validate a data driven module that leverages state-of-the-art techniques from Artificial Intelligence (AI) domain.
4. Focusing on operational faults and AHUs utilized in Dutch Built-Environment, demonstrate the technique into a software module that can be integrated with a CMS (for example InsiteSuite).
5. Deploy the tool and evaluate results at shortlisted buildings.

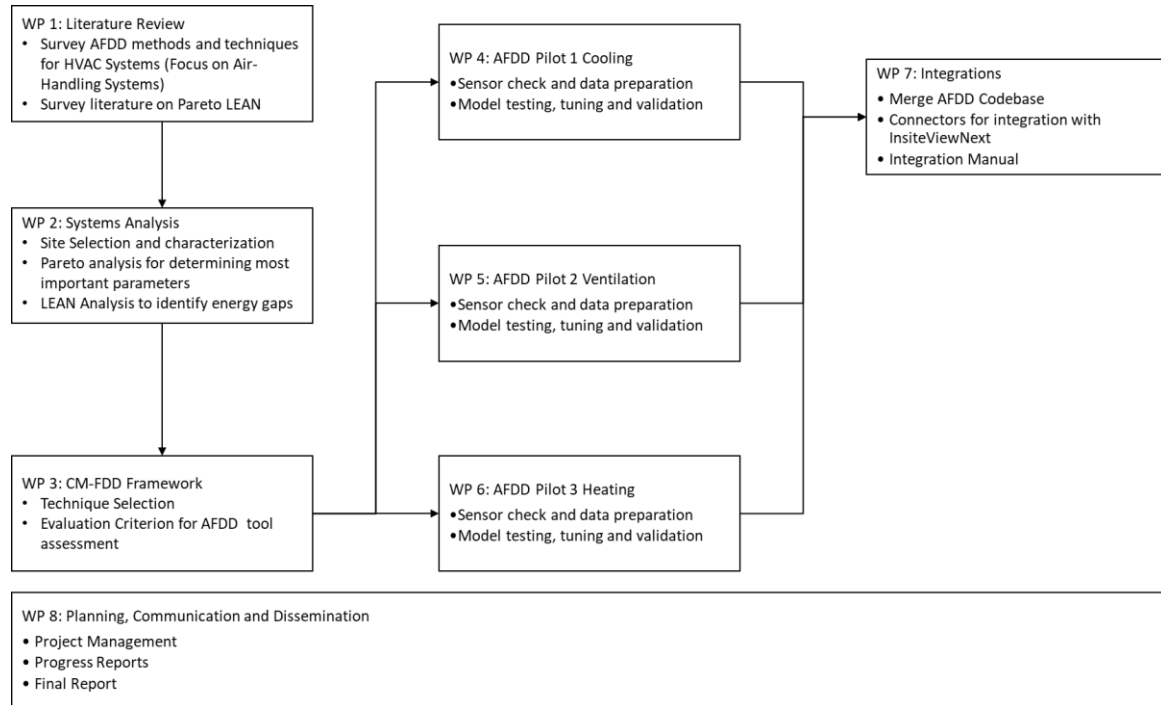


Figure 6: Project methodology

It is understood that a more personalized approach with subjective feedback collected from occupants is required for improving human comfort. This aspect is taken care of in a parallel project titled APK2.0 and hence only objective key-performance indicators pertinent to comfort have been considered as inclusions in this project. To achieve the stated objectives, the overall planning for the project is divided into work packages (WP) shown Figure 6. Briefly, the project would commence with reviewing literature (see WP 1 on Figure 6) in-order to deeply understand the domain, and identify the available state-of-the-art. Before designing and developing the AFDD tool, a systems analysis (see WP 2 on Figure 6) step has been introduced to firstly characterize the system and reduce the design variables. More specifically, a systematic approach termed Pareto analysis has been considered to minimize the data preparation requirements. This is aimed at reducing the time spent in data preparation (often at least 80%) before any ML models can be trained. Further, it also includes a sensor impact analysis to identify critical sensors required for preparing FDD models. The results from this analysis are utilized to propose a framework for FDD that can be combined with deployed CM systems termed 'CM-FDD' (see WP 3 on Figure 6). With the reduced datasets and the CM-FDD framework, the project would step into testing and validation of the AFDD tool in-situ at the shortlisted building sites. For planning purposes, the project tasks are further broken down to pursue distinct initiatives in cooling, heating, and ventilation (see WP 4,5,6 on Figure 6). These align with the primary functions of an AHU. Alongside a pilot initiative in each direction integration with CMS (InsiteSuite) platform (see WP 7 on Figure 6) would be undertaken. The work package 8, is a supervisory work package that's been designed to monitor and report project's progress continuously.

#### 1.4 OUTLINE OF THE REPORT

The overall design methodology for prototyping the AFDD tool and case studies considered for verification and validation of the AFDD tool are discussed in Chapter 2. In effect WP 1, 2, and 3 outlined in Figure 6, contributed to the development of this method. In Chapter 3, the results from applying the developed method to considered case-studies are presented. The chapter also includes results from pilot deployment of models developed for fault detection and diagnosis for cooling, heating and ventilation (see WP 4,5,6 on Figure 6). The developed FDD tool using the discussed methodology, and its integration with the CMS (see WP 7 on Figure 6) is presented in

Chapter 4. In Chapter 5, the compliance of the designed concept is verified and the financial feasibility along with risks associated with the deployment are discussed. The report is then concluded in Chapter 6.

## 2 DESIGN APPROACH AND METHODOLOGY

A systematic approach that emphasizes on continuous verification and validation of the design has been adopted for the project and is presented in this section. Using this approach, first the requirements for the design of the AFDD tool are identified and discussed in section 2.1. In line with these requirements, the overall design methodology for prototyping the AFDD tool is discussed in section 2.2.

### 2.1 REQUIREMENTS

The complete requirements for the software are identified as a) user requirements and b) system requirements [47]. For identifying the user requirements for a stakeholder analysis is performed to assess their interests and is presented in section 2.1.1. Thereafter, system requirements are identified from published literature and is presented in section 2.1.2. Keeping the various interests in view, and upon careful examination of literature on the subject, a comprehensive set of requirements are iterated in section 2.1.3.

#### 2.1.1 Stakeholder analysis and their interests

The stakeholders for the project are mapped on Figure 7. This map clearly identifies who are the relevant project stakeholders, and how each one of them is connected. Further, the individual motivations ('Why?') of the various stakeholders are described in form of User stories. The User stories are written in form of actions and benefits, wherein the actions translate to specific requirements and benefits address the corresponding stakeholder motivation. This way each software requirement is clearly linked to the value delivered for the project participant (stakeholder).

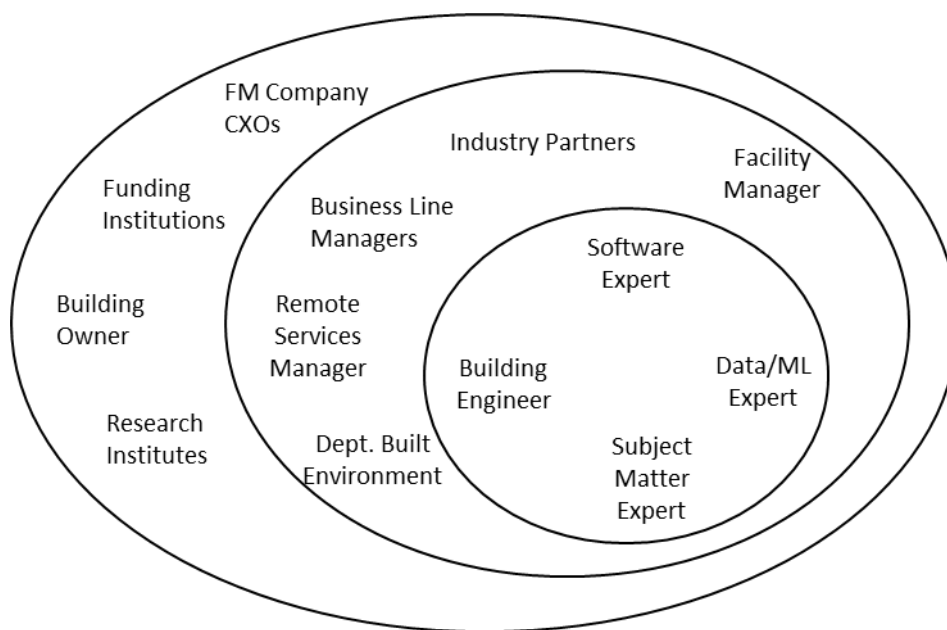


Figure 7: Stakeholder map

On this map stakeholders are grouped as per their roles on the project. The stakeholders in the innermost ellipse formulate the core user group for the proposed AFDD tool. The proposed tool upon commissioning would be directly utilized by this group and carry highest interest in the features to be developed. The second concentric ellipse comprises of stakeholders that together represent the gatekeepers group. This group directly influences the decision-making process and are concerned with the overall outcomes of this project. Sponsors for the project are mapped on the third concentric ellipse. The stakeholders within this sponsors group are mainly concerned with the impact of this project. Stakeholders' interests within the scope of this project are explored further and are more concretely presented as user stories in Table 1.

Table 1: User stories

#	Stakeholder	Example	Role	I want to [Action]	so that [Benefit]
<b>Inner ellipse (direct users)</b>					
A	Building engineer	Technicus, Kropman	User	Be informed of actions to be taken for fault correction	avoid comfort complaints and prevent energy wastage
				Be informed of fault diagnosis and root cause	prioritize and undertake maintenance action
				utilizing a reliable and user-friendly tool	ignore any false alarms
B	Software expert	Software engineer, Kropman	User	integrate FDD outcomes with the company's CMS	provide better insights to users
				enhance company's CMS with advanced visualizations	deliver information in a user-friendly manner
C	Data/ML expert	Software engineer - Machine Learning, Kropman	User	integrate advanced machine learning use-cases into the company's ML framework	deliver intelligence powered by machine learning to 100+ end users
				enhance current machine learning capabilities	keep the current framework updated with state-of-the-art in predictive modeling
D	Subject matter expert	Advisor O&T, Kropman	User	evaluate innovative techniques and their potential for deployment	advise company on the accurate potential for deploying advanced AI based methods
<b>Middle ellipse (influencers in the decision making process)</b>					
E	Facility manager	Project Leider, Kropman; Project Manager Radboud UMC	User	test new techniques for fault detection and diagnosis, and create demonstrable examples for the organization	contribute to organizational development on the knowledge scale
F	Industry partner	System Air, Kropman	Influencer	test and validate new ideas for improving service delivery and operational efficiency	lead innovations on the marketplace, create a differentiated value proposition for my customer, organizationally adapt to the future
G	Business line manager	Director Gebouwautomatisering, Kropman; Hoofd Technical Competence Center, Kropman	Decision-maker	evolve from current rules-based approaches to novel data-driven/AI based techniques for fault detection and diagnosis	automate FDD processes and use it as an example for larger digital transformation required within the organization
				explore data-driven models whose outputs can be	develop confidence within the organization to shift to data-driven

#	Stakeholder	Example	Role	I want to [Action]	so that [Benefit]
				explained	solutions
				continuously push the boundaries for innovation within the company	maintain a competitive advantage on the marketplace
H	Remote services manager	Manager Insite Remote Services, Kropman	Influencer	steer my current operations through automation	can be future ready for managing multiple sites with limited and less experienced resources as compared to before
				become more operationally efficient	remain financially competitive in providing my services
I	Dept. Built environment (TU/e)	Professor, TU/e	Decision-maker	promote innovative and state-of-the-art ideas	contribute to upgradation and upskilling of building installations company
				minimize carbon footprint of buildings	contribute development of a climate neutral built environment
		Post-doc, TU/e	Sponsor	deliver high-quality output	contribute to better research and design outcomes
Outer ellipse (sponsors)					
J	FM Company CXOs	Kropman	Promotor	be a profitable and climate friendly enterprise	maintain differentiated proposition on the marketplace and
				develop a robust software platform for continuous monitoring of building installations	bid and execute more DBMO (Design, Build, Maintain and Operate) type contracts
K	Funding institutions	Eindhoven Engine, Rijksdienst voor Ondernemend Nederland	Promotor	mobilize positive initiatives	contribute to energy transition and promote technology that would combat climate change
L	Building owner	ROC, Kropman	Promotor	operate my building in a sustainable manner	avoid unwarranted carbon emissions from my building
M	Research institutes	ISSO	Promotor	cross-fertilize research initiatives	contribute to development of collective knowledge that would contribute to a more sustainable future

### 2.1.2 AFDD tool requirements from literature

In addition to the requirements identified through stakeholder interactions (ref. section 2.1.1), key requirements identified through literature search are presented in this section. These system requirements are identified along two directions: a) application specific requirements and b) algorithmic requirements. Herein, application specific requirement implies the requirements constraining the design of the overall FDD tool, whilst algorithmic requirements are identified to constrain the plethora (ref section 1.2.1) of competing FDD techniques.

- a) The application specific requirements are viewed as functional and realization aspects of the system [48]. Using this categorization, some desirable characteristics proposed by [5,8,13,40,49] are presented in Table 2.

Table 2: AFDD Tool - desirable characteristics

Functional Aspects	Realization Aspects
High accuracy	Adaptability
Quick detection and diagnosis	No need for handcrafted AFDD algorithms
Robustness	Low Cost
Explanation facility	Interoperability
Isolability - ability to distinguish between multiple failures	Low storage and computational requirements
Novelty identifiability	Limited modelling requirements
Heuristic observations as evidence	Automation level in configuration
Multiple fault identifiability	Evaluation and decision support capabilities

- b) For algorithms, the following have been identified as key to successful implementation and widespread adoption:
- Linkage between AI or data-driven model and the underlying system, such that deployed models are explainable to the user [21].
  - Overcome the uncertainty within models trained with history data, which is inherent due to limited information about historical operation and how well it represents normal behavior [50].

### 2.1.3 Requirements Summary

The composite system requirements are specified in this section. These system requirements are further classified as domain, functional, and non-functional requirements for developing the AFDD tool and are enlisted in Table 3, Table 4, and Table 5 respectively [47]. Further, upon consultation with key decision makers a priority order has been identified. Using this process, finalized requirement along with its linkage to user story and priority is specified in the tables presented below. The priority order is utilized for planning and development purposes.

Table 3: Prioritized domain requirements

Linkage to user stories	Requirement	Priority
A, D, E, F, H	Select and show key performance indicators that can track system performance	High
A, D, E, F, H, I	Select and prioritize key faults that cause the largest energy performance gap	High
A, C, D, E, F, G, H, I	Express clear linkages between developed diagnosis strategy and HVAC system	High
A, C, D, E, F, G, H, I	Explain predictions of deployed machine learning models	High
A, D, E, F, H, I	Isolability, Evaluation and decision support capabilities: Utilize Bayesian methods that can deal with uncertain information. Further, embed features to evaluate outcomes and support decision making.	High
A, D, E, F, H, I	No. of Sensors/Masurement Requirements: For modelling utilize as less sensors as possible to avoid sensor uncertainty	Medium

Linkage to user stories	Requirement	Priority
B, C	Ease and Automation of training and tuning, Limited need for handcrafting of algorithms: Model training and tuning procedure to be completely automated	Low
A, C, D, E, F, G	Detection Time: Detection time for detecting abrupt faults needs to be minimal	Low
B, C	Computational requirements (Memory): Model deployment for a single building should be supported on a standard PC with 16GB memory	Low

Table 4: Prioritized functional requirements

Linkage with User-Stories	Requirement	Priority
C, G, I	Provide support for training, testing, evaluating, and deploying Bayesian networks	High
B, D, G, I	Visualize diagnostic Bayesian networks including symptom states and fault probabilities	High
C, I	Provide support for training, testing, evaluating, and deploying machine learning models	High
A, E, H	Validate datasets before utilizing them for serving predictions	High
G, I	Software should be able to interface with CMS (InsiteSuite) over API	High
B, C, G	Store meta information about the underlying HVAC system	Medium
A, E, H	Visualize diagnosed faults in a clear manner	Medium
A, E, H	Provide supporting evidence and information on diagnosed faults	Medium
C, G, I	Develop a fault library that can store fault and meta information on faults	Medium
C	Provide support for tracking performance of deployed machine learning models and raise flags for retraining	Medium
A, E, H	Software should support date, time and text filter and sort functionalities wherever applicable	Medium
C	Provide support for utilizing state-of-the-art feature selection techniques	Low
C, I	Feature to compare results from multiple regression modelling frameworks such as gradient boosting, decision tress	Low
I	Software should support dynamic Bayesian networks	Low
G, I	Software should be able to interface directly with BMS deployed on site for data ingestion	Low
B, C, G	Software should support APIs for data export from developed application	Low
C, G, I	Software should carry a mechanism to input expert information that can be further utilized for labelling or correction purposes	Low

Table 5: Prioritized non-functional requirements

Linkage to user stories	Requirement	Priority
F, G	<b>Security:</b> Only designated and authorized use of client data	High
G, I	<b>Maintainability:</b> Software should be free of poor coding practices and should carry ample documentation and annotations for easy maintainability Data tags utilized in the software should be human understandable	High
G, I	<b>Interoperability:</b> Should be designed in a manner that it can support open interfaces for connectivity with external applications	High
C, G	<b>Scalability:</b> Should be deployed and tested over multiple building use-cases Should be able to handle multiple data sources Should be able to accommodate newer algorithms	High
A, E, H, G	<b>Portability:</b> Software should be agnostic to operating system environment. It can be deployed on any local or cloud environment that carries sufficient memory and support Python	Medium

Linkage to user stories	Requirement	Priority
	Software visualization layer should support standard browser interfaces	
A, E, H, G	<b>Performance:</b> Should be able infer and generate results by processing real-time data streams Should be able to validate inputs and clearly indicate errors	Low
G, I	<b>Reusability:</b> Software dependencies should be clearly expressed Machine learning and Bayesian network modelling blocks should be reusable	Low

## 2.2 DESIGN METHODOLOGY

To design and engineer the AFDD tool, systems thinking approach has been adopted [51]. For the AFDD tool development, Python is the utilized programming language as it is popular and has a large collection of continuously maintained packages supporting AI based development. The proposed architecture for AFDD software is conceived with modularity, reusability, and scalability considerations. This is to address the non-functional requirements as stated in Table 5.

### 2.2.1 AFDD Tool Overview

The overall system architecture of the AFDD tool is presented in Figure 8. Herein, the implemented workflow is represented with solid arrows. The architecture comprises of several layers namely data acquisition, data validation and pre-processing, business, post-processing, and visualization. In the data acquisition layer, all aspects concerning data transactions with external interfaces, its protocol, and security are maintained. The acquired data is then parsed through as key value pairs into downstream software layers.

The design of the FDD tool hereafter can be envisioned as *User Agnostic* and *User Specific developments* as shown in Figure 8. The *User Agnostic development* concerns design of data preparation and data mining operations on acquired data. These operations are carried out in the *Data Validation and Pre-Processing Layer* and the *FDD Business Layer* respectively. The *User Specific development* is to provide a user-friendly interface for efficiently realizing outputs from *FDD business layer* and enable human-in-the-loop diagnostics. The design of the business layer encapsulates majority of the focus of this project and is discussed next in section 2.2.2. The methodology for designing the user interface for the tool or the *Data Visualization Layer* is presented in section 2.2.3. The method for designing other layers (see Figure 8) that essentially play a supporting function are briefly discussed in section 2.2.4.

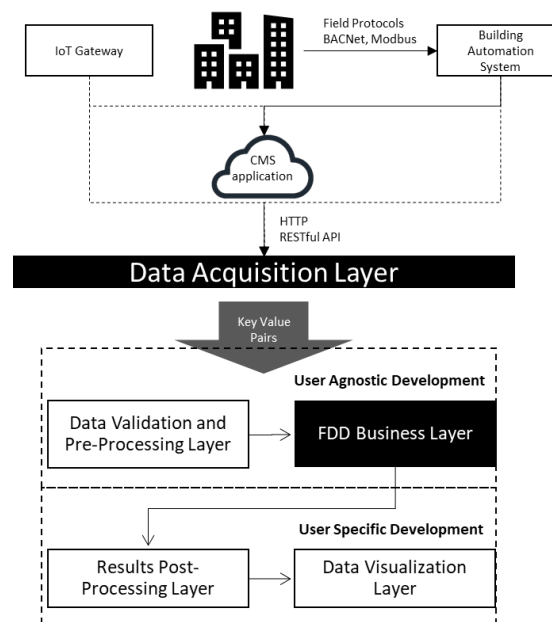


Figure 8: System architecture

### 2.2.2 FDD business layer

The FDD business layer has been conceived with the intention of wrapping critical information such as faults, FDD algorithms, detection thresholds, fault & symptom associations. It has been designed with keeping key domain specific requirements such as robustness, isolability, and early detection and diagnosis under consideration (see Table 3). In view of these requirements, multiple competing FDD approaches have been studied (ref. section 1.2). Before, applying these techniques in practice a systems analysis step has been introduced (see Figure 9).

Systems analysis supports the realization of stakeholder needs into definitive product outcomes [52]. Various systems analysis techniques have been proposed to support the product development process across its lifecycle [52]. In this project, systems analysis has been conducted early in its life cycle to: a) support planning and development; b) avoid costly design modifications in the latter phases of the AFDD tool development. Two specific steps in fault and sensor impact analysis formulate this systems analysis step. This approach is also known as Pareto-LEAN approach [53]. However, is referred to fault and sensor impact analysis hereafter.

The faults to be included in the AFDD tool are prioritized using a fault impact analysis. Herein, faults often studied in literature are rank ordered based on their computed energy gap realized through a simulation approach [23]. Such a prioritization is vital to maximizing the energy saved through the designed tool. A typical large building installation can carry hundreds of sensed and controlled variables. Through the sensor impact analysis sensors are prioritized and relationship between faults and analytical symptoms are understood. Using this approach, the design variables involved in the FDD process are constrained. This approach is dwelled upon further in Chapter 3.

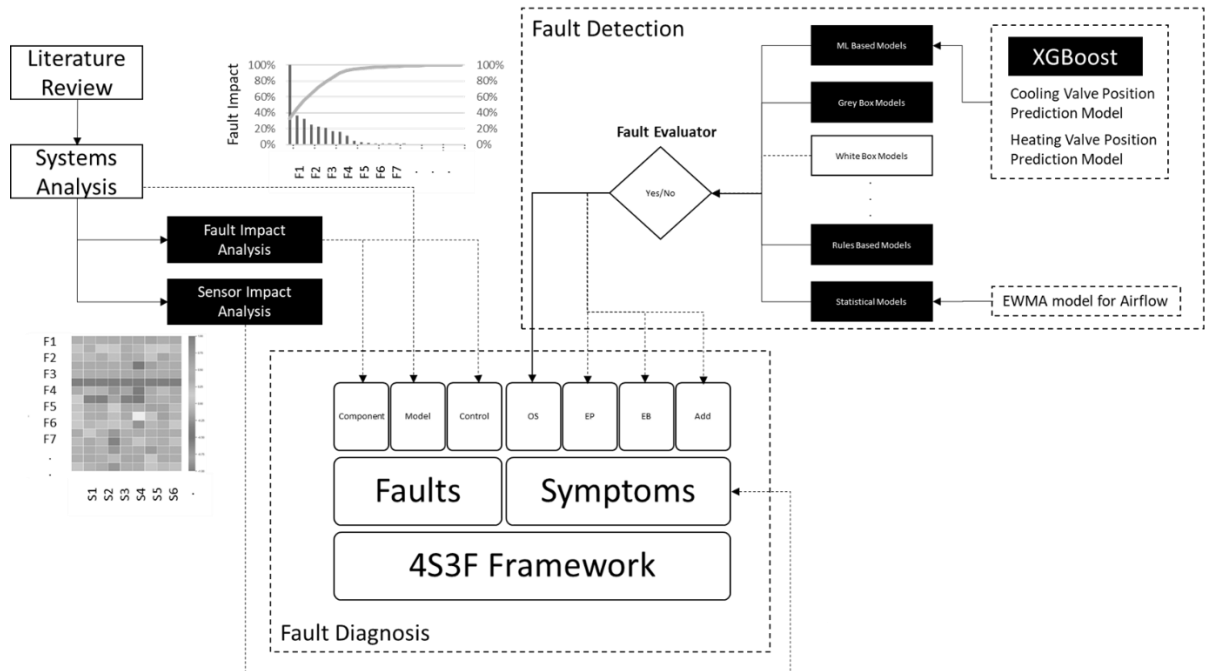


Figure 9: FDD Business Layer

It has been identified that DBNs can successfully handle the uncertainty associated with the FDD process. The DBN based 4S3F framework demonstrates clear linkage between the underlying HVAC system and the diagnosis process [21]. The probabilistic nature of this approach allows a way to eliminate failure modes, which is also synonymous with how HVAC engineers work [21]. Further, the relationships between faults and symptoms are characterized using a belief network [33]. These belief networks lessen the reliance on accuracy of the fault detection algorithm [30]. Furthermore, simplified models can be utilized instead of complex algorithms that offer lesser generalizability [30]. Citing these reasons, the 4S3F framework (see Figure 9) is selected for developing the business layer of the proposed FDD tool.

As the name implies, the 4S3F method classifies faults into three categories: component faults, control faults, and model faults [21].

1. **Component faults:** Referred to as hard faults that are caused due to design, poor selection, performance degradation or complete failures [21].
2. **Control faults:** Also known as soft faults. As the name suggests, these faults refer to issues arising due to improper control such as set points and controller issues [21].
3. **Model faults:** These are also called soft faults and are caused because of models deployed for quantitative estimation [21].

For the faults included in the DBN, the prior beliefs are derived using literature search [31,32,54]. The conditional probabilities are prepared using HVAC expert knowledge. In this regard, a sensitivity analysis by [50] revealed that if the set probability values are reasonable, the likely diagnosed outcome is not affected.

In a DBN, symptom nodes are variables that are utilized to update prior beliefs on presence or absence of a fault. In buildings, these nodes are supplied with evidence using data collected from the BMS. It is desirable to utilize smaller Bayesian networks to keep the size of the conditional probability tables manageable as otherwise the size of these tables grow exponentially [35]. NoisyMax simplification is utilized as convention for child nodes with more than two parents [35].

Focusing on the symptoms block shown in Figure 9, four kinds of symptom nodes have been proposed by [21]

1. **Operational state (OS):** The OS symptom node represent deviation in operational state from its expected state. The OS symptoms can be further classified into control-based OS indicators and design-based OS indicators [45].
2. **Energy Performance (EP):** The EP node is representative of normalized key performance indicators such as COP, KWh/m<sup>2</sup> that are conventionally utilized to gauge or compare performance within or between systems. They can be further declassified into performance factors, capacity indicators, or energy outliers [45].
3. **Energy Balance (EB):** The EB node encapsulates system design principles that tend to promote balanced behavior beyond some transient aberrations. Therefore, instead of detailed white box modelling approaches, fundamental balancing equations are utilized [21].
4. **Additional (Add.):** Additional symptom nodes are utilized to pass qualitative or quantitative information received from other available information sources such as maintenance logs, or manufacturers input, or user satisfaction[45].

These symptom nodes are activated using fault detection models encapsulated in the Fault Detection Layer (see Figure 9). Diving further into the fault detection layer, it comprises of a modelling layer and a fault evaluation layer. For fault detection, amongst the data-driven based approaches (ref section 1.2), regression-based and statistical modelling approaches have been utilized to set performance benchmarks to distinguish between faulty and normal behaviour. However, the framework is designed with enough flexibility to replace the utilized methods with any competing or superior method given a use-case scenario. This is done to ensure that developed prototype can be continuously improved with evolution in the AI domain. The fault evaluation is done by setting thresholds on the residual generated through this process. In the event, these thresholds are breached a fault is considered detected, and the corresponding symptom is passed to the DBN for diagnosis.

This way in the *FDD Business layer*, the fault diagnosis process that concerns root-cause elimination is separated from the fault detection process which is more aligned with the so-called anomaly detection process. This separation between layers is highly recommended as it allows for multiple techniques from various domains and sub-domains to be combined in a common framework [13]. For example, through this project an advanced AI algorithm called XGBoost (extreme gradient boosting) is utilized in the fault detection process and its outputs are fed into the symptom nodes [55]. The modelling strategies utilized for FDD are elaborated upon in Chapter 5. To validate the robustness of the *FDD Business layer*, experimental validation is utilized. Case studies utilized in this process are discussed in section 2.3.

### 2.2.3 Data visualization layer

Effective visualization is key to promoting human-in-the-loop (HITL) diagnostics. HITL diagnostics implies a synergetic cooperation between a human expert and AI models, wherein this combined strength is harnessed, whilst simultaneously overcoming limitations of each party [56]. For designing the user interface (UI) for the proposed tool, a product discovery method referred to as design sprint is applied[57]. Using this approach, specificities desirable for users are incorporated and objectively evaluated before considering them for development. Multiple visual concepts are prototyped in Figma, a graphics editor utilized for designing user

interfaces. These design concepts of this layer are tested with key stakeholders and result from the process are summarized in APPENDIX A. This way, the user specific development (see Figure 8) is realized.

#### 2.2.4 AFDD tool integration

Besides the veracity of the business logics, a robust coupling between the AFDD tool and the deployed CMS (InsiteSuite) is key to its usefulness. For integration with this CMS system an application programming interface (API) approach is adopted. Using this strategy, data can be securely acquired over standard web protocol such as HTTP. For this project, the *data acquisition layer* (see Figure 8) has been customized to the available API environment. Although, it can be expanded upon to interface directly with on-premises servers or Internet of Things (IoT) gateways as shown in Figure 8. This is a first step towards ensuring the desirable interoperability of AFDD application (see Table 5). Further, it also ensures that evidence from the BAS deployed on-site is continuously collected and inferred through the utilized FDD strategy.

As the proposed tool utilizes AI approaches, the software architecture needs to attune to this atypical programming environment. Ameisen in [58], discussed how development of machine learning applications at its core comprises of two pipelines namely the training pipeline and the inference pipeline. For deploying the discussed XGBoost fault detection model (see 2.2.2), the two stitched pipelines are shown in Figure 10. The training pipeline starts with data acquisition over the API and ends with a trained model. The performance of the trained model is ensured through the intermediary steps of pre-processing, evaluation through cross-validation, feature selection, and tuning [59]. The specific steps employed for various models trained for the application are discussed in Chapter 4. To ensure multiple modelling approaches such as (ANN, Gradient Boosting etc.) can utilize same datasets, the steps until feature selection shown in the training pipeline below are bucketed into the *data validation and pre-processing layer* (see Figure 8).

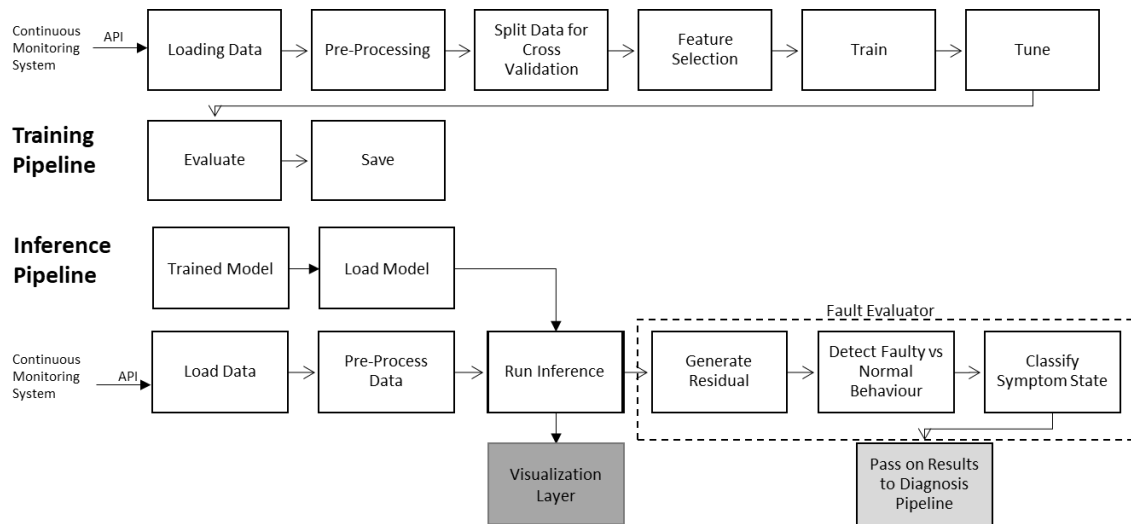


Figure 10: Training and inference pipelines for fault detection

In the inference pipeline, data is requested over the same API and results are inferred using a saved model from the training pipeline. Given the use-case, the inference pipeline splits into two data streams. One is utilized for plotting results from the trained model for visual diagnosis and the other to the fault evaluator. In the fault evaluator, the generated residual is classified as normal or faulty using a fixed or dynamic threshold [60]. Hereafter, the results are prepared for treatment in the diagnosis pipeline. For example, the measured continuous variables are converted to discretized as required for the diagnosis pipeline realized using DBNs. The training and inference pipelines for other trained ML models as well as the Bayesian network are designed using a similar approach.

Besides, the treatment of data within the *FDD business layer*, for effective visualization as required in the *Data visualization layer* an intermediary layer is proposed called *results post-processing*. Herein, the data is for example aggregated to be presented in charts or other tabular visualization schemes. In effect, the *results post-processing* layer can support multiple visualizations schemes across the AFDD tool and is therefore designed as a separate component.



selected cases, four cases are from the Netherlands including a simulation case wherein Dutch weather file has been utilized to have more examples representative of Dutch built environment. The only foreign example included in the mix is Energy resource station building. Datasets collected from this building for ASHRAE's RP-1312 project have been utilized by several researchers from across the world to demonstrate competing FDD approaches for AHUs [64–66]. These datasets therefore provided a consistent baseline for comparison.

Table 6: Case study comparison

Description	Case-Studies				
	#1: 5-Zone Building	#2: Energy resource station	#3: Hoofddorp office	#4: Breda office	#5: Nijmegen school
Simulation/Real Case	Simulation	Real	Real	Simulation and Real	Real
Non-Residential Building Type	Office building	Laboratory Facility	Office building	Office building	School
Location	Netherlands	Iowa, USA	Netherlands	Netherlands	Netherlands
Purpose	Systems Analysis, Verification	Verification	Verification	Systems Analysis and Validation	Validation
AHU description	One central AHU supplying to five-zones	Two central AHUs supplying to three zones each	Four central AHUs	One central AHU supplying to three zones (North, South, and Office 105)	Two central AHUs
Fans	CAV	VAV	CAV	CAV	CAV
Coils	1 heating and 1 cooling coil in central AHU and 5 reheat coils	1 heating and 1 cooling coil in central AHU	1 heating and 1 cooling coil in central AHU	1 heating coil in central AHU and 3 cooling coils along supply air path	1 common heating and cooling coil in central AHU
Heat-Recovery	Rotary Heat Exchanger	Air-Side economizer	Rotary Heat Exchanger	Rotary Heat Exchanger	Rotary Heat Exchanger
Project Deliverables					
Simulation model					
Fault models					
Fault Impact analysis					
Sensor Impact analysis					
Fault Detection models					
Fault Diagnosis models					
FDD application deployment					

## 1) 5-zone building

The 5-zone building model is one of sixteen prototype building models developed by U.S. Department of Energy [67]. The building emulates character of a non-residential small office (total floor area of 463.6 m<sup>2</sup>) type building. The building has four exterior and one interior zone with 0.61m high return plenum and an overall building height of 3.05m. The default AHU configuration provided with the reference building has been modified to emulate Air-handlers installed at the real-building cases studied and typifies AHU installations in the Netherlands. These modifications include a 100% outdoor air system and a rotary heat exchanger for heat recovery. The detailed HVAC characteristics of the building are summarized and compared with the other case-studies in Table 7. The developed simulation model has primarily been utilized for fault modelling, fault impact and sensor impact analysis. Results from fault and sensor impact analysis are presented in section 3.1 and 3.2.

Table 7: HVAC characteristics 5-zone building, Breda office, and Nijmegen school

Description	5-zone	Breda office	Nijmegen school
No. of Chillers	2	1	1 Heat Pump
Chiller Type	Screw Type	Screw Type	NA
Chiller Flow Control Strategy	Constant Flow	Constant Flow	NA
Chiller Capacity [kW]	13.7 * 2	63.7	NA
Chiller Pump Configuration	Constant Primary Variable Secondary	Constant Flow	
Chilled Water Loop Design Exit Temp [C]	6	6	10
Chilled Water Loop Design Temp Difference [delta K]	6	6	10
No. of Boilers	1	1	NA – ATEs Type System
Boiler Capacity [kW]	26.96 * 1	156	NA
Boiler Flow Control Strategy	Leaving Set Point Modulated	Leaving Set Point Modulated	NA
Boiler Pump Configuration	Variable Flow	Constant Flow	NA
Hot Water Loop Design Exit Temp [C]	82	90	40
Hot Water Loop Design Temp Difference [delta K]	11	20	10
<b>Central AHU/s</b>			
Air Handling System type	CAV	CAV	CAV
Maximum Supply Air Flow Rate [m <sup>3</sup> /s]	0.91	North Zone – 2.26 South Zone – 1.27 105 Zone – 0.67	AHU 1 and AHU 2 - 12.22
100% OA	Yes	Yes	Yes
Air Side Heat Recovery type	Rotary heat exchanger	Rotary heat exchanger	Rotary heat exchanger
Cooling Coil Capacity [kW]	28.67	North Zone – 39.30 South Zone – 24.40 105 Zone - 14.50	130.4 (Sensible: 36.1kW, Latent: -137.62kg/h)
Heating Coil Capacity [kW]	8.01kW + 5 reheat coils of total ~17kW capacity	84.10	495.1 (Sensible: 348.4, Latent: 211.33 kg/h)
Setpoints	Outdoor Air reset	Outdoor air reset	Outdoor air reset
AHU Operation	<b>Weekdays:</b> 07:00-21:00 <b>Weekends:</b> -	<b>Weekdays:</b> 06:00-17:00 <b>Weekends:</b> -	Varied on daily basis

## 2) Breda office

The first case-study considered for validation and prototyped tool deployment is an office building commissioned in 1993 and renovated in 2009. The characteristics for the HVAC installation at site are tabulated in Table 7. The heating and cooling demand for the building is fulfilled by an onsite gas boiler and electric chiller units respectively. The central AHU supplies to three centrally conditioned zones name North & Canteen (North),

South, and 105. This constant air volume (CAV) AHU contains the supply and return fans, heating coil, supply, and return filters, and an enthalpy type heat recovery wheel (HRW). Whereas, in the supply path of the AHU post the supply fan, three individual cooling coils have been placed for each of the supply zones. Flow through the heating and cooling coils is regulated using a three-way control valve. An air-terminal unit is placed along the air path of 105 zone that regulates the airflow to maintain concentration of CO<sub>2</sub>. To maintain the heating supply air temperature a master-slave control strategy is employed, wherein master implies PID control between heating supply air and water temperatures and slave implies the control loop between hot water supply and the 3-way control valve (see Figure 12). Further, the heating setpoint is set as the maximum of desired setpoint in the three zones. The zone setpoint is controlled using a cascaded control strategy, wherein return air setpoint is determined using prevailing outdoor air condition and which cascades further to determine the supply air setpoint. The cooling supply air temperature on the other hand, is controlled directly using PID control (ref TC in Figure 12) between supply air and cooling coil control valve.

A zoomed in portion of the P&I diagram for the central AHU and North zone is shown in Figure 12. The complete P&I diagram is provided in APPENDIX B. This building has been modeled in simulation environment using DesignBuilder and EnergyPlus [68,69]. The HVAC layout of the simulation is also provided in APPENDIX B. In the developed simulation model, to emulate the prevailing control strategy following simplifications have been made:

1. For fault modeling purposes and due to an atypical HVAC design at Kropman Breda, the heating and cooling operation of the AHU are modeled separately using different layouts. For emulating heating mode operation, the cooling coils placed in the air path are modeled with a Fan Coil Unit object in EnergyPlus. Whereas cooling mode operation is modeled using three separated Air-Handling Units.
2. For heating mode operation, the master-slave control is simplified and calibrated using a direct control of supply air temperature with hot water flow through the heating coil.

The developed models are validated by comparing the simulation predictions with measurements at the site. The methodology and results for validation are presented in APPENDIX B.

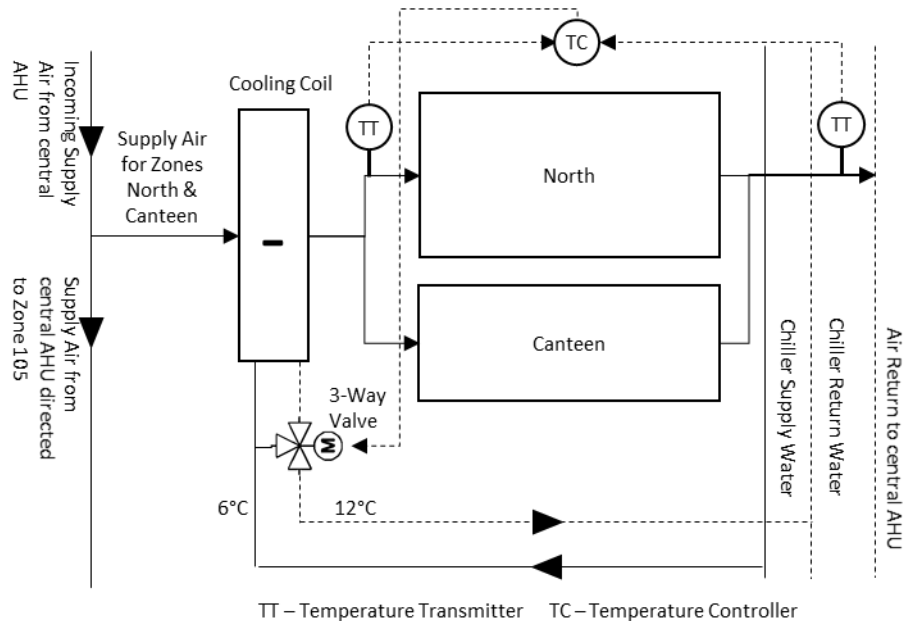


Figure 12: P&ID Breda office – central AHU and North zone

### 3) Nijmegen school

The second building considered for validation and FDD tool deployment is a school located in Nijmegen. It was commissioned in the year 2010. The HVAC installation at the building comprises of an Aquifer Thermal Energy Storage (ATES) system supported by a heat pump on the generation side. On the distribution side two central AHUs are installed that operate with a CAV control strategy. The supply air temperature is directly controlled using two-way control valves that regulate supply water through a common cooling and heating coil. In

comparison with the Breda office building, a single casing houses all the AHU components. A zoomed in portion of the P&I diagram for the AHU1 is shown in Figure 13. The complete P&I diagram is provided in APPENDIX B.

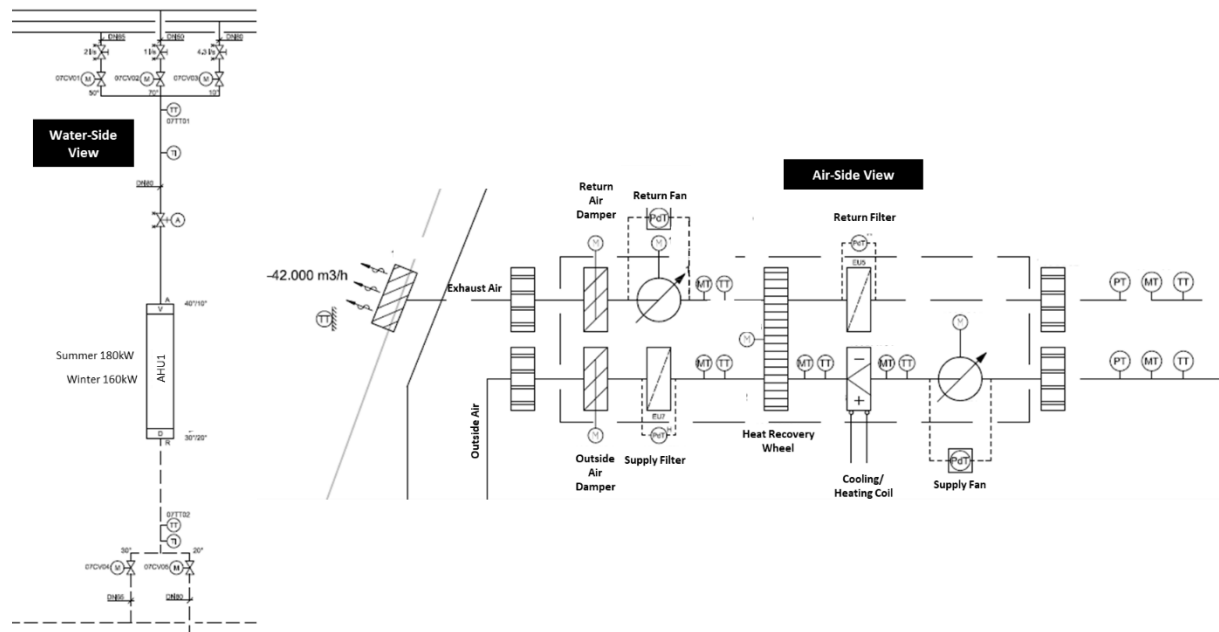


Figure 13: P&ID waterside (left) and airside (right) for Nijmegen school: AHU One

### 3 FDD BUSINESS LAYER

The FDD business layer discussed in section 2.2.2 encapsulates core business logics. In other words, it's the brain of the proposed AFDD tool. In line with the discussed method in section 2.2.2, the two key systems analysis steps namely fault impact analysis and sensor impact analysis are discussed in section 3.1 and section 3.2 respectively. For this analysis, the simulation models prepared for 5-zone building and Breda office (ref section 2.3) are utilized. The results from this step such as critical faults and sensors are directly utilized in the FDD processes discussed next.

Several advanced AI methods have been utilized in the *FDD business layer*. Most demonstration of these techniques in published literature either utilize prepared datasets or datasets prepared using simulation models. Data collected from real buildings though is prone to uncertainty. Therefore, for ensuring a reliable development of this layer, a large set of verification and validation cases (ref section 2.3.2) have been considered. In total four case studies are utilized namely: Energy resource station, Hoofddorp office, Breda office and Nijmegen office. Initially, the trained fault detection models using a black-box approach are verified using Hoofddorp office and Energy Resource station buildings. Then for experimental validation of the trained detection and diagnostic models Breda office and Nijmegen office are utilized. In section 3.4, the developed fault detection models using XGBoost algorithm are presented. In section 3.5, the DBNs developed for the two validation cases are presented. In section 3.6, *FDD business layer* is concluded.

#### 3.1 FAULT IMPACT ANALYSIS

Faults can be inexpensively modeled in a simulation environment to understand their impact on energetic and comfort performance. Several researchers in the past have demonstrated this approach at system and component level using various methods and simulation tools. Few of these approaches are summarized in Table 8. Of the over 174 plus tools listed on International Building Performance Simulation Association (IBPSA's) website, only a few possess fault modelling capabilities [23]. Further, a comprehensive review on these tools by [19] revealed advantages and higher capabilities of EnergyPlus [68]. Furthermore, the tool is being actively developed and offers several possibilities for co-simulation [70]. Upon careful evaluation of available options, EnergyPlus has been preferred for this project. The methodology utilized for fault impact analysis using EnergyPlus is discussed next in section 3.1.1.

Table 8: Previous research fault impact analysis – buildings and HVAC domain

Sr. No.	Author & Year	Topic	Simulation Tool	Summary
1	[71]	The Energy Impact of Faults in U.S. Commercial Buildings	-	Quantified impact of 13 different faults observed in US Commercial buildings and estimated their impact on a national level
2	[72]	A study on the energy penalty of various air-side system faults in buildings	EnergyPlus	Energy cost impacts of a range of common system faults in variable air volume (VAV). Use a 40 Storied building typical of one's found in Hong Kong and study a total of 9 VAV faults.
3	[73]	Modeling and simulation of HVAC faults in EnergyPlus	EnergyPlus	Characterize and prioritize common faults of HVAC equipment and control systems using a list of faults covered in an International Energy Agency (IEA) Report. Modeled a total of 19 faults.
4	[23]	Common Faults and Their Prioritization in Small Commercial Buildings	EnergyPlus	Studied and rank ordered a list of 20 top priority faults from a list of 39 faults found in US small commercial buildings
5	[73]	An innovative fault impact analysis framework for enhancing building operations	EnergyPlus	Studied a large set of 41 faults at Building level and quantified their impact across various weather scenarios. Also, provide an innovative framework for fault modelling by introducing fault probabilities into the fault model, and demonstrate the approach on typical US medium sized office building

6	[74]	A holistic fault impact analysis of the high-performance sequences of operation for HVAC systems: Modelica-based case study in a medium-office building	Modelica	Focus on high-performance control sequences recommended by ASHRAE Guideline 36. Demonstrate fault impact analysis over 359 different scenarios across three operating conditions (cooling, heating and shoulder). Measure the adaptability of the proposed control sequences.
---	------	---	----------	---

### 3.1.1 Methodology

For carrying out a fault impact analysis, a list of faults, a baseline model, and weather are three key considerations. Using studies carried out by [23,75], surveying published literature of nearly 20 years, a comprehensive list of 39 faults pertinent to AHUs is presented in APPENDIX B-Table 24. A baseline model is indicative of normal system behavior and is utilized as reference for comparison with fault models. The observed difference on selected energy and comfort indicators is quantified as the fault impact.

For this project, the 5-zone building, and Breda office are included to understand and compare fault impact in a general and specific context. Faults cause dissimilar impacts across different weather conditions [23]. To isolate this impact and understand the granularities, the fault impact analysis is split into peak (winter, summer) and shoulder (spring, autumn) weather periods observed at the location. The considered weather period for fault modelling is shown in Figure 14.

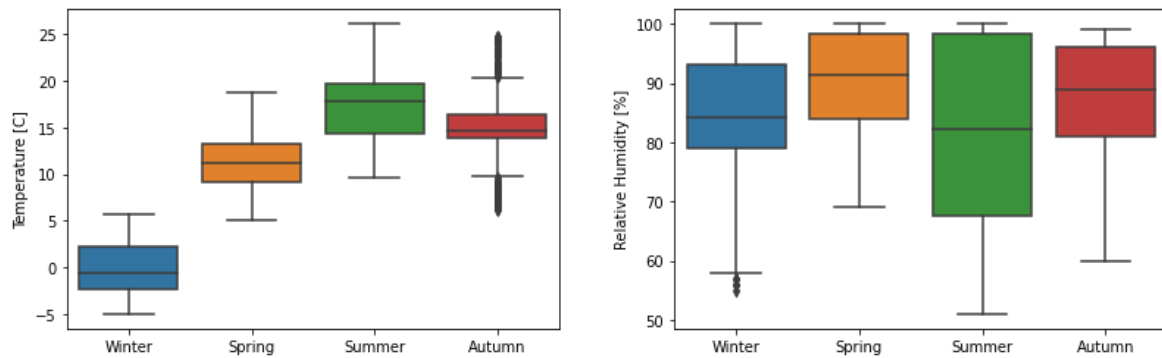


Figure 14: Outdoor air Dry-bulb temperature and Relative Humidity conditions prevailing in the considered weather periods for fault impact analysis of 5-zone building

### 3.1.2 Results and Discussion

- 30 and 26 fault models are prepared for 5-zone building and Breda office respectively. Cooling coil and its valve related faults are not modeled for Breda office, as chiller control strategy does not allow its operation in the considered weather period (winter).
- For the considered scenarios, the percentages of faults that cause nearly 80% of the energy performance gap are shown in Table 9. The observed results nearly follow the Pareto principle or the 80:20 rule [76]. This implies that vital few faults can be prioritized using this approach.

Table 9: Percentages of faults that cause nearly 80% of the energy performance gap estimated through fault impact analysis

5-zone building		Breda office
Peak weather period	Shoulder weather period	Peak winter period
26.7%	30.0%	30.8%

- The variation observed in normal vs faulty behavior is more prominent during shoulder months in comparison with peak weather months. This points towards utilizing more conservative thresholds for differentiating between faulty vs normal behavior during peak summer/winter months viz-a-viz shoulder months.
- Although, the considered cases (5-zone building and Breda office) differ in their HVAC design and control strategy, the distribution of faults that cause largest impact doesn't alter significantly.

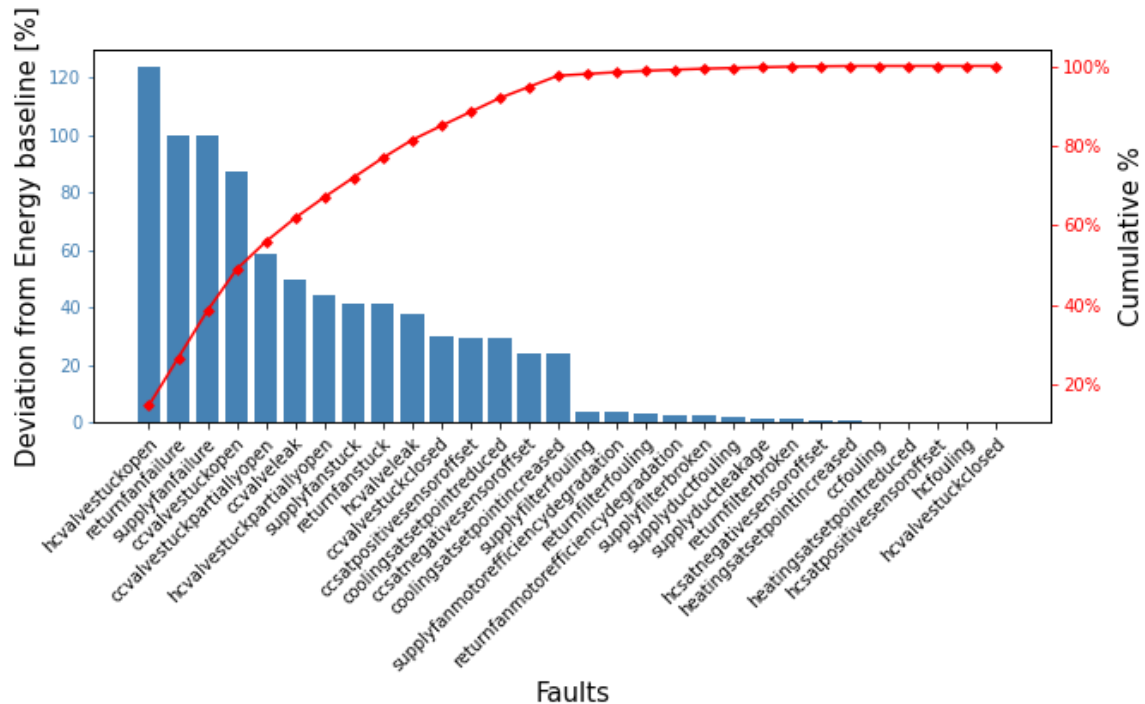


Figure 15: Fault impact analysis with 5-zone building for shoulder weather period

- Estimated fault impact of control or soft faults (Ref 2.2.2) such as stuck valve or fan, leaking valve, or sensor offset is larger than component faults such as performance degradation of fan motor or coil/duct/filter fouling. Therefore, control faults are prioritized for the development of the AFDD tool.
- Amongst the control faults valve and fan related faults cause larger impact than sensor faults.

The current fault impact analysis doesn't account for fault occurrence that determines its frequency or prevalence [23]. Further, the faults are modeled with their behavior representative of a step function [23]. These are possible directions to improve the accuracy of carried out fault impact analysis. Since detailed fault impact analysis is not the main objective of this project, faults prioritized using the adopted method are proceeded with.

### 3.2 SENSOR IMPACT ANALYSIS

Varying kind and number of sensors are installed in buildings due to sensitivity of most building owners to costs during a building's design phase [77]. Consequently, installed building sensors are limited to sensors important from control standpoint, and relatively expensive sensors such as flow rate, pressure, and power are often found missing [4]. This impedes the standardization and scalability of FDD approaches [21]. To this end, a survey of building practitioners by Zhang et al. discussed in [77] found that sensors for FDD carry the least level of importance. To understand the implications of these considerations on this project, a comparative analysis of available sensors at two case-studies (ref section 2.3.2) selected for FDD deployment namely Breda office and Nijmegen school is presented in Table 10. Here, the available sensors deployed at building are compared against list of sensors commonly observed on AHUs worldwide [78]. In Table 10, presented sensors are also differentiated between typical sensors, sensors that carry potential and high potential for FDD [78].

Table 10: Comparative analysis Air-Handling Unit sensors

Measurement	Typical Sensors	Highly potential Sensors	Potential Sensors	Breda office	Nijmegen school
Outside air temperature	x			*	x
Mix air temperature	x			*	x
Supply air temperature	x			x	x
Heating coil outlet air temperature			x	x	x
Cooling coil outlet air temperature			x	x	x

Return air temperature		x		x	x
Outside air humidity		x		*	x
Supply air humidity		x		x	x
Return air humidity		x			x
Supply air duct static pressure	x			x	x
Supply fan differential pressure		x			x
Return fan differential pressure		x			x
Supply airflow rate	x			*	x
Return airflow rate		x			x
Outdoor airflow rate			x		
Supply fan total power meter	x				
Return fan total power meter	x				
Supply fan speed signal	x			x	x
Return fan speed signal	x			x	x
Mixing box damper position signal	x			x	x
Heating coil valve position signal	x			x	x
Cooling coil valve position signal	x			x	x
Heating coil water flow rate			x		
Cooling coil water flow rate			x	*	

\* Proposed and deployed during the project

Sensor measurements inevitably are uncertain, and this uncertainty is heavily reliant on the kind (temperature, pressure etc.) and accuracy of the deployed sensors [79]. The former is unavoidable, however latter can be directly linked to cost of sensors [4]. Keeping this along with the need for limiting the size of Bayesian network (ref section 2.2.2) in view, it's important to identify the most important sensors from FDD standpoint. Kim and Comstock et al. in [71 and 79], demonstrated a simulation model-based approach to measure the sensitivity of sensors to faults. Simulation models are helpful in overcoming the discussed limitations with sensors.

### 3.2.1 Methodology

Fault models discussed in section 3.1 have been utilized to understand impact of faults on various sensors. For quantifying this impact normalized mean-biased error (NMBE) has been selected as indicator [81].

### 3.2.2 Results and Discussion

The sensor impact analysis for peak weather periods carried out with 5-zone building and Breda simulation model is provided in APPENDIX B, whilst for shoulder weather period is presented in Figure 16. Upon comparing the results, it can be observed that amongst the sensors listed in Table 10, maximum impact is felt on the mass flow rate sensors deployed on the heating and cooling coils. Although, a highly potential sensor mass flow rate measurement is typically lacking in buildings and as is also the case at the considered building cases.

Besides AHU sensors, to understand the impact in general some additional power measurements are also included in the sensor impact analysis. On these sensors too impact of faults is clearly observable and hence can be useful in the FDD process. However, power measurements can be quite exorbitant and hence are deployed seldomly [6]. The bifurcation of sensor impact across different weather periods (see Figure 14) showcases the lack of impact observed in peak weather situations, thereby making the FDD process difficult. Fouling of coils along with duct leakages are the hardest to detect amongst the considered list of faults. Either additional measurements or detection techniques that stretch beyond the utilized objective measurements are required for fault detection. Hence, these faults are not considered in this project.

Besides mass flow rate, impact that is lesser in magnitude is observed across temperature measurements such as temperature at cooling or heating coil air outlet. These measurements are therefore considered as additional operational state symptoms (ref section 2.2.2). This way the sensor impact analysis using a simulation model is not just helpful for prioritizing the sensors but also for systematically identifying the symptom nodes that can be included in a DBN. The utilized approach can further reduce the dependency on experts for realizing a DBN.

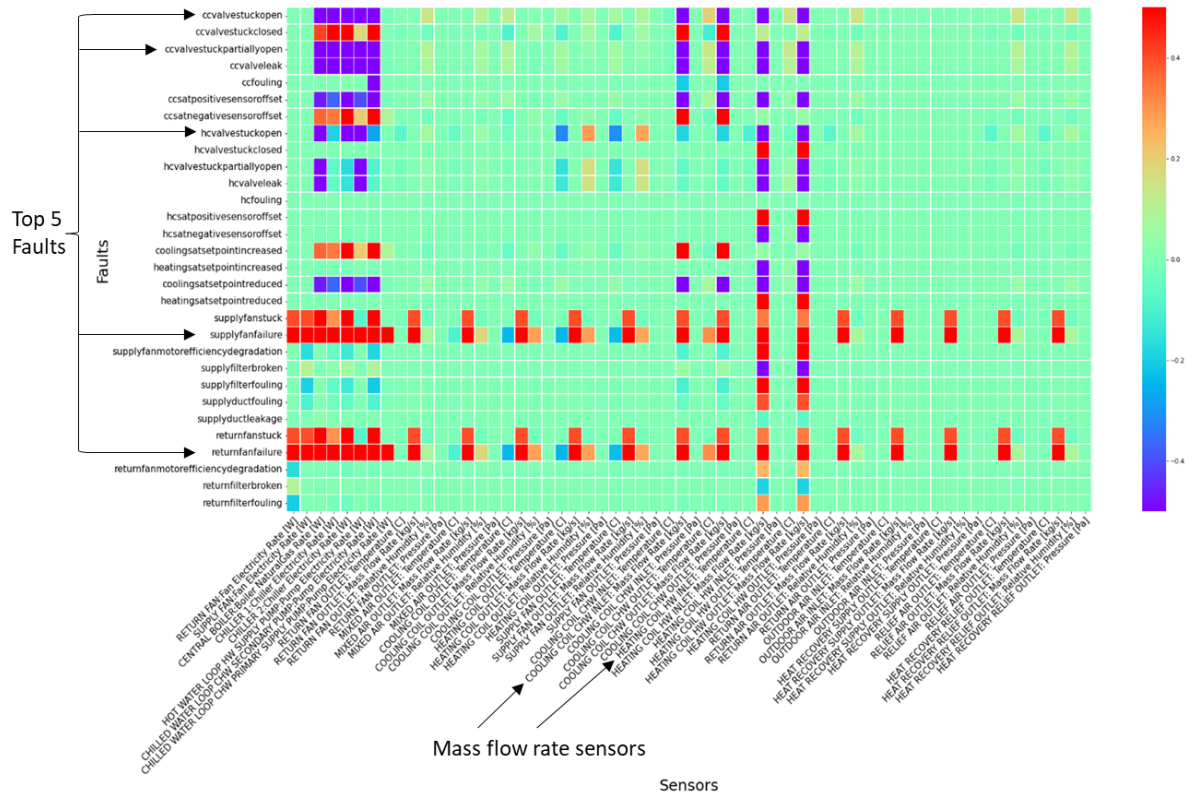


Figure 16: Sensor impact analysis – 5-zone building – Shoulder weather period

### 3.3 CONCLUSION – FAULT AND SENSOR IMPACT ANALYSIS

Using a fault and sensor impact analysis, the uncertainty associated with using data collected from building measurements is overcome. Through simulation models, faults such as stuck valve or fouling are modelled in an inexpensive way, which otherwise would have been too energy or labor intensive to study. Further, studying leakage fault in a real-system is nearly impossible as it can directly compromise occupant health. Of the list of 39 faults considered, a few vital faults are identified using the fault impact analysis. Similarly, using a sensor impact analysis from the possible list of 50 plus considered sensors, some key sensors are shortlisted.

Based on the systems analysis for AHU, following choices have been made for development of the AFDD tool:

- Control faults have been prioritized over component faults such as performance degradation. The prioritized list of faults includes stuck or leaking control valve, fouled duct, fouled or broken filter, stuck or complete fan failure, sensor offset and inappropriate supply air setpoints.
- Mass flow rate measurement along with some key temperature measurements (for example temperature after cooling/heating coil) are prioritized for developing the FDD strategy further.
- Of the four faults discussed in for the heat recovery wheel in APPENDIX B-Table 23, control faults including VFD bypass and control faults have been prioritized after consultation with stakeholders and project partner (System Air). Frosting fault has been excluded given availability of an override within BAS to tackle this. Fouling/Scaling fault has been deprioritized due to reasons discussed in section 3.2.2. Using the discussed simulation approach, leakage fault can be modelled, and an accurate diagnosis model can be prepared. This is recommended for future work.

### 3.4 FAULT DETECTION

For fault detection, a reference benchmark is obtained by training a model using historical data collected at the site. The trained model has then been utilized to compare the actual measurement with the predicted value to generate a residual. This process of fault detection is commonly referred to as regression-based approach [4] and is shown in Figure 17.

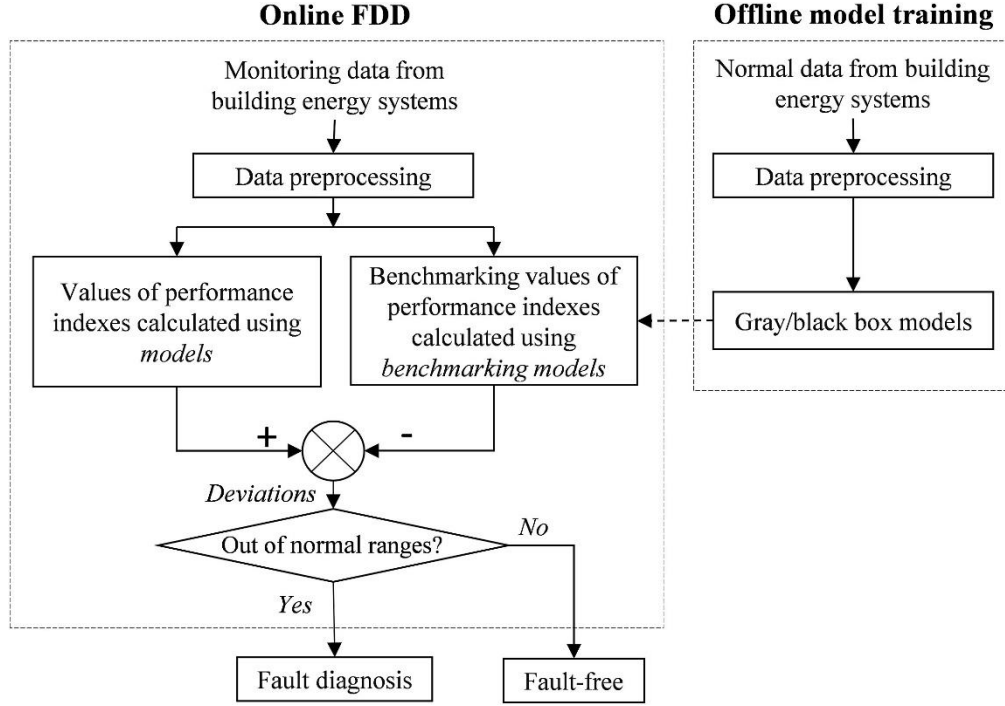


Figure 17: Regression-based fault detection [4]

In this project, XGBoost framework has been utilized in the offline model training process (see Figure 17) given its superior performance [28,29,82]. XGBoost is a scalable and end-to-end machine learning framework for boosted trees [55]. Its success is attributable to popular machine learning theory that multiple weak learners perform better than a single strong learner. In its implementation with decision trees, multiple simultaneous trees are populated much like random forest, and then the predictions from each of these trees are iteratively improved to minimize a loss function such as a squared-error loss or in other words mean squared error. The simplified version of objective function for the algorithm is shown in equation (1) [55].

$$\tilde{\mathcal{L}}^{(t)} = \sum_{i=1}^n [g_i f_t(x_i) + \frac{1}{2} h_i f_t^2(x_i)] + \Omega(f_t) \quad (1)$$

Here, the first term comprises of the first and second order gradient statistics or the gradient and the hessian of the convex loss function. The second term  $\Omega$  is the regularization parameter that penalizes the complexity of the model and helps with its generalization process. The XGBoost implementation allows for the objective function to be customized for different loss functions from its default squared loss error to log-loss or logistic in line with the learning objective. Further, to account for the bias-variance trade-off multiple hyperparameters have been provided to regularize the complexity of the model. The complete list of hyperparameters is provided in [83]. Typically, random or grid search methods are employed to find the best combination of hyperparameters. Despite their advantages, random or grid search methods are more intuition driven than model driven hence making the process of hyperparameter tuning less scalable. R. Shi et al. in [84] utilized a sequential model-based optimization (SMBO) that uses Bayesian optimization updates the hyperparameters in an informed manner. This makes the process more generalizable and less resource intensive. Model driven hyperparameter tuning process is utilized in this project.

For developing an accurate model, feature selection is of paramount importance. Using minimal features is key to preventing model from overfitting and reducing its complexity. To select relevant features for the model the adopted framework is shown in Figure 18. Besides, the available sensed information new features are engineered. Then, using an iterative process unimportant features are dropped. The process begins with a coarse feature selection [85]. In this step, multi-collinear features are filtered out using Pearson Correlation Coefficient (PCC) scores. It is followed by a wrapper-based feature selection method known as recursive feature elimination and cross validation (RFECV). This algorithm recursively eliminates features that carry less impact on the model performance measured using cross-validation [86]. The wrapper-based method follows the coarse feature

selection process as it is computationally expensive and compensates for the uncertainty associated with coarse method [85]. Lastly, Shapley additive explanations (SHAP) framework is invoked for dropping features further [87].

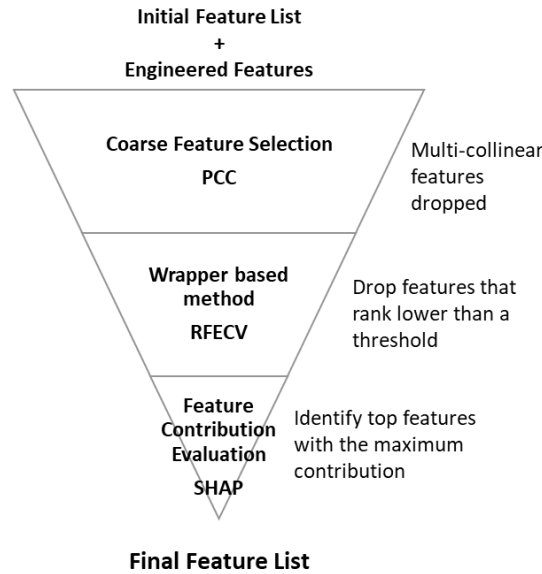


Figure 18: Feature selection framework

Black box models such XGBoost are often difficult to interpret due to the non-linear relationships explored within these models. SHAP is a game theory based explainable AI framework, that is helpful for interpreting a trained black-box model. Using SHAP, features that increase model complexity can be removed using an objective evaluation, which improves the model's reliability and generalizability. At its core, lie the shapley values which are an average of marginal contribution of all permutations of features/predictors supplied to a model. SHAP is an extension of shapley values that offers local as well global explanations for a predictor. This implies that each prediction made by the model can be individually interpreted, which makes this approach very powerful.

A baseline model is trained using the features selected with RFECV and multiple candidate models are trained by iteratively dropping features identified as less importance using SHAP. Candidate model with minimal possible but adequate number of features are selected to prevent uncertainty in sensor measurements from carrying into the inference process.

### 3.4.1 Valve position prediction model

In the sensor impact analysis discussed in section 3.2, it was identified that mass flow rate measurement can be utilized a key performance indicator for the considered faults. However, as identified in Table 10, mass flow rate is not a commonly deployed measurement in AHUs. This also holds true for the case studies considered, except Breda office where a mass flow rate sensor has been deployed as part of this project. To overcome this challenge and keep the FDD strategy generalizable, valve position has been utilized as a proxy for mass flow rate measurement. The relationship between the two variables is explained in APPENDIX B-Figure 44.

Using the discussed XGBoost framework, cooling and heating coil valve prediction models are prepared. For verification of the complete fault detection approach Energy Resource Station and Hoofddorp office case studies (see APPENDIX B) are utilized. The available datasets deployed at these sites have been partitioned to prepare training and test sets. The accuracy of the trained XGBoost models is quantified using the key performance indicators such as R2 Score, Mean Absolute Error (MAE), Root Mean Squared Error (RMSE) and Cross-Validation Root Mean Squared Error (CV-RMSE) and reported in Table 11 [29,81].

Table 11: Results from verification of trained XGBoost models for valve position prediction

Case-Study Building Name	Energy resource station	Hoofddorp office	Energy resource station	Hoofddorp office
Cooling/Heating Valve Position Prediction Model	Cooling Coil Valve Position Prediction	Heating Coil Valve Position Prediction	Heating Coil Valve Position Prediction	Heating Coil Valve Position Prediction
AHU Reference	AHU B	AHU 2	AHU B	AHU 2
Data Sampling frequency	1 min	8 mins	1 min	8 mins
# Training samples	8606	9190	10257	56095
# Test samples	2151	9190	2565	14024
Test Scores	R2 Score: 0.93 RMSE [%]: 2.89 CV-RMSE 0.06	R2 Score: 0.88 RMSE [%]: 6.79 CV-RMSE 0.08	R2 Score: 0.971 RMSE [%]: 0.643 CV-RMSE: 0.033	R2 Score: 0.902 RMSE [%]: 5.252 CV-RMSE: 0.221

As part of the ASHRAE's RP-1312A project, fault experiments were carried out over three seasonal periods between 2007-2008 at Energy resource station building [66,88,89]. Experiments carried out in summer of 2007 between August 19<sup>th</sup> and September 09<sup>th</sup> are utilized for verifying the complete fault detection process. Here, two Air-Handling Units (AHU-A&B) shown in APPENDIX B - Figure 47 were operated simultaneously, wherein AHU-B operated in normal condition whilst faults were introduced in AHU-A. Since, both AHUs supply conditioned air to identical thermal zones and are of the same capacity, learned parameters of XGBoost model trained for AHU-B transfer to AHU-A.

The residual between measured and predicted values is utilized to detect faults. Further, a threshold of  $\pm 10\%$  on 0-100% scale has been utilized. Since the fault labels are known apriori the detected fault label is compared with the true label and the results are plotted on a confusion matrix shown below in Figure 19. Setting the threshold at a high of  $\pm 10\%$  results in specificity exceeding 97%, however compromising the sensitivity of the detection algorithm. To balance this trade-off, threshold can be tuned by plotting a Receiver Operator Characteristics (ROC) curve as shown in APPENDIX A-Figure 56. To this end, a dynamic threshold setting method has also been explored and discussed in APPENDIX A. The dynamic threshold method showed encouraging results and has hence been recommended for future improvements over the fixed threshold method utilized in this project.

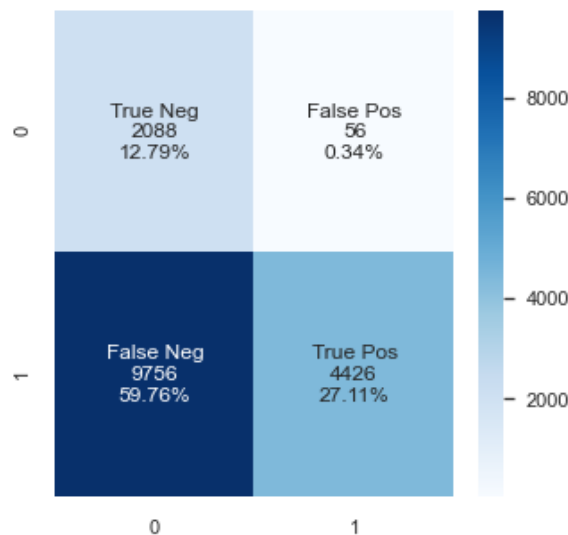


Figure 19: Confusion matrix for fault detection using the developed model

The introduced feature selection framework has been utilized for selecting the final list of features utilized for XGBoost model training. The features selected at each stage of the process are listed in Table 12. The last step of the feature selection process (see Figure 18) using SHAP is presented in APPENDIX A-Figure 58.

Table 12: Feature selection for Breda office: North zone cooling coil valve position prediction model

	#Features	Feature Names
AHU Features available from building automation system	19	Outside temperature (North East, South-West), Chiller leaving water temperature, Chiller entering water temperature, Chiller weighted leaving water temperature, Supply air temperature north, Calculated supply air temperature north, Calculated return air temperature north, Return air temperature north and canteen, Supply air temperature central AHU, Room temperature canteen, Relative humidity central AHU, Average static pressure supply air channel, Delta pressure over return air filter, Absolute humidity central AHU supply air, Supply fan speed, Return fan speed, Supply air setpoint,
Engineered Features	5	hour of day, day of week, day of year, week of year, month
Total Features	24	
Features dropped using PCC	1	Supply air temperature
Features Selected Using RFECV	-	None
Feature Selected Using SHAP	7	Supply air temperature (central AHU) Chiller entering water temperature Supply air temperature setpoint (Zone north) Supply air temperature setpoint (central AHU) Chiller leaving water temperature Supply air pressure Week of year
Final Features	7	Supply air temperature (central AHU) Chiller entering water temperature Supply air temperature setpoint (Zone north) Supply air temperature setpoint (central AHU) Chiller leaving water temperature Supply air pressure Week of year

Since, the developed fault detection models are trained with historical data there is a certain lead time before such models can be deployed in operation. To identify the lead time required for training such models, three cases namely Hoofddorp office, Breda office and Nijmegen office have been considered. Here, the models are iteratively trained with datasets partitioned over varying time horizons (month for Hoofddorp and Breda; weeks for Nijmegen). This variation is synonymous with the length of available dataset. For example, data from Hoofddorp building is available since 2011, and hence has been partitioned in months, whereas data from Nijmegen is only available since March 2020 and has been partitioned in weeks. Starting with dataset from first available time horizon, at each iteration the length of dataset utilized for training is increased by one. For instance, if dataset is partitioned in weeks, then first iteration involves training with dataset from first available week and second iteration involves training with data from first week and next available week. This way, it was identified that to train an accurate cooling coil valve position prediction models data from at least 20 weeks or nearly a complete cooling season in the Netherlands would be ideal. The results detailing these experiments are presented in APPENDIX A (Figure 59 and Figure 60).

Using the discussed XGBoost algorithm, cooling and heating valve position models are trained for Breda office and Nijmegen school. The scores of these models on the performance indicators discussed previously are tabulated in Table 13. Between the heating and cooling valve position prediction models, it can be observed that heating coil valve position prediction models have better performance scores. Given this better fit and higher accuracy, these models can be utilized with lower thresholds for fault detection and hence are useful for identifying faults with lower severity. On the CV-RMSE indicator scores of all trained models is less than 0.3, and hence it can be said that they are useful for engineering applications and are proceeded with further for fault diagnosis[29].

Table 13: Accuracy metrics for the trained ML models for heating and cooling valve prediction

Model	Site	AHU	Key Performance Indicator	Score
Cooling Coil Valve Position	Breda office	North Zone Cooling Coil	R2 Score	0.94
			MAE [%]	2.63
			RMSE [%]	4.86
			CV-RMSE	0.11
	Nijmegen school	AHU One	R2 Score	0.98
			MAE [%]	2.65
			RMSE [%]	4.25
			CV-RMSE	0.09
Heating Coil Valve Position	Breda office	Central AHU Heating Coil	R2 Score	0.99
			MAE [%]	0.98
			RMSE [%]	2.18
			CV-RMSE	0.05
	Nijmegen school	AHU One	R2 Score	0.99
			MAE [%]	0.91
			RMSE [%]	1.72
			CV-RMSE	0.02

### 3.4.2 HRW supply temperature and relative humidity prediction models

To measure the effectiveness of heat exchange process, several key performance indicators (KPIs) such as effectiveness measured for latent, sensible, enthalpy exchange or number of thermal units (NTUs), moisture removal rate (MRC), dehumidification coefficient of performance (DCOP) have been utilized in literature. These KPIs have been summarized in Table 14. KPIs such as MRC, and DCOP are more relevant for desiccant type wheels, whilst KPIs such as effectiveness or UA (conductance area) are indicative of fouling/scaling of heat recovery wheels. Therefore, given the type of heat wheel, its KPIs can be set and continuously monitored for tracking its performance. Theoretically, each of these KPIs can be utilized in the fault detection process. In Table 14, these KPIs are further classified using the symptom classification approach proposed in the 4S3F framework.

Table 14: Key performance indicators – Rotary heat exchanger

#	KPI	Symptom classification as per 4S3F	Reference
1	Effectiveness (T/Rh/Enthalpy) *	Balance symptoms	[90–99]
2	NTU	Balance symptoms	[99]
3	Conductance-area product (UA) *	Balance symptoms	[100]
4	Temperature difference / LMTD *	Balance symptoms	[100]
5	Heat transfer rate *	Balance symptoms	[100]
6	Frost formation boundary/Absolute Humidity	Operation State symptoms	[101]
7	Moisture removal capacity (MRC) **	Balance symptoms	[94,102]
8	Dehumidification coefficient of performance (DCOP) **	Energy Performance symptom	[102]

\* FDI – Fouling Detection Indicator

\*\* Relevant for desiccant HRWs

To model the HRWs, white and black box approaches have been utilized. These approaches have been summarized in APPENDIX A-Table 34. White box approaches typically range from reduced to complex numerical models that focus on emulating the heat transfer character within some constraints. This is a key limitation of this approach as the resulting model is either too specific (to its geometric construction or desiccant properties) to the underlying system or can only predict its behaviour in a narrow operational range. Black-box models on the other hand can overcome these issues, however, require training datasets and are often difficult to interpret. Black-based models have been successfully utilized for modelling HRWs (ref APPENDIX A-Table 34). Most of these models try to predict the temperature and/or relative humidity at the supply side outlet of the HRW. Madhikermi et al. in [103] compared neural networks and support vector machines for fault detection in HRWs and explained their black-box model with framework called LIME (an alternative to SHAP utilized in this project).

Using the XGBoost framework introduced, temperature and relative humidity at the supply outlet of HRW are predicted for AHU One at Nijmegen school (ref section 2.3.2). These models are prepared using measured air temperature and relative humidity in the suction, supply and return streams along with air velocity measurements. The SHAP contributions of the various features utilized for Temp prediction model is shown in Figure 20. Using these SHAP values it can be said that for the trained model contribution of return temperature and suction air temperature is considerably higher than other features, which is expected given the energy balance equation (2). The impact of return air temperature is explored further and the dependence of the model on this feature is plotted on Figure 21

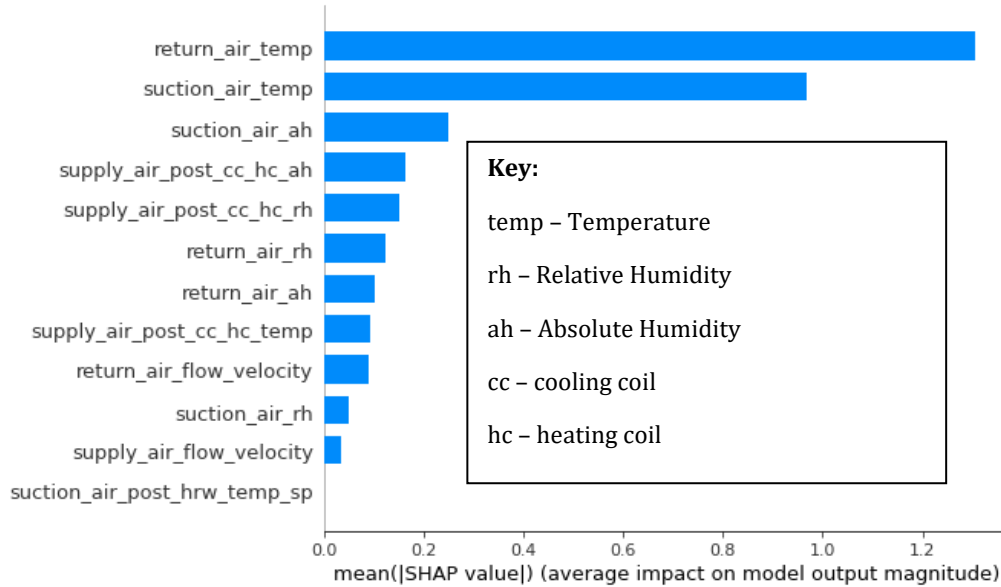


Figure 20: Feature impact for predicted suction air post HRW temperature computed using SHAP for AHU One

In Figure 21, the dependence of predicted suction air post HRW is explained with return air temperature. On the secondary Y-axis SHAP automatically selects the feature that carries highest correlation with the independent feature. Expectedly, as the return air temperature increases so does the supply air temperature. This way the opaqueness of the trained XGBoost model can be reduced, and the dependence of the model on its features can be studied in detail. Also, the most important features (see Figure 20) can be tracked for issues such as drift to ensure the predictions made using such a model are correct. This is discussed further in APPENDIX E.

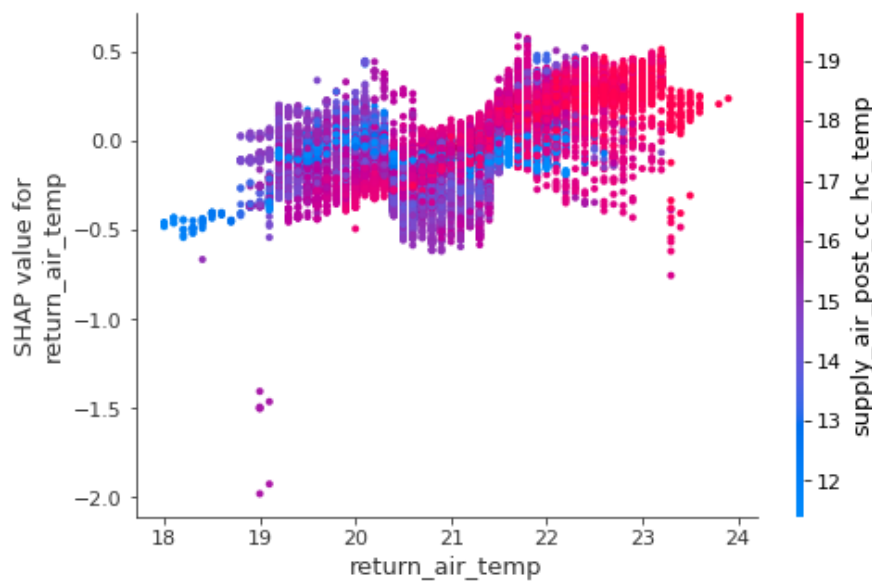


Figure 21: Explainability of black-box model using SHAP – Dependence of predicted suction air post HRW on return air temperature

In line with the discretization strategy discussed previously, separate black-box models have been developed for heating and cooling mode operation of the AHU. Outdoor temperatures less than 18°C and complete range of HRW control have been considered for heating mode operation. The complete rules utilized for determining the operation modes are provided in APPENDIX A. Model features and targets are split in 80:20 ratio for training and testing purpose. From the suction air and return air streams conditions shown in Figure 22, it can be observed that a wide DBT operation has been considered for testing the model.

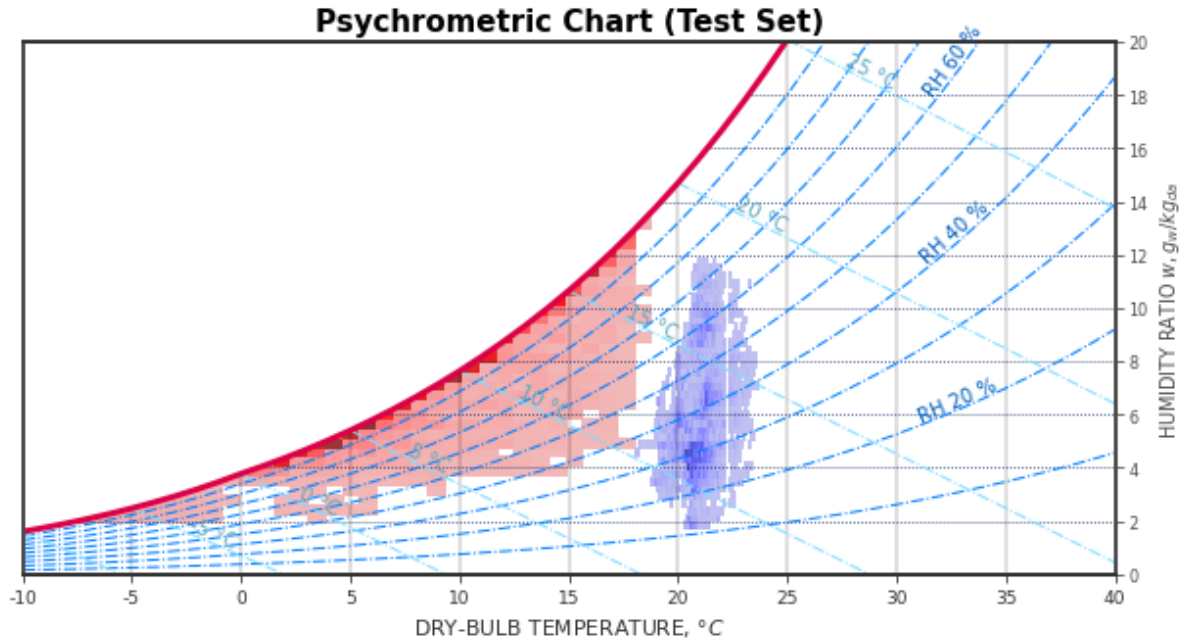


Figure 22: Dataset utilized for testing the HRW temperature and relative humidity prediction models for heating mode operation of AHU one (supply air condition indicated in red and return air condition indicated with purple)

The results from testing the model performance are summarized in Table 15. Using the discussed approach models have been trained for AHU One deployed at Nijmegen school and Breda office. The performance of these models on the selected performance indicators is tabulated in Table 15 for comparison. It can be observed that highly accurate models that can explain more than 93% variability in the test sets are trained. On comparing the models, it is observed that model trained for Breda office are slightly less accurate than model for Nijmegen school. At Breda office new sensors were proposed during the project and were installed in February 2022. Therefore, these models could only be trained with very limited data. Despite this limitation, the models are accurate enough to distinguish between faulty and normal operation as observable in APPENDIX A-Figure 69. Further, using the CV-RMSE indicator, these models have been found useful. Although, the usefulness of these models for fault detection needs to be ascertained and is discussed next.

Table 15: Fault detection models trained for HRW supply temperature, relative humidity prediction

Model	Site	AHU	Key Performance Indicator	Score
Supply Temperature Prediction	Nijmegen school	AHU One	R2 Score	0.98
			MAE [°C]	0.18
			RMSE [°C]	0.35
			CV-RMSE	0.02
	Breda office	Central AHU	R2 Score	0.96
			MAE [°C]	0.41
			RMSE [°C]	0.80
			CV-RMSE	0.04
Supply Rh prediction	Nijmegen school	AHU One	R2 Score	0.99
			MAE [%]	0.95
			RMSE [%]	1.54
			CV-RMSE	0.03
	Breda office	Central AHU	R2 Score	0.93

			MAE [%]	0.98
			RMSE [%]	2.53
			CV-RMSE	0.09

The usefulness of the developed models for fault detection is understood by understanding their ability to generate an analytical symptom (ref section 1.1). This ability to generate symptoms is determined visually by observing the mean and variance spread of the residual generated using these models. In Figure 23, impact on multiple possible symptoms such as residuals between predicted and measured temperature (temp\_residual) and relative humidity (rh\_residual); residual between measured temperature and its setpoint at HRW supply outlet (temp\_sp\_residual); temperature (temp\_eff) and humidity efficiencies (moist\_eff) discussed in Table 14 are presented. Two control faults (ref APPENDIX B-Table 23) a) HRW failure and b) HRW operated with bypassed rotational control have been introduced. Details for these faults are provided in APPENDIX A-Table 35. In Figure 23, upon comparing data from faulty (indicated with maroon) and fault free operation (indicated with peach) residuals generated using the developed prediction models are clearly distinguishable and can be isolated. Further, as anticipated the two control fault events generate residuals that are centred on either side of mean residual. This information is helpful towards setting rules for fault diagnosis. Impact of faults is also observable on the utilized HRW KPIs, and hence these are included in the application (ref section 4.2.1).

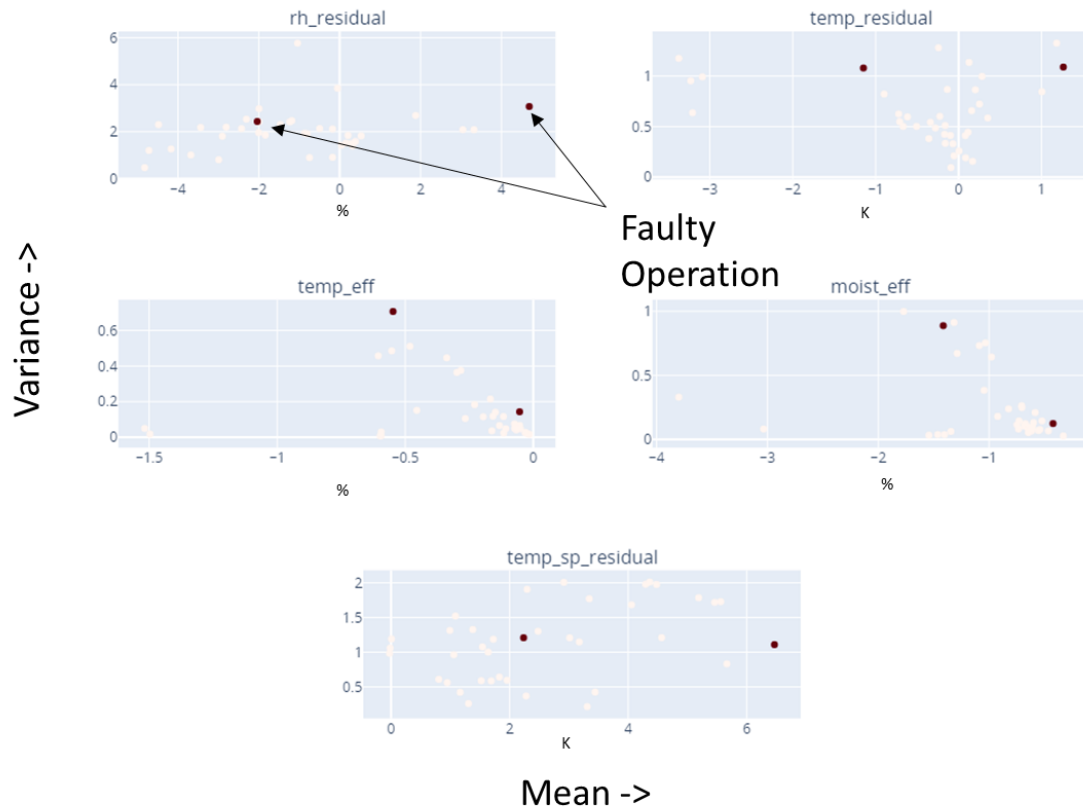


Figure 23: Symptom impact analysis for Nijmegen school: Operation of Heat Recovery wheel during heating mode

### 3.5 FAULT DIAGNOSIS

Using the introduced 4S3F framework, the developed DBN models evolve from the P&I diagram. Further, the development of DBNs for the AHU has been discretized. It implies that separate DBNs have been prepared for cooling and heating mode operation of the AHU. These DBNs are then activated using the control strategy deployed at the AHU (ref section 2.3). In this section the developed DBN models for the two validation cases are first described and then results from their experimental validation are presented. In section 3.5.1, the DBNs for cooling mode operation of the considered AHU cases are discussed, whilst section 3.5.2 contains description and

validation of DBNs for heating mode operation. In section 3.5.3, DBN utilized for diagnosis of HRW faults is presented.

### 3.5.1 Cooling mode operation

The P&I diagram for the zone North & Canteen of Breda office is shown in Figure 12: P&ID Breda office – central AHU and North zone. The DBN model that emanates from this P&I diagram is shown in Figure 24. In this figure, the fault nodes are depicted in purple, wherein the Airflow fault node is an abstraction for upstream air side faults in components such as ducts, fans, or filters that can alter the supplied airflow to the zone. Reduced supply air temperature (SAT) and cooling coil valve (CCV) Stuck nodes depict reduced setpoint and cooling coil control valve stuck faults respectively. Airflow fault node and CCV Stuck fault nodes encapsulate three fault scenarios that are higher and lower than desired condition or fault-free condition. Whereas Reduced SAT node encapsulates only two fault scenarios namely fault present or fault-free. The higher and lower fault conditions is additional information that further describes the fault present condition and is helpful for building manager in understanding the impact of the fault.

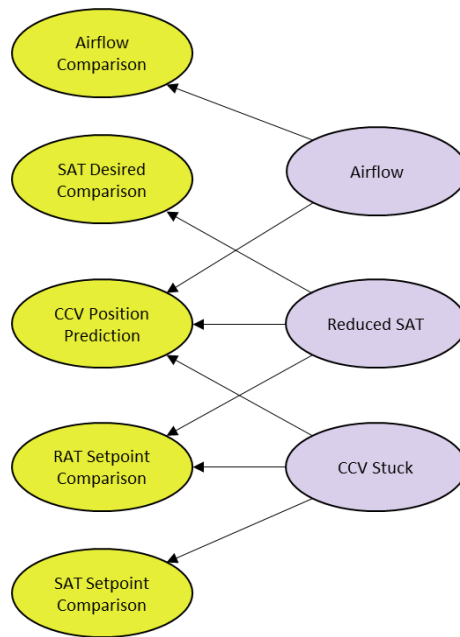


Figure 24: DBN for cooling mode operation – North & Canteen zone at Breda office

The symptom nodes are generated using a combination of multiple modelling approaches. The rules for passing evidence to the symptom nodes are provided in Table 16. The airflow comparison node and CCV prediction nodes are activated using predictions from a statistical model and machine learning model respectively. Here, the airflow prediction is made using an exponentially weighted moving average (EWMA) model [104]. The EWMA model predicts the air velocity based on a historical moving average and is tuned to identify abrupt variations in airflow. A moving average prediction is utilized in comparison with design airflow condition, as air flow in nearby Zone 105 is modulated to meet a CO<sub>2</sub> setpoint and hence the usual constant air volume supplied to the zone varies in magnitude. For predicting the cooling coil valve position the discussed XGBoost model (ref section 3.4.1) has been utilized.

Table 16: Symptom Nodes description for cooling mode DBN – Breda office

#	Symptom Node	Symptom State	Rules for setting the state
1	Airflow Comparison	High	$F_{act} - F_{pred} > \Theta$
		Low	$F_{act} - F_{pred} < -\Theta$
		Fault-free	$F_{act} - F_{pred} \leq \Theta$
2	SAT Desired Comparison	Negative	$T_{set} - T_{set,des} < -\Theta$
		Fault-free	$T_{set} - T_{set,des} \leq \Theta$
3	CCV Prediction	Positive	$X_{ccv} - X_{ccv,pred} > \Theta$
		Negative	$X_{ccv} - X_{ccv,pred} < -\Theta$
		Fault-free	$X_{ccv} - X_{ccv,pred} \leq \Theta$

#	Symptom Node	Symptom State	Rules for setting the state
4	RAT Setpoint Comparison	Positive	$T_{ra}-T_{ra,set}>\Theta$
		Negative	$T_{ra}-T_{ra,set}<-\Theta$
		Fault-free	$T_{ra}-T_{ra,set}\leq\Theta$
5	SAT Setpoint Comparison	Positive	$T_{sa}-T_{sa,set}>\Theta$
		Negative	$T_{sa}-T_{sa,set}<-\Theta$
		Fault-free	$T_{sa}-T_{sa,set}\leq\Theta$

**Key:** **F** - Flow Rate in m<sup>3</sup>/s, **T** - Temperature in °C, **X** - Control Position in %, **Θ** - Threshold, **act** - Actual, **pred** - Predicted, **ccv** - Cooling coil valve, **des** - Desired, **sa** - Supply air, **ra** - Return air, **set** - Setpoint

For experimental validation of the developed diagnosis model, several experiments were carried out wherein faults were artificially introduced. Faults shown in DBN (see Figure 24) were introduced between 23<sup>rd</sup> June 2021 and 20<sup>th</sup> August 2021. The chronology of these experiments is provided in APPENDIX A-Table 27. Besides introducing different faults, same faults with varying severities are also introduced to understand precision of the diagnosis approach.

On 16<sup>th</sup> July 2021, an experiment was carried out and a stuck valve fault was introduced in the north zone cooling coil at Breda. The position of the three-way control valve that regulates the flow was fixed at 75% at 15:30 in the afternoon using a BMS override. It can be observed from Figure 25 that the predicted valve position deviates significantly from the measured actual valve position post introduction of this fault and generates a residual exceeding +30%. This activates the CCV Prediction node and SAT Setpoint Comparison nodes (see Table 16). Consequently, the probability measure of the fault state (Positive Stuck) changes from a low (<5%) to a high likelihood (~70%) of fault presence.

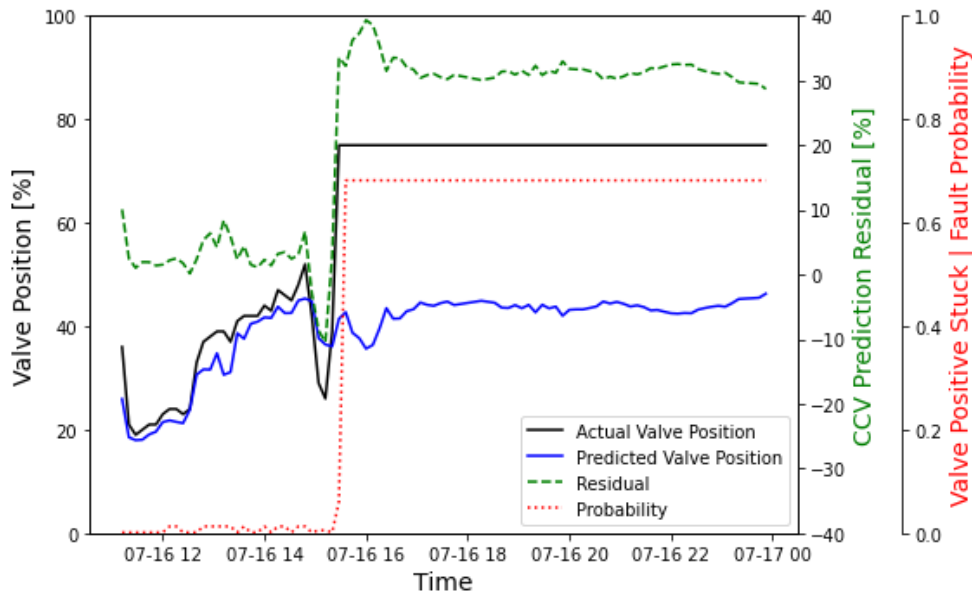


Figure 25: Stuck valve fault experiment at Breda office on 16th July 2021

The computed posterior probabilities for all introduced faults at various severities are summarized in Table 17. It can be observed that across multiple severity scenarios' fault presence is successfully diagnosed.

Table 17: Computed posterior probability using DBN model developed for Breda office

Fault	Severity	Computed Posterior Probability
Stuck Valve	Stuck at 50% open	0.68
	Stuck at 75% open	0.68
Reduced SAT	16°C	0.88
	17°C	0.88
Lower Airflow	60% of maximum speed*	0.93
	70% of maximum speed*	0.93
Higher Airflow	100% of maximum speed*	0.93

\*Typically, the fan operates at 85% of maximum speed

The long-term operational performance of the developed DBN (see Figure 24) along with the contributing fault detection models have been tested over an experimental period between 23rd June 2021 and 20th August 2021. During this period a mix of fault and fault-free days (on days no fault experiment is carried out) are considered. The confusion matrix in Figure 26 showcases the accuracy and robustness of the developed fault diagnosis strategy.

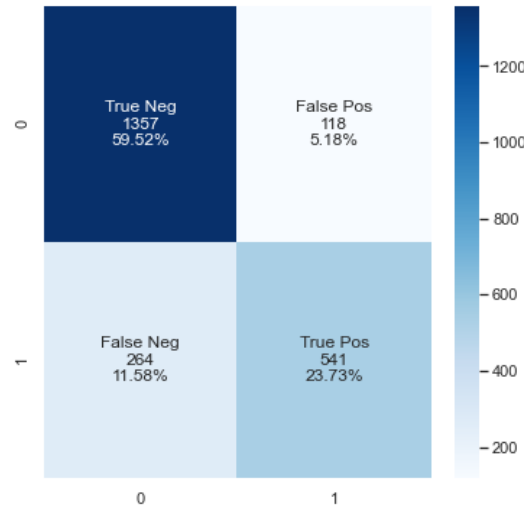


Figure 26: Experimental validation - Confusion Matrix – North and Canteen zone at Breda office - Cooling mode operation

Based on the number of true/false positive and negatives recorded, some KPIs that quantitatively indicate performance of the developed FDD business layer are computed [105]. Precision, Recall/Sensitivity, and Specificity are indicative of the quality of diagnosis, whilst labelling accuracy is indicative of the overall diagnosis accuracy. The formulas for computing these metrics are provided in APPENDIX A. Labelling Accuracy implies if the diagnosed label and the true label are the same. Sensitivity and Specificity are frequently utilized in medical diagnosis to compare quality of tests [106].

Table 18: Experimental validation of developed DBN models for cooling mode operation

Case Study	Period	Results	
Breda Office	23 <sup>rd</sup> June 2021 to 20 <sup>th</sup> August 2021	<b>Precision</b>	82.1%
		<b>Recall/Sensitivity</b>	67.2%
		<b>Specificity</b>	92.0%
		<b>Labelling Accuracy</b>	83.2%
Nijmegen school	01 <sup>st</sup> July 2020 and 31 <sup>st</sup> August 2020	<b>Precision</b>	83.3%
		<b>Recall/Sensitivity</b>	84.5%
		<b>Specificity</b>	94.5%
		<b>Labelling Accuracy</b>	92.1%

Using similar approach as adopted for Breda office, experimental validation of the diagnosis model developed for Nijmegen school is carried out. The developed DBN model and detailed results for Nijmegen school are provided in APPENDIX A. The computed performance indicators for both Breda office and Nijmegen school are tabulated in Table 18. Comparing the two outcomes, a high diagnosis specificity exceeding 90% is realized over a long-term testing period spanning nearly 2 months. A sensitivity of nearly 85% is realized with the DBN model deployed at Nijmegen, whilst the DBN model for Breda office is tuned to realize a high specificity. It should be noted though that the DBN model at Breda is exposed to varying fault conditions (ref APPENDIX A-Table 27) in comparison with Nijmegen school. Despite the lower sensitivity, the DBN model at Breda office can successfully identify all fault conditions although with a time delay. This delay is a consequence of the utilized fixed thresholds in the fault detection process. This can be addressed if required by using dynamic thresholds for early detection (ref APPENDIX A). The traded-off sensitivity is accepted since it's found high enough to diagnose the faults considered. Further, the high specificity addresses a key concern of building managers regarding reliability of the FDD system (see Table 3). Further, a positively diagnosed condition in a test with high specificity is helpful

in ruling in the disease. It implies that a positive diagnosis of fault with the algorithm would impute a very high confidence in fault presence, thereby warranting corrective action to prevent energy waste.

### 3.5.2 Heating mode operation

The heating mode operation for the AHU is its sequence of operation wherein supply air is heated by pumping hot water through the heating coil to meet the desired supply temperature. The rules for filtering this sequence of operation along with the rules utilized for cooling operation are provided in APPENDIX A. The P&I diagram for central AHU deployed at Breda office is shown in APPENDIX B-Figure 48. Using this P&I, the developed DBN model is shown in Figure 27. In comparison with the DBN for cooling mode operation, a single DBN model is developed as opposed to discretized DBNs for each of the zones. This is since discretization doesn't offer any advantage in this case.

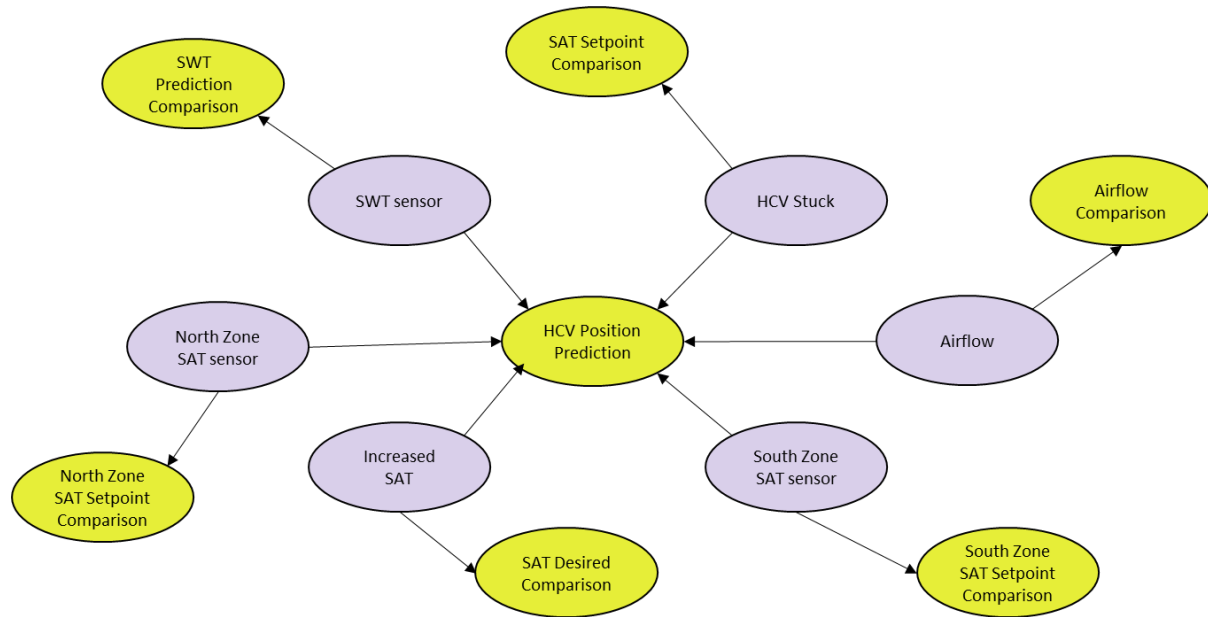


Figure 27: DBN for heating mode operation - Breda office

As with the DBN shown in Figure 24, Airflow fault node is an abstraction for the air side faults in components such as ducts, fans, or filters that can alter the supplied airflow. Increased supply air temperature (SAT) and heating coil valve (HCV) Stuck nodes depict increased setpoint and heating coil control valve stuck faults respectively. For the heating mode operation prioritized sensor faults (see APPENDIX B-Figure 55) such as SAT sensors deployed in North & South Zones and supply water temperature (SWT) sensor faults are also included. Except Increased SAT node, all other fault nodes encapsulate three fault scenarios that are higher or lower than desired condition or fault-free condition. Increased SAT node encapsulates only two fault scenarios namely fault present or fault-free. The higher and lower fault states provide additional information on the fault present condition.

The symptom nodes for the DBN are generated using a combination of modelling approaches. The rules for passing evidence to the symptom nodes are provided in Table 19Table 16. The airflow comparison node and HCV prediction nodes are activated using predictions from a statistical model and machine learning model respectively. For predicting the heating coil valve (HCV) position the discussed XGBoost model (ref section 3.4.1) has been utilized. For each of the fault node, HCV position prediction is the common symptom node, whilst an additional node symptom node that compares the measured value against its controlled reference is considered. Through data analysis it was noted that comparison of supply water temperature node with its setpoint was not sufficient for generating residuals, given the available tolerance in its PID control. Therefore, a supply water temperature prediction has been generated using an XGBoost model, that approximates the master slave relationship between the valve position and supply water temperature (ref section 2.3.2 for details on control strategy). The noisy max simplification discussed in section 2.2.2, is utilized for HCV position prediction node given it carries multiple parent nodes. Otherwise, it would have been nearly impossible to compute the complete marginal over this distribution.

Table 19: Symptom Nodes description for heating mode DBN – Breda office

#	Symptom Node	Symptom State	Rules for setting the state
1	Airflow Comparison	High	$F_{act}-F_{pred} > \Theta$
		Low	$F_{act}-F_{pred} < -\Theta$
		Fault-free	$F_{act}-F_{pred} \leq \Theta$
2	SAT Desired Comparison	Positive	$T_{set}-T_{set,des} > \Theta$
		Negative	$T_{set}-T_{set,des} < -\Theta$
		Fault-free	$T_{set}-T_{set,des} \leq \Theta$
3	HCV Position Prediction	Positive	$X_{hcv}-X_{hcv,pred} > \Theta$
		Negative	$X_{hcv}-X_{hcv,pred} < -\Theta$
		Fault-free	$X_{hcv}-X_{hcv,pred} \leq \Theta$
4	SWT Prediction Comparison	Positive	$T_{sw}-T_{sw,pred} > \Theta$
		Negative	$T_{sw}-T_{sw,pred} < -\Theta$
		Fault-free	$T_{sw}-T_{sw,pred} \leq \Theta$
5	SAT Setpoint Comparison	Positive	$T_{sa}-T_{sa,set} > \Theta$
		Negative	$T_{sa}-T_{sa,set} < -\Theta$
		Fault-free	$T_{sa}-T_{sa,set} \leq \Theta$
6	North Zone SAT Setpoint Comparison	Positive	$T_{nsa}-T_{nsa,set} > \Theta$
		Negative	$T_{nsa}-T_{nsa,set} < -\Theta$
		Fault-free	$T_{nsa}-T_{nsa,set} \leq \Theta$
7	South Zone SAT Setpoint Comparison	Positive	$T_{ssa}-T_{ssa,set} > \Theta$
		Negative	$T_{ssa}-T_{ssa,set} < -\Theta$
		Fault-free	$T_{ssa}-T_{ssa,set} \leq \Theta$

**Key:** **F** - Flow Rate in m<sup>3</sup>/s, **T** - Temperature in °C, **X** - Control Position in %, **Θ** - Threshold, **act** - Actual, **pred** - Predicted, **hcv** - Heating coil valve, **des** - Desired, **sw** - Supply water **sa** - Supply air, **ra** - Return air, **set** - Setpoint, **ssa** - South Supply air, **nsa** - North Supply air

For experimental validation of the developed diagnosis model, several experiments were carried out wherein faults were artificially introduced. Faults shown in DBN (see Figure 27) were introduced between 18<sup>th</sup> October 2021 and 09<sup>th</sup> December 2021. The chronology of these experiments is provided in APPENDIX A.

To understand the long-term performance of the developed model, a period between 15<sup>th</sup> October 2021 and 31<sup>st</sup> December 2021 is considered. The confusion matrix shown in Figure 28 showcases the accuracy and robustness of the developed fault diagnosis strategy.

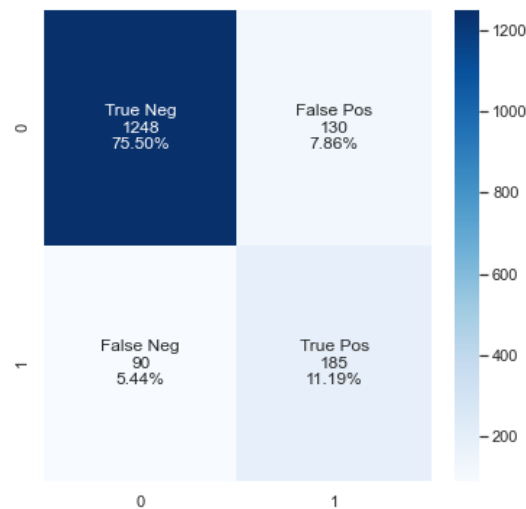


Figure 28: Experimental validation - Confusion Matrix - Breda office - Heating mode operation

Using similar approach as Breda office, experimental validation has been carried out at Nijmegen school. The results for this are provided in 84APPENDIX A. The computed performance indicators for both Breda office and Nijmegen school for heating mode operation are tabulated in Table 20. As with cooling mode operation the

diagnosis specificity has been traded off with its sensitivity to reduce the number of false positives and a highly specific (>90%) model has been developed. The precision in the case of Nijmegen school is lower given the imbalance of positive and negative labels in the considered datasets. Only 1% of all the considered samples belong to faulty operation or in other words are true positive samples. In both cases, it has been observed that a lot of false positives are encountered during system start-up. To address this issue, an additional fault confirmation layer has been programmed, that counts a positive diagnosis only when three consecutive positive results are obtained. As samples in the CMS are collected every 8 minutes, this implies that fault condition is confirmed as positive only if it persists for 20 minutes or more.

Table 20: Experimental validation of developed DBN models for heating mode operation

Case Study	Period	Results	
Breda Office	15 <sup>th</sup> October 2021 to 31 <sup>st</sup> December 2021	<b>Precision</b>	58.7%
		<b>Recall/Sensitivity</b>	67.3%
		<b>Specificity</b>	90.5%
		<b>Labelling Accuracy</b>	86.7%
Nijmegen school	01 <sup>st</sup> July 2020 and 31 <sup>st</sup> August 2020	<b>Precision</b>	31.6%
		<b>Recall/Sensitivity</b>	66.7%
		<b>Specificity</b>	98.4%
		<b>Labelling Accuracy</b>	98.0%

A robust diagnosis strategy would involve not only identification of faulty operation but also ability to isolate the faults from each other. To this end, the isolability of the diagnosis algorithm has been assessed and summarized in plot shown in Figure 29. Viewing across the diagonal from the bottom right, it can be observed that nearly all faults are successfully isolated and labelled correctly. In percentage terms, Airflow fault is misdiagnosed as fault free most often. This is since, the fault uses an EWMA model, that has been tuned for early diagnosis which is acceptable. The increased SAT fault exhibits similar symptoms are SWT sensor fault and hence, there it is sometimes misdiagnosed as SWT sensor fault. Under such an event, knowledge of the building engineer can be utilized by providing probabilistic outcomes and evidence of both faults. The true negatives are mostly encountered after fault has developed and persists in the system. To overcome such situation early diagnosis and early correction is recommended.

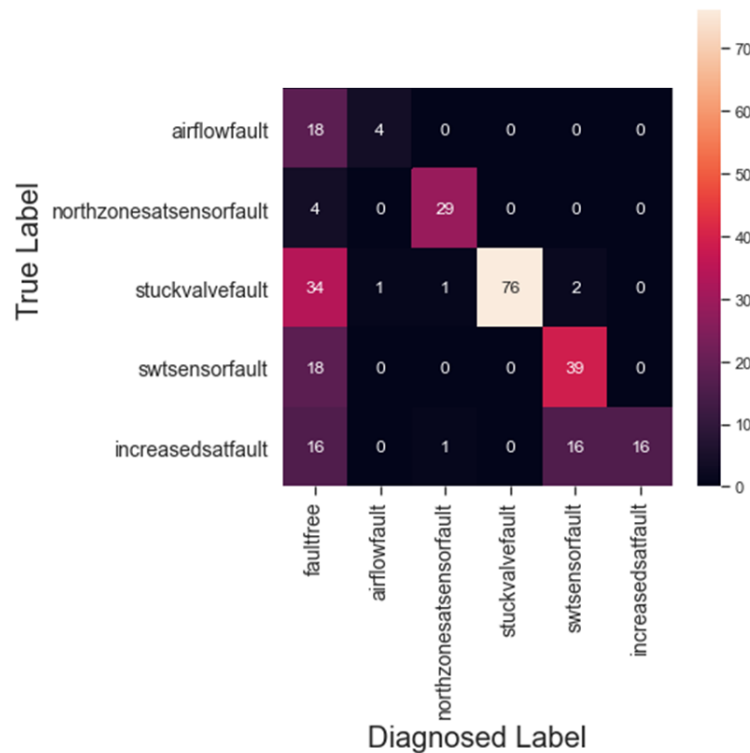


Figure 29: Isolability of the DBN model developed for Breda office's heating mode operation

### 3.5.3 Heat Recovery Wheel

Despite there being some research towards fault detection of HRWs [107], there are no demonstrable literature examples for fault diagnosis of HRWs. Through, this project a first model for HRW control fault diagnosis has been developed using the energy balance symptoms (ref section 2.2.2) of the 4S3F framework. The temperature and relative humidity prediction models discussed in section 3.4.2, are considered as energy balance symptom nodes of the DBN shown in Figure 30.

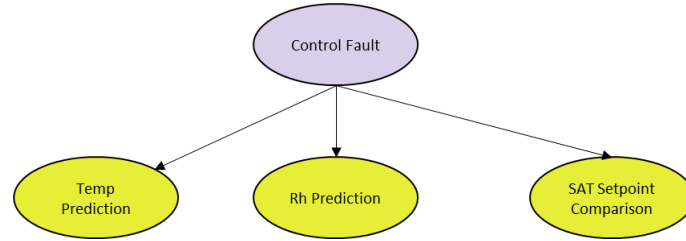


Figure 30: DBN for HRW - Nijmegen school

In the shown DBN for Nijmegen school (see Figure 30) besides the balance symptoms an additional operational state symptom node in SAT setpoint comparison has been included that measures the deviation of suction air temperature post HRW from its setpoint. Rules for generating symptoms through these nodes are tabulated in Table 21. Discretized symptoms such as positive, negative, or fault-free are generated using set thresholds determined through experiments.

Table 21: Symptom node description for HRW DBN – Nijmegen school

#	Symptom Node	Symptom State	Rules for setting the state
1	Relative Humidity Prediction	Positive	$Rh_{act} - Rh_{pred} > \Theta$
		Negative	$Rh_{act} - Rh_{pred} < -\Theta$
		Fault-free	$Rh_{act} - Rh_{pred} \leq \Theta$
2	Temperature (Temp) Prediction	Positive	$T_{act} - T_{pred} > \Theta$
		Negative	$T_{act} - T_{pred} < -\Theta$
		Fault-free	$T_{act} - T_{pred} \leq \Theta$
3	SAT Setpoint Comparison	Positive	$T_{act} - T_{set} > \Theta$
		Negative	$T_{act} - T_{set} < -\Theta$
		Fault-free	$T_{act} - T_{set} \leq \Theta$

**Key:** Rh - Relative Humidity in %, T - Temperature in °C,  $\Theta$  - Threshold, **act** - Actual, **pred** - Predicted, **set** - Setpoint

For validation of the developed diagnosis model, fault experiments are carried out at Nijmegen school on two days in March 2022. The chronology of these experiments is provided in APPENDIX A-Table 35. The diagnosis ability of the developed model is tested with data collected over 20 days, and its performance is shown on a confusion matrix (see Figure 31).

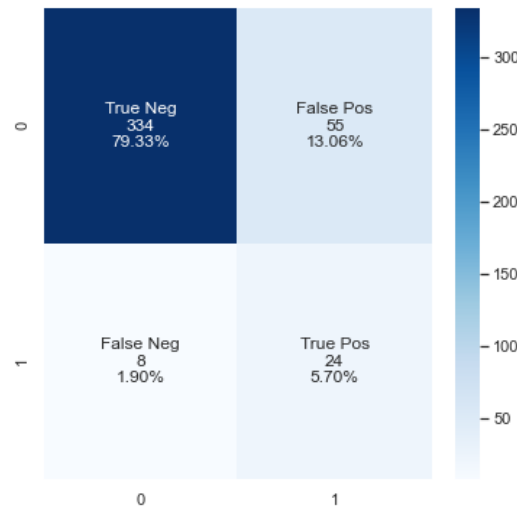


Figure 31: Confusion matrix - DBN HRW experimental validation

Observing the overall accuracy of diagnosis summarized in Table 22, it is observed that the developed model is quite sensitive towards identifying the fault sample, and yet retains its specificity (~86%). Some of the model's sensitivity is traded off for higher specificity by limiting the analysis to only period between 08:00-18:00, as operation periods outside these hours at the building are found erratic. Also, as with heating mode operation a positive sample is confirmed positive if the diagnosis algorithm concludes a positive diagnosis on two consecutive occasions. Its low precision is attributable to lower number of positive samples considered on the test, and its labelling accuracy is found sufficient. Further, the developed model not only identifies the fault presence with a good sensitivity but is also able to correctly isolate the underlying fault condition on both days system operated under faulty condition.

Table 22: Experimental validation of developed DBN model for heat recovery wheel

Nijmegen school	10 <sup>th</sup> March 2022 and 31 <sup>st</sup> March 2022	<b>Precision</b>	30.4%
		<b>Recall/Sensitivity</b>	75.0%
		<b>Specificity</b>	85.9%
		<b>Labelling Accuracy</b>	85.0%

### 3.6 CONCLUSION

The proposed FDD business layer scheme is congruent with the requirements identified in section 2.1.3 and is highly scalable and flexible. The developed fault detection models are very accurate (explain >90% of variability in the datasets) and have been found useful towards generating fault symptoms. The features utilized for training these models are iteratively identified using the demonstrated feature selection process. The lead time associated with deploying such models is a key consideration and needs further exploration. However, such black box models have been found useful in filling gaps associated with lack of sensors. For example, for the heating mode operation of Breda office and Nijmegen school supply water temperature and supply air temperature prediction models are prepared using just a single measurement. Otherwise making an accurate prediction using a first principles approach would have been quite cumbersome. Further, the models developed for HRW can predict over its complete control range (0%-100%), which is seldom done in literature.

Upon experimentally validating the developed diagnosis models, encouraging results with diagnosis specificity exceeding 90% across two different non-residential buildings with different HVAC schemes are obtained. Using the P&I schemes for the buildings, the DBNs discretized well and were able to successfully isolate all fault conditions. The DBN prepared for heating mode operation is an example of how a large probabilistic model might shape up, and what are the associated complexities with training such a network. All the DBNs are programmed in Python, which implies they can be integrated directly or as an API service for inference. This is discussed in the next Chapter 4. Lastly, a concept for diagnosing faults associated with HRW has been demonstrated. The developed diagnosis model is highly specific and isolates the fault conditions on all occasions. For extending this network, leakage fault is recommended to be included next given its important in the current context.

## 4 AUTOMATED FAULT DETECTION AND DIAGNOSIS - TOOL

Using the methodology discussed in section 2.2 and keeping the requirements identified (ref section 2.1), a prototype for automated Fault Detection and Diagnosis of Air-large Handling Units faults has been conceived. The overall concept of tool is discussed next and if followed by the developments towards *FDD business layer* and *Data Visualization layer* (see Figure 8).

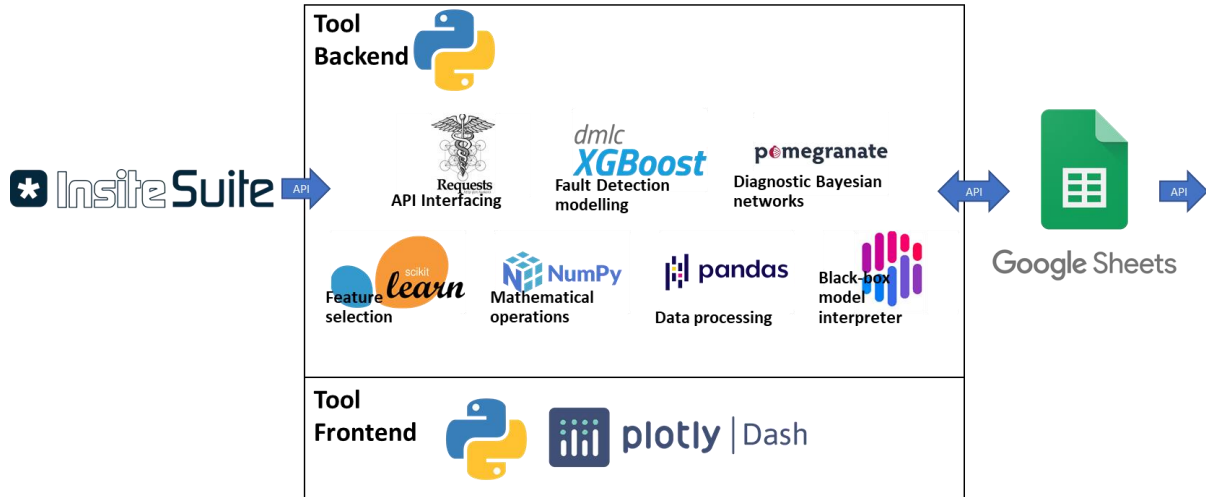


Figure 32: Interfaces and packages - AFDD Tool

The entire AFDD tool is realized in Python. Besides popularity of Python, the realized Pythonic application benefits from dozens of Python packages (see Figure 32) and its object-oriented structure. Further, the Pythonic realization makes it possible to use the tool across multiple OS environments [108]. The current implementation has been tested on windows OS version 10. The entire tool can be viewed as backend (*data acquisition layer*, *data validation and pre-processing layer*, *FDD business layer*, and *results post-processing layer*) and frontend (the *data visualization layer*) developments and are discussed in 4.1 and 4.2.

### 4.1 AFDD TOOL BACKEND

The four layers discussed in section 2.2.1 namely *data acquisition layer*, *data validation and pre-processing layer*, *FDD business layer*, and *results post-processing layer* together form the application backend. In the discussed *data acquisition layer* (see Figure 8), the data for model training and FDD is acquired using the InsiteSuite API support (see Figure 32, left) provided by the project partner (Kropman Installatietechniek). To enable this interface and acquire data securely over HTTP, Python's *requests* package has been utilized. Once access is granted, data is continuously acquired using a secure tokenization.

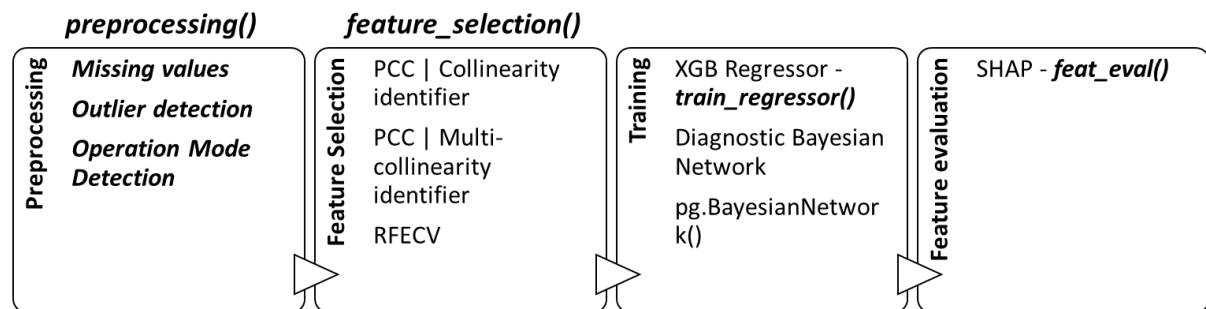


Figure 33: Class diagram - Model training pipeline for FDD tool

The next backend layer (see Figure 8) namely *data validation and pre-processing layer* has been enabled using Python classes (see Figure 33). This has been done to program these layers in an object-oriented manner,

thereby creating objects that can be repurposed. This development is built atop Python's base libraries such as *Pandas*, *scikit-learn*, and *NumPy* (see Figure 32) [86,109–111]. The pre-processing of data involves multiple steps. First, the acquired raw data is validated. This validation process involves steps such as a) the meta information for acquired data such as its timestamps, name tags are corrected for maintaining consistency and interpretability within the tool; b) treating missing values with interpolation techniques or dropping them; c) treating incorrect values (for example cooling coil valve position > 100) or outliers. Second, the validated data is further processed to filter AHU's operation mode. Third, the pre-processed data is utilized for feature selection (ref section 3.4).

Data from *data validation and pre-processing layer*, is passed further into the *FDD business layer* wherein critical model information such fault thresholds utilized in the fault evaluator (ref section 2.2.2), model hyperparameters, model features, prior and conditional probabilities are maintained. For enabling the training of XGBoost model and Bayesian network, two classes namely *train\_regressor* and *pg.BayesianNetwork* (see Figure 33, 3<sup>rd</sup> card from left) have been utilized. Their utilization (see Figure 32) has been made possible by using the API of *XGBoost* and *pomegranate* packages [112]. To provide interpretability to the user on the trained black-box models (ref section 3.4), *shap\_eval()* class has been programmed. In between the various classes, data is exchanged using comma separated values (CSV) and Java Script Object Notation (JSON) formats, which are flexible and light weight. This reduces the processing time and resource involved in this process.

The trained XGBoost models utilized in the fault detection process are maintained at the backend using a model management framework. The model management framework in essence tracks key model features (identified with *shap\_eval()*) for issues such as data drift, and across key performance indicators such as RMSE, and R2 Scores. In case of observed issues, this tracking mechanism generates an alarm if the observed model performance on the tracked KPIs is less than desired, or a data drift issue is observed. In the 4S3F framework, model faults are one of the three fault categories (ref section 2.2.2). Generated model alarms from model tracking can be incorporated to infer the correct posterior probability under such a situation.

As discussed, the diagnosis models are trained to probabilistically emulate faults and symptoms. Maintaining these relationships at scale can get overwhelming as DBNs would include more faults and corresponding symptoms. Therefore, to support the *FDD business layer* a database structure termed 'Fault Library' has been conceived and is discussed in 4.1.1. Thereafter, in 4.1.2 the developed pipeline to continuously acquire data and utilize the trained models for automated FDD is discussed.

#### 4.1.1 Fault Library

To maintain a unified taxonomy of faults along with more information such as its root cause, prioritization order, and other information that can support corrective action a database of faults has been conceived. This database structure is referred to as a 'fault library'. It is envisaged that the list of faults included in the current project is extensible and would be continuously updated. For such a scenario, a database scheme serves well as it helps avoid data redundancy. The various included faults along with its corresponding fault states (ref section 2.2.2) are identifiable in the database records using a unique fault code as shown in Figure 34. Alongside, faults qualitative information such as fault priority, its differentiating characteristics such as operation mode, category, its description, and recommended actions are also maintained. Further, the prior probabilities utilized for training the Bayesian network are also stored. In another table in the same database, fault events diagnosed by the FDD application are also stored. This way a unique record of faults and fault events is maintained.

For storing the discussed information, a lightweight database has been created using Google Sheets which is a royalty free spreadsheet program offered by Google. Instead of using the popular database languages such as SQL, Google Sheets has been preferred for its ease-of-use and familiarity of prospective users with spreadsheet programs. The spreadsheets are accessible over Google's API via Google's Cloud platform infrastructure. Through Google's infrastructure, the program is portable across mobile and desktop devices. A wrapper (named *gapi*) that includes methods for handshake with this API is included in the AFDD Tool. Using this wrapper data can be uploaded and downloaded from this cloud hosted database in a universal JSON data-interchange format. The FDD Tool's alarms page discussed in section 4.2, utilizes this database as backend.

fault_code	operation_mode	fault_number	name	priority	category	type	description	action	prior_probability
stuck_valve_positive	cm	f1	stuck valve fault	high	waterside	abrupt	Valve is stuck at higher position. It can increase your chiller and pump energy consumption	Manually check	0.02
stuck_valve_negative	cm	f2	stuck valve fault	high	waterside	abrupt	Valve is stuck at lower position. It can affect comfort conditions	Manually check	0.02
stuck_valve_faultfree	cm	f3	stuck valve fault	high	waterside	abrupt	Its all cool	Manually check the valve	0.96
reduced_sat_fault	cm	f4	reduced SAT fault	high	airside	abrupt	Supply air temperature setpoint is lower than desired. It can increase your energy consumption	Manually check the valve	0.05
reduced_sat_faultfree	cm	f5	reduced SAT fault	high	airside	abrupt	Its all cool	Manually check the valve	0.95
airflow_high	cm	f6	airflow fault	high	airside	abrupt	Airflow is higher than required. It can impact cooling performance.	Manually check the valve	0.03
airflow_low	cm	f7	airflow fault	high	airside	abrupt	Airflow is lower than required. It can impact ventilation requirements.	Manually check the valve	0.03
airflow_faultfree	cm	f8	airflow fault	high	airside	abrupt	Its all cool	Manually check the valve	0.94
increased_sat_fault	hm	f9	increased SAT fault	high	airside	abrupt	Supply air temperature setpoint is higher than desired. It can increase your energy consumption	Manually check the valve	0.05
increased_sat_faultfree	hm	f10	increased SAT fault	high	airside	abrupt	Its all cool	Manually check the valve	0.95
sat_sensor_offset_positive	cm	f11	sat sensor offset fault	high	airside	abrupt	Supply air temperature sensor has a positive offset. Extra cooling may be provided.	Manually check the valve	0.02
sat_sensor_offset_negative	cm	f12	sat sensor offset fault	high	airside	abrupt	Supply air temperature sensor has a negative offset. Cooling demand may not be met.	Manually check the valve	0.02
sat_sensor_offset_faultfree	cm	f13	sat sensor offset fault	high	airside	abrupt	Its all cool	Manually check the valve	0.96
svt_sensor_offset_positive	hm	f14	svt sensor offset fault	high	waterside	abrupt	Supply water temperature sensor has a positive offset. Required heating may not be provided.	Manually check the valve	0.02
svt_sensor_offset_negative	hm	f15	svt sensor offset fault	high	waterside	abrupt	Supply water temperature sensor has a negative offset. Extra heating might be provided.	Manually check the valve	0.02
svt_sensor_offset_faultfree	hm	f16	svt sensor offset fault	high	waterside	abrupt	Its all cool	Manually check the valve	0.96
stuck_valve_positive	hm	f17	stuck valve fault	high	waterside	abrupt	Valve is stuck at higher position. It can increase your gas consumption	Manually check the valve	0.02
stuck_valve_negative	hm	f18	stuck valve fault	high	waterside	abrupt	Valve is stuck at lower position. It can affect comfort conditions	Manually check the valve	0.02
stuck_valve_faultfree	hm	f19	stuck valve fault	high	waterside	abrupt	Its all cool	Manually check the valve	0.96
airflow_high	hm	f20	airflow fault	high	airside	abrupt	Airflow is higher than required. It can impact heating performance	Manually check the valve	0.03
airflow_low	hm	f21	airflow fault	high	airside	abrupt	Airflow is lower than required. It can impact ventilation requirements.	Manually check the valve	0.03
airflow_faultfree	hm	f22	airflow fault	high	airside	abrupt	Its all cool	Manually check the valve	0.94
sat_sensor_offset_positive	hm		offset fault	high	airside	abrupt	Supply air temperature sensor has a positive offset. Required heating may not be provided.	Manually check the valve	0.02
sat_sensor_offset_negative	hm		offset fault	high	airside	abrupt	Supply air temperature sensor has a negative offset. Extra heating might be provided.	Manually check the valve	0.02
sat_sensor_offset_faultfree	hm		offset fault	high	airside	abrupt	Its all cool	Manually check the valve	0.96

Figure 34: AFDD tool - unique faults and faults events library

The API infrastructure is open for data sharing not just with designed FDD tool but is also useful for allowing secure third-party access. In other words, using this media information can be securely exchanged with third-party applications for enabling Interoperability (ref Table 5).

#### 4.1.2 AFDD inference

The results from trained models are inferred in an automated manner using the developed AFDD tool. This implies combining the inference pipelines of detection and diagnosis processes. This combined inference pipeline is realized as an online pipeline that follows the same process as utilized in training (see Figure 8) except in this case model parameters are known and not learnt (ref section 2.2.4). The *data acquisition layer* continuously checks for availability of new data and updates the local database with this newly acquired data for inference. Via this established link the inference using the *FDD business layer* occurs with minimal delay and is helpful towards diagnosing faults early. For inference using the trained XGBoost models, a separate class called *infer\_regressor* (see Figure 33, 3<sup>rd</sup> from left) has been developed that is initialized using trained models and features. Further, it contains a method for evaluating predictions on KPIs that are useful for model management discussed previously. Inference for diagnosis with the trained DBNs is supported with the help of a Python module created named *dbn\_inference* for this purpose. This module has been developed to infer posterior probabilities as new data is acquired. Through a series of underlying functions, continuous values collected from the CMS are inferred through the FDD models and faults diagnosed are reported. These faults are then parsed over the API, into the google spreadsheet (see section 4.1.1). The results from the inference process are visualized using a web application interface discussed in section 4.2.

## 4.2 AFDD TOOL FRONTEND

The *data visualization layer* or the frontend of the AFDD tool (see Figure 32) is encoded in Dash by Plotly [113]. It presents the results inferred from the tool's backend. This encoding wraps HTML, Java Script, and CSS code blocks in a Pythonic syntax thus keeping the complete AFDD software limited to Python. This is beneficial as it reduces the need for separate skills for programming front-end. An evaluation of the selected package on key functional and realization aspects is provided in APPENDIX E. The realized application frontend is accessible across and tested with web-browser interfaces including Google Chrome, Mozilla Firefox, Internet Explorer, thereby keeping the application system agnostic.

The architecture of the designed *visualization layer* is shown in Figure 35. Herein, the entire frontend is subdivided into web pages (or 'dashboards'). For maintaining a hierarchy within this layer, the designed webpages are grouped into application pages and sites specific pages. Application pages contain root/index of the prototyped application to provide its entry point for example Home Page (see Figure 39). Site pages comprise of the sites or building specific pages to modularize the addition or deletion of use-case buildings for example the current prototype is demonstrated with two buildings - Breda office and Nijmegen school (ref section 2.3). This

hierarchy is created to a) ensure site specific data is not mixed; b) pages in future can be developed in both cases. For example, the current tool doesn't include a user management page which would have application pages as its parent and a new building addition would have sites pages as its parent. This provides scalability (ref Table 5) to the developed frontend.

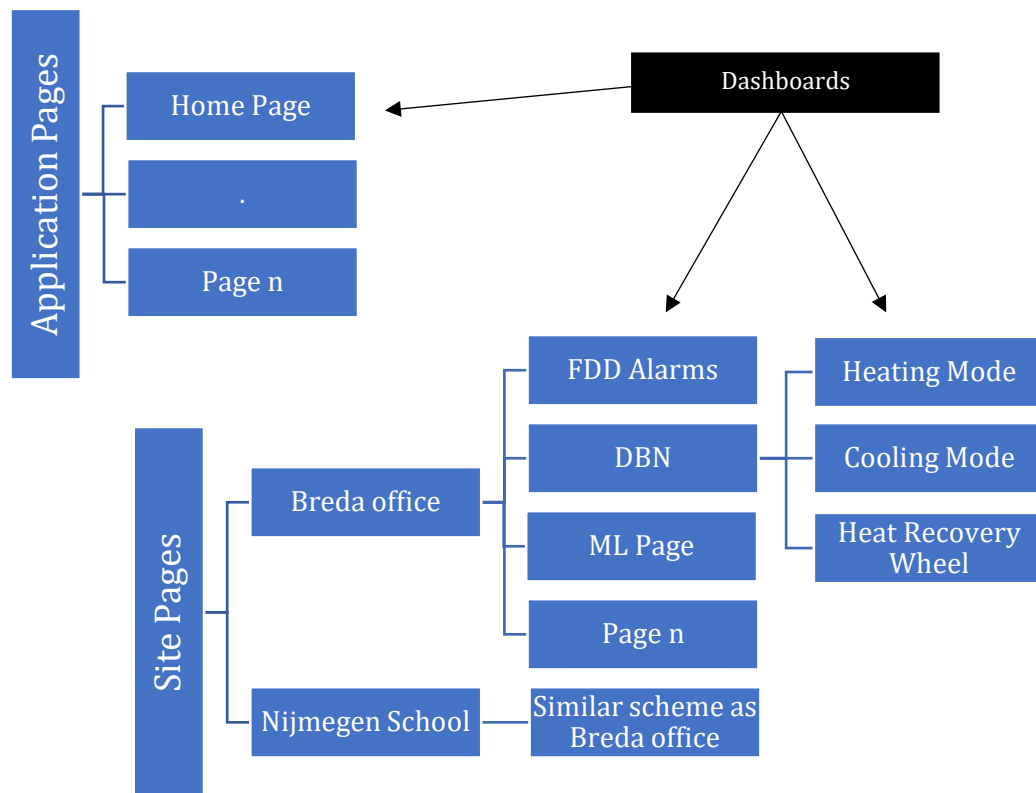


Figure 35: Data visualization layer hierarchy

Some key elements of the dashboard such as KPIs and virtual sensors are discussed in 4.2.1 and 4.2.2 respectively. KPIs are developed using the available sensors, whilst virtual sensors are provided to overcome the lack of sensors. The resulting dashboards are discussed in section 0,

#### 4.2.1 Key Performance Indicators (KPIs)

System performance can be effectively quantified using KPIs. The adoption of appropriate KPIs is key to realizing energy efficiency goals [114]. H. Li et al. in [115] surveyed literature and classified building performance KPIs at three levels: **a)** whole-building level, **b)** system level, **c)** component or equipment level. At system level, the KPIs can be structured by impact (for example energy or comfort), value (for example single or series), aggregation level (for example hourly, daily), associated faults or abnormalities, and improvement or corrections upon observing deviation [115]. A challenge associated with development of these KPIs is availability and reliability of sensors (ref section 1.2).

Through the fault impact analysis presented in section 3.1, impact on energy KPIs such as chiller energy, boiler energy, pump energy, and comfort KPIs such as unmet hours have been measured. Through this process a clear association between simulated faults and KPIs is identified. Further, these KPIs are treatable as the energy performance symptoms in the utilized 4S3F framework (ref section 2.2.2) and KPIs are considered for inclusion in the developed FDD tool. The KPIs are laid out atop the developed diagnostics page (see Figure 41). Since, the DBNs have been discretized (ref section 3.5), the KPIs on the application page correspond with this discretization. For example, on the north zone cooling coil diagnostics page shown in Figure 41, the cooling unmet hours imply the number of hours cooling setpoint remains unmet in the north zone.

In Figure 36, KPIs corresponding with the cooling mode operation are shown. KPIs such as chiller cycles, chiller shutoff (1a in Figure 36) and unmet hours are indicative of energetic and comfort performance of the cooling sub-system. Along with each indicator (1c in Figure 36), a deviation from baseline indication (1d in Figure 36) and the aggregation level (1b in Figure 36) has also been provided. As H. Li et al., (2020) indicate, defining the

baseline for comparison is challenging due to complexity, configuration and stochasticity, simplified baselines have been considered. For example, chiller cycles are aggregated daily, and compared against the chiller cycles recorded on the previous day. The indicated deviation from baseline (red: deterioration /green: improvement), is designed to aid the user (such as facility manager or building engineer) efficiently keep track of performance and initiate action if required.

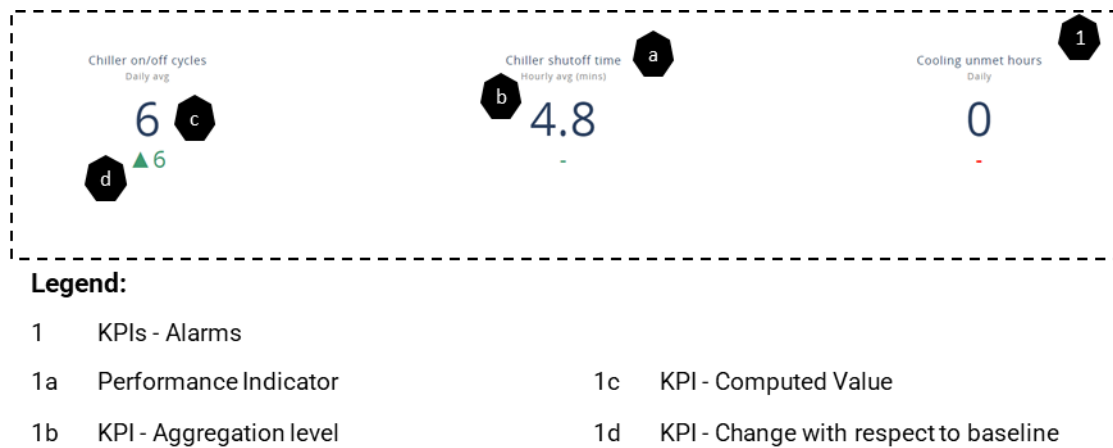


Figure 36: AFDD tool - key performance indicators cooling mode operation – Breda office

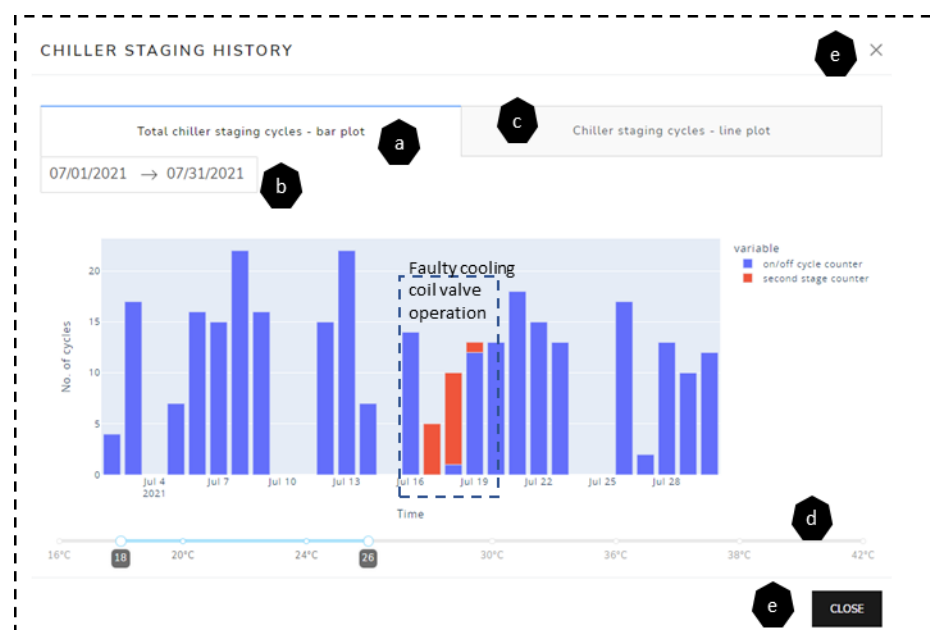


Figure 37: AFDD tool - key performance indicator - chiller staging - detailed view

To further explore each KPI and for leveraging building engineer's or a subject matter expert's (SME) knowledge for diagnostics, each KPI is designed as an interactive component. This implies that upon clicking the KPI (clicking

1c on Figure 36), a window pops open (see Figure 37) that provides information to view development trends of that KPI. Using the example of chiller cycles, it can be observed from Figure 37 that between July 17-18, 2021, the deployed chiller at Breda office operated with cycled less in comparison with July 16 or July 19. Further, it operated mostly at second stage thereby consuming higher energy than previous day despite both days falling in the same temperature band (see d on Figure 37). From case presented in Figure 25, it can be correlated that a stuck valve fault caused this behaviour. This additional information as seen is clearly useful for a building engineer to diagnose faults and track health of key energy consuming components of the HVAC system. Further, additional features for analysis such as switching between bar or line plot (a or c on Figure 37) or filtering out data for weather conditions (slider d on Figure 37), or dates are also provided (see b on Figure 37). This combination of expert knowledge aided with effective visualizations is a step that promotes human-in-the-loop diagnostics.

#### 4.2.2 Virtual Sensors

Virtual sensors are often developed in HVAC systems to fill in the gaps left by missing, misplaced or out-of-calibration sensors [116]. Therefore, they are helpful in either replacing missing information voided by lack of sensors or in assessing the reliability of collected data through sensors. This added information is useful in the FDD process [117]. For example, the mass flow rate sensor has been identified as vital to detecting faults in an AHU (ref section 3.2) and is often found missing in building installations. On this note Choi & Yoon in [118], demonstrated the use virtual enthalpy sensor for sensor calibration.

Virtual sensors can be developed using white, grey, or black-box approaches [116]. During the project additional sensors are installed at Breda office (see Table 10) and three virtual energy meters (see Figure 38) have been applied using the energy conservation equations for an AHU [116].

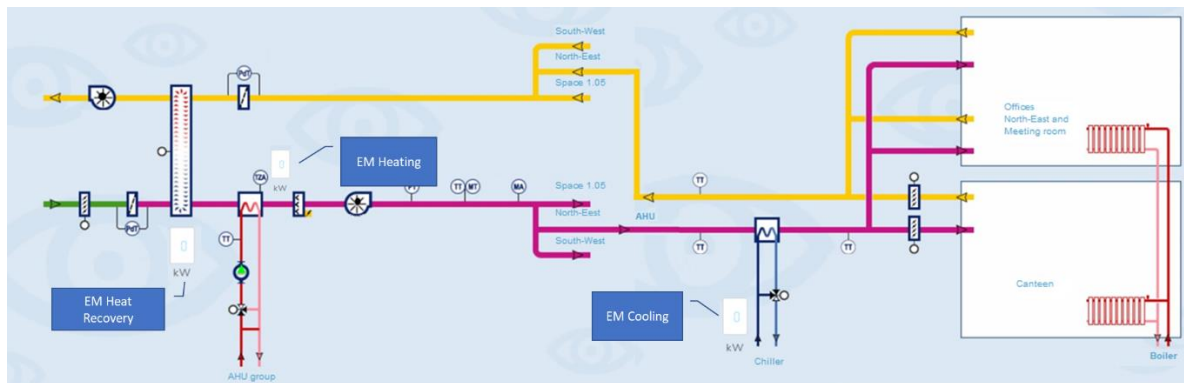


Figure 38: Virtual energy meters overlayed on P&I of Breda office - central AHU + north zone cooling coil

Ready availability of such information is handy for the user (for instance a building engineer or an HVAC expert) and reduces their effort spent data curation thereby unlocking time for analysis. For example, using these three energy meters building engineer can quickly observe energy flows and for example detect unwarranted use of simultaneous heating or cooling installations.

#### 4.2.3 Data Dashboarding

The designed visualization layer comprises of four key dashboards (see Figure 35) that have been realized iteratively starting with the more abstract requirements presented in section 2.1. The requirements for the dashboard are identified through the design sprint methodology discussed in section 2.2.3.

The Home Page for the FDD tool (see Figure 39) comprises of the list of integrated sites and a global view into the diagnosed outcomes. The integrated sites are overlayed on a geographical map using a bubble, whose size indicates the number of faults diagnosed using the FDD tool. This way a user (such a remote services manager) responsible for monitoring several building installations can quickly identify the installation requiring more attention. As shown in Figure 39, on hovering (see 1a) over the bubble more quantitative information is provided, which can be expanded in content. More importantly, as the FDD tool would be scaled to a larger number of sites such a representation is quite helpful for remotely located teams in planning and coordination with on-site engineers. For navigating through the entire tool, an explore option is provided on the main navigation bar (see Oa on Figure 39). All developed pages integrated into the application are directly accessible from here. Further, the developed pages are categorized for easy access. For example, all the DBN pages are grouped together in this menu (see Oa on Figure 39).

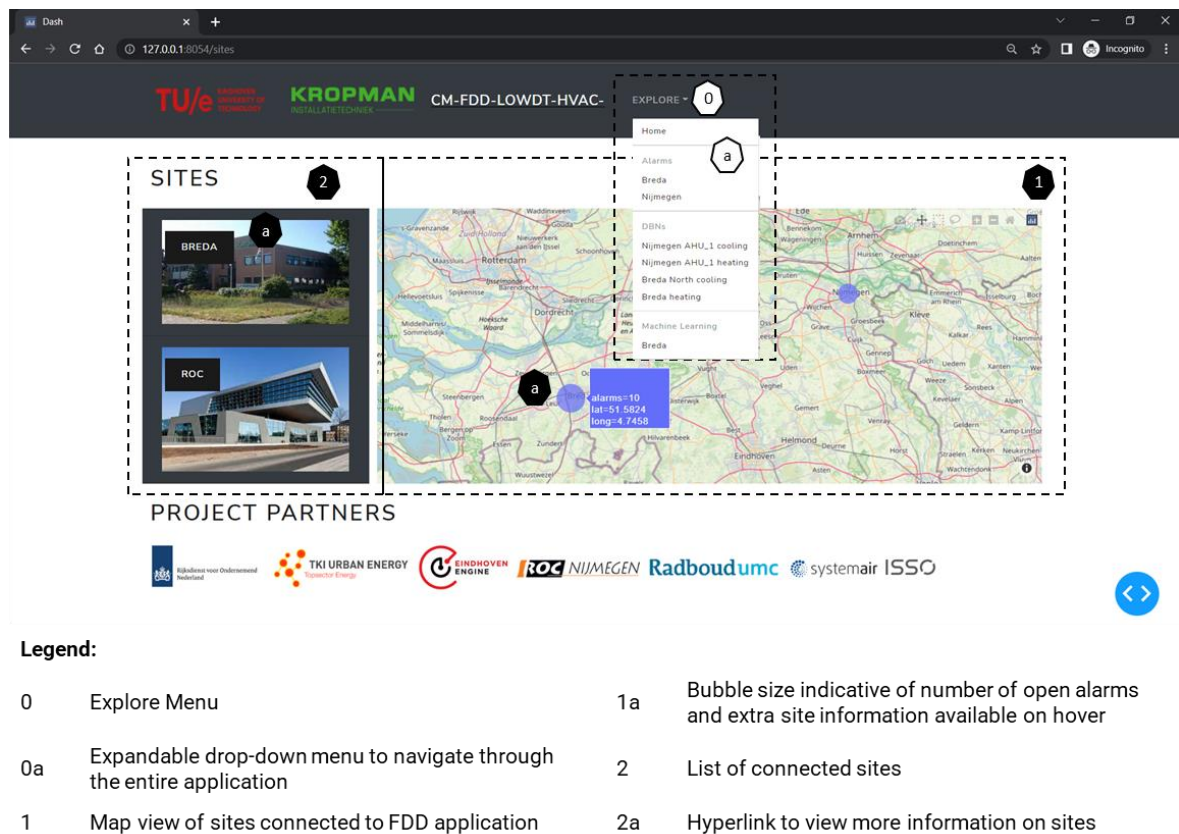


Figure 39: AFDD tool - Home Page

Besides, the explore drop-down menu the user can also navigate to the alarms page using an embedded link on the site's image (see 2a Figure 39). Upon clicking the link, the user is directed to the site-specific alarms page (see Figure 40). Here, faults diagnosed by the FDD tool are presented as alarms for user. At the start of the page some key performance indicators are populated (see 1 on Figure 40). Using these key performance indicators, facility manager can keep a track of the faults diagnosed on a specific time horizon such as week, month, year. Each performance indicator is compared with a reference value derived using the previous time instance. For example, faults diagnosed in the current week are compared with diagnosed faults from previous week. Using such quantitative information, a facility manager can initiate action through a service engineer or building engineer for fault correction.

For the building engineer's record, a detailed list of diagnosed of faults (or alarms) is populated. Alongside each alarm, qualitative information such as fault priority, category, type, description about the raised alarm is provided. This information is obtained from the fault library explained in section 4.1.1. Using this information, the building engineer can prioritize response and take recommended action or refer to an SME for further information on diagnosis. Besides information on the faults, the user is also equipped with filtering, searching, and sorting functionalities (see 2 a, d, e, f on Figure 40) for an enhanced user experience. Through these features the user can slice through the presented data for dates, categories, fault types. For example, the building engineer can prioritize airside faults for correction over waterside faults or vice-versa.

During an initial roll-out, all building engineers or facility managers, might not be equipped with the AI-based approaches utilized at the AFDD tool backend for diagnosis. This can generate queries directed towards a software expert or ML expert to provide further information on the diagnosed outcome. To tackle these issues, the complete information on diagnosis is provided on a detailed diagnostics page shown in Figure 41.

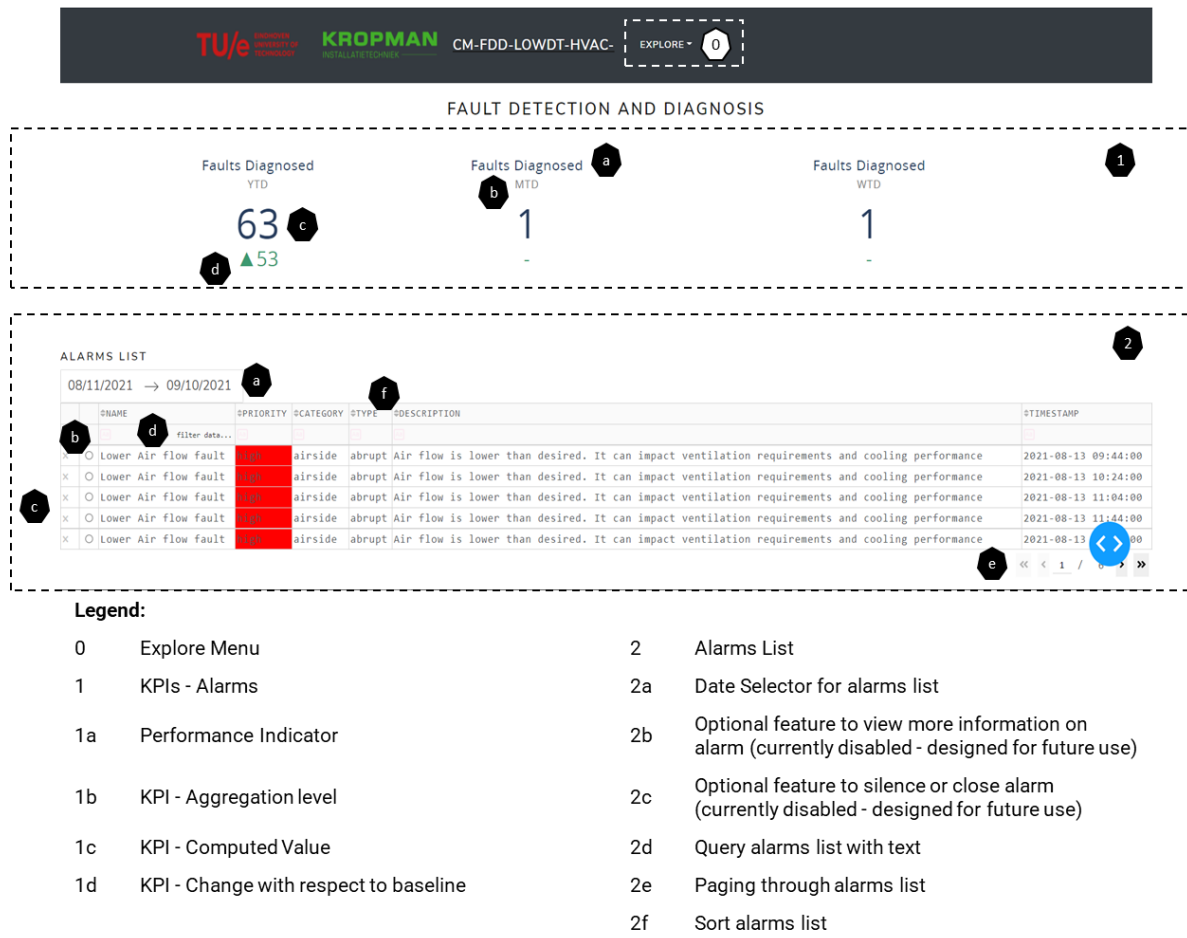


Figure 40: AFDD tool - Alarms page

For ML expert, or an SME, the traceability of the diagnosis is of more importance such that they can track the outcomes of the developed models. To support such a use-case, a page specific to Bayesian networks utilized for fault diagnosis has been developed. The page allows the user to track information flow through the discussed steps within the *FDD business layer*. At the centre of this page (see Figure 41), lies the developed DBN model for fault diagnosis. To support the additional checks, augmented information such as key performance indicators (ref section 0) and virtual sensors (ref section 4.2.2) are also located on the top and bottom of DBN pages respectively. In line with the discretization process discussed in section 3.5, the user can switch between DBNs for cooling, heating, or HRW (see 1 on Figure 41). This toggling feature allows the user to quickly switch between these DBNs and view the corresponding Bayesian networks as well as KPIs.

The nodes of the developed DBN are designed as interactive clickable elements (see 3a and 3b on Figure 41), whereby upon clicking the fault node fault probability is displayed (see Figure 42) and symptom residuals (see Figure 43) are displayed upon clicking the symptom nodes. Further, on mouseover the fault node, the user is also indicated of the location and its connection with the P&I diagram shown after the Bayesian network on the DBN page (see 4 on Figure 41). This way interpretability of the developed DBN model is improved for a building engineer or a facility manager.

As mentioned, the fault probabilities (upon clicking 3a on Figure 41) and symptom residuals (upon clicking 3b on Figure 41) are displayed as pop-ups on the screen. Additional features are provided to support an ML and or an SME in comparing computed posterior probabilities and understanding their development on a time horizon. For example, for the stuck valve fault discussed in section 3.4.1 the computed posterior probability is nearly over 68% (see b on Figure 42), thereby indicating fault presence and its development and correction in time. This information can be accessed for all evidence provided to the developed DBN and the computed posterior probabilities thereof for all faults by using features of date selection (see a in Figure 42) and checklist (see c in Figure 42). For the expert, to be able to share such extra diagnosis information with the building engineer, additional features such as downloading a plot or zooming into a particular section are also provided (see d & f in Figure 42).

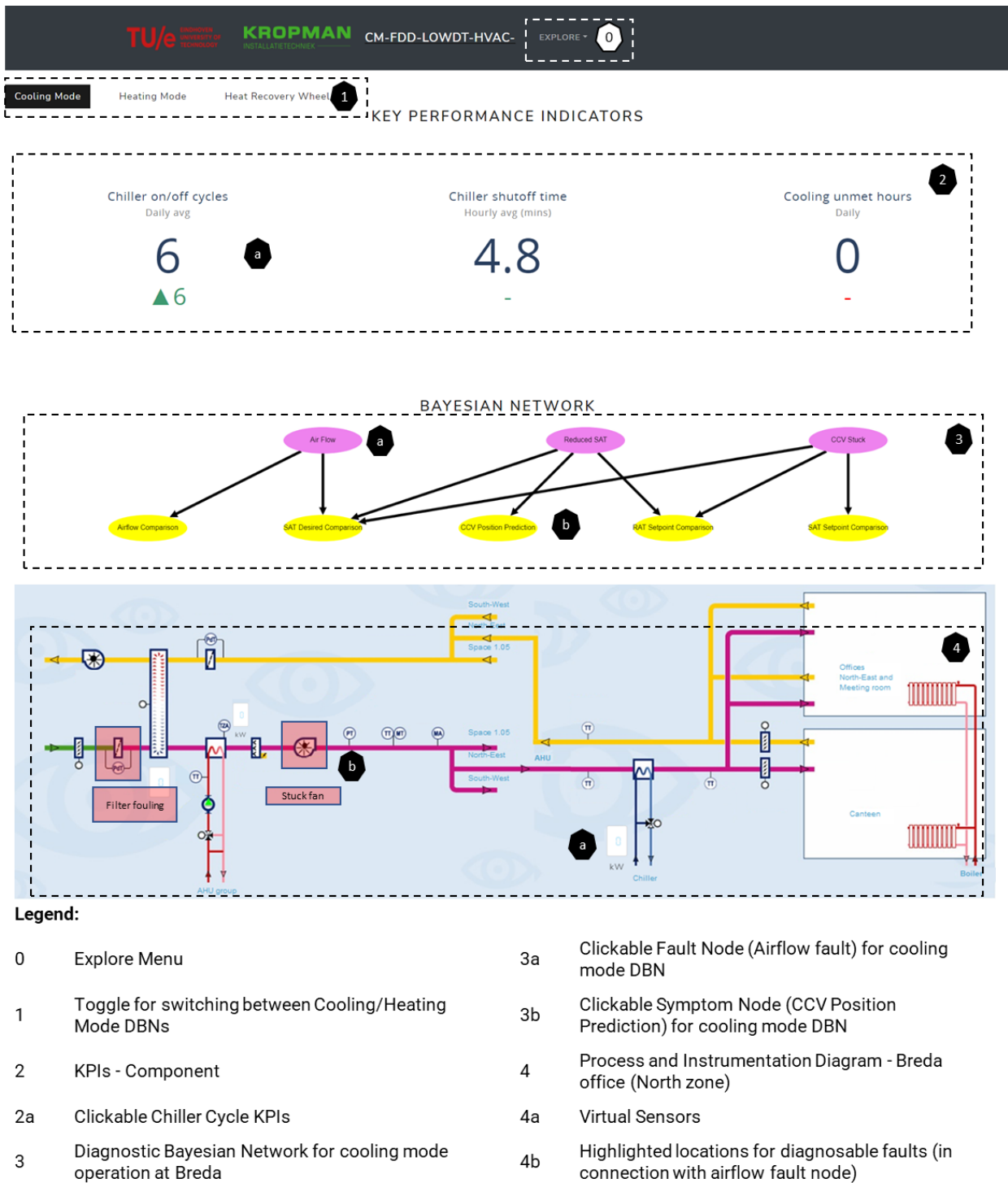
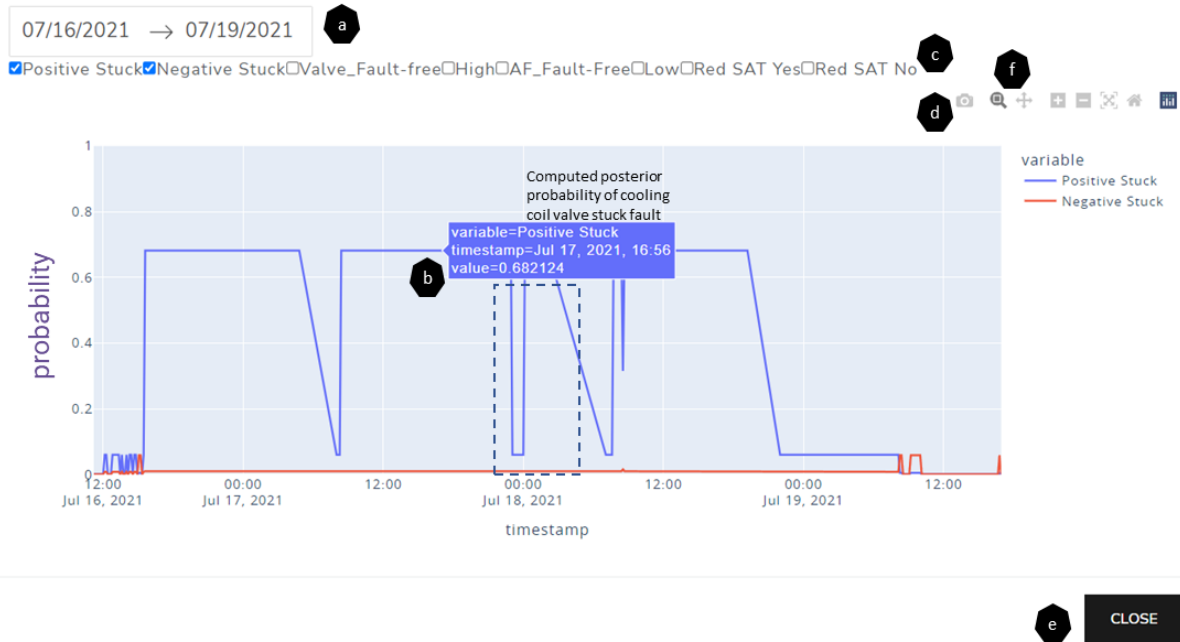


Figure 41: AFDD tool - Cooling mode diagnostics page for Breda office North zone

## FAULT PROBABILITIES



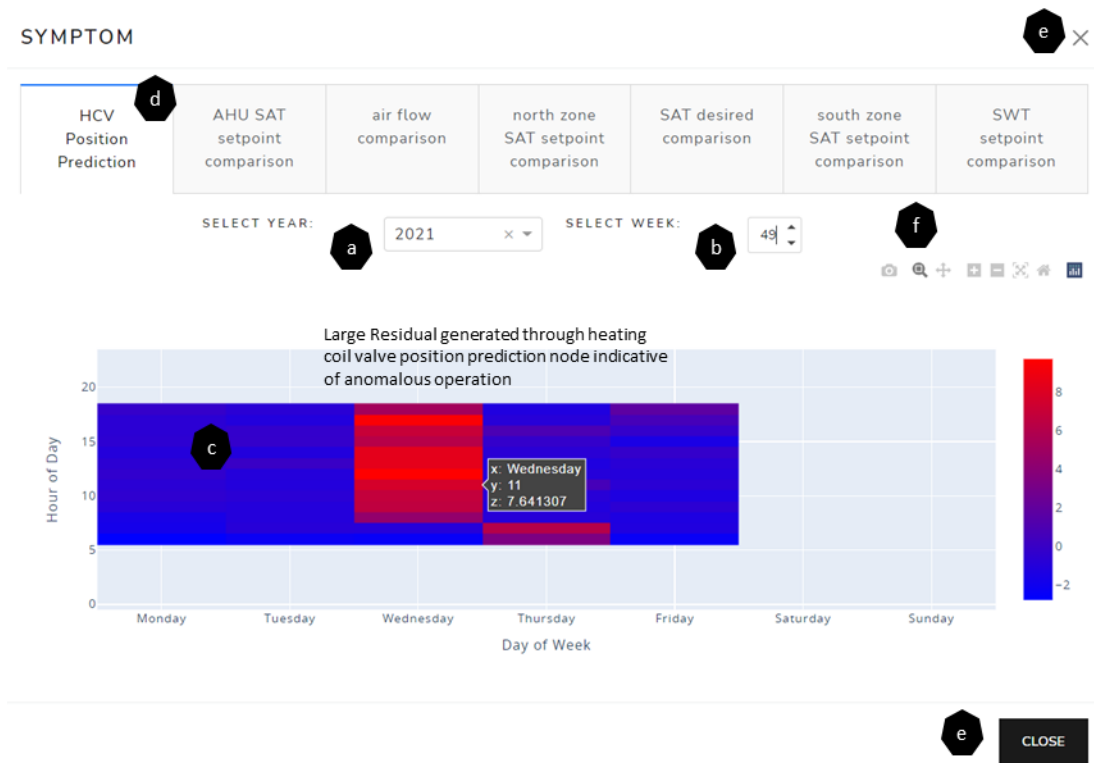
### Legend:

- |   |  |   |                    |
|---|--|---|--------------------|
| a | Date selector                            | d | Download Plot      |
| b | Computed posterior probabilities in time | e | Close pop-up       |
| c | Check list of all fault states           | f | Zoom In or Pan-out |

Figure 42: AFDD tool - computed posterior probabilities inferred using DBN developed for cooling mode operation at Breda office

On the symptom residual pop-up (see Figure 43), computed residuals using for instance formulas in Table 19, are visualized on a heatmap representation. The intensity of the colour (RGB scale) on heatmap (see c on Figure 43) indicates the magnitude of the residual on the positive (blue) and negative (red). For example, on the Wednesday 8<sup>th</sup> December 2021 a supply water temperature sensor offset fault was introduced (ref section 3.5.2). This provides an expert a lucid view into the utilized fault detection process. Further, using such information a building engineer, who perhaps is unaware of the complexity of black-box model can easily differentiate between anomalous and normal operation. Although the fault diagnosis process has been completely automated in the tool, a building engineer using such information can augment the diagnosis process. For example, a building engineer can rule out false positives through additional checks or considering available site information or on the contrary confirm true positives that can later be utilized for labelling collected operational data.

The diagnosis process utilizes several AI models, for example for cooling coil or heating coil valve position prediction. To ensure a reliable diagnosis, it's imperative to track the performance of the trained models over time and identify issues such as data drift that impact the quality of the prediction [119]. To visually observe the performance of trained models over time a specific page has been realized and is discussed in APPENDIX E.



### Legend:

- |   |  |   |  |
|---|--|---|--|
| a | Year selector  | d | Tabs to observe other residuals                    |
| b | Week selector  | e | Close pop-up                                       |
| c | Heat-map indicating residual intensity (blue normal, red – high) | f | Common features for download, zoom in-out, and pan |

Figure 43: AFDD tool - generated symptom residual through XGBoost models

## 5 DISCUSSION

---

The concept presented in Chapter 4 is assessed in this section from technical, financial and deployment risk perspectives. Firstly, its technical viability is discussed in section 5.1. Secondly, in section 5.2 the overall concept is assessed from a financial feasibility viewpoint. Lastly, in section 5.3, the risks associated with deploying the concept at scale are discussed.

### 5.1 ASSESSMENT OF TECHNICAL VIABILITY

The presented concept for the AFDD tool is verified by comparing with the prioritized requirements in section 2.1 and assessed if it technically satisfies needs of various project stakeholders. The compliance of the developed tool with respect to identified requirements is presented in APPENDIX F - Table 36. In this matrix, complete compliance is indicated with green and partial compliance or improvement needed is indicated with yellow. It is observable that the developed tool complies with majority of the identified requirements.

Focusing on the domain specific requirements, a robust diagnosis strategy is desirable for the most important faults. Using the 4S3F framework multiple discretized DBNs have been developed. For their discretization, P&I diagram of the underlying HVAC system has been utilized. This way the diagnosis model traces its origins back to the HVAC design and is synonymous with how a building practitioner would go about the diagnosis process. As opposed to utilizing classification-based approach (see Figure 4), an interpretable diagnosis strategy has been employed. To improve interpretability of developed black-box models for fault detection, SHAPley framework has been implemented. The framework was also found useful in features selection process. Widespread use of such frameworks would not only help reduce dimensionality of datasets, but more importantly inspire confidence within building practitioners to trust a black-box model's predictions.

In the project an initial concept for model management is presented. For its commercial application, there can be improvements made in the direction of extending this framework in the direction of complete automation. Currently it included only a few indicators such as R2 Score and RMSE to track model performance and can identify issues such as data drift with human support. However, it can be automated through extensive collaboration with teams focused on this topic. Although, the developed ML models are fit-for-purpose, the current modelling framework should be extended to include algorithms from the deep learning and other domains. This would help users to actively compare modelling paradigms and understand their differences. The currently application has been developed and tested on a Windows PC with 16GB memory. Although, the utilized Python based framework offers cross platform support, this aspect needs to be tested further. This can be achieved through testing it first on a Linux machine. Although, to ensure this portability out-of-the-box it is recommended to containerize the developed tool. To this end, an open-sourced containerization platform called Docker has been found useful [120].

For integrating Bayesian networks into software continuously values residuals generated in the fault detection process have been discretized into states [36]. Some information is lost during this discretization process for reducing model complexity, that can be regained. This would improve the specificity of the desirable action and its priority. For instance, the fault states are currently discretized as positive, or negative, or fault-free. A positive stuck valve fault implies a valve is open more than desired. However, discretizing the positive fault state further can help the building engineer or facility manager in understanding its severity and thereby prioritize their response. Further, the developed Bayesian network infer posterior probabilities using Bayes rule. However, each inference in a time-series is a prediction using fixed prior and conditional probabilities. Using this process, the information contained in the time dimension of data is lost. Therefore, it is desirable to regain this lost information using dynamic Bayesian networks that can update conditional probabilities by learning over time [34]. This would prevent misdiagnosis of faults as pointed to in section 3.5.2, and thereby improve the isolability of the designed network.

To support building practitioners further, a comprehensive list of faults studied in literature for AHUs have been prioritized using a fault impact analysis presented in section 3.1. It was observed that Pareto principle is applicable and faults causing highest energy performance can be prioritized. Although, this approach was found useful, it can be improved in three directions. Firstly, the fault modelling approach utilized for this analysis uses a stepwise approach to model fault character in time. Fault behaviour that is more often drift-like or incipient (for example fouling, leakage), needs to be studied further. This would be helpful towards calibrating the detection and diagnosis approach for such faults. Secondly, more fault models with multiple simultaneous fault

occurrences are recommended. This would help towards creating more test scenarios which are helpful in improving the isolability of the diagnosis models further. Lastly, the current simulation models approximate the actual building's behaviour with reasonable error, the tolerance considered can be reduced through more detailed modelling and thereby realizing a complete digital twin of the building. These digital twins could then be utilized for energy performance benchmarking and for feature selection.

The developed application comprises of KPIs populated across each developed page, for tracking performance of the underlying system being continuously monitored. These KPIs always include a benchmark or reference value to measure performance. For example, on the alarms page (see Figure 40) it is easier to compare faults diagnosed in current week with diagnosed alarms over the previous week. However, component KPIs such as energy performance of a chiller or boiler cannot be usefully compared using similar method due to variations in weather and/or occupancy. Further development in this direction would require a rigorous effort in defining appropriate baselines. Furthermore, often these KPIs do not include user or occupant feedback into consideration, which is highly desirable. Such feedback is often subjective and not continuously valued as objective measurements in a building. However, Bayesian networks can assimilate such information as discrete valued inputs in the additional information node (ref section 2.2.2) of the 4S3F framework. The ongoing APK2.0, and Brains for Buildings focus on these topics.

## 5.2 ASSESSMENT OF FINANCIAL VIABILITY

In Chapter 1, it was identified that up to 30% building energy can be saved using effective use of data collected through CMS systems. Through the developed FDD tool, faults introduced in the system are successfully diagnosed (see Chapter 3). The case presented in Figure 25 is used to estimate the preventable energy waste. On the 16<sup>th</sup> of July 2021 (Friday) a stuck valve fault was introduced in the afternoon and corrected the following Monday. The chiller's energy consumption between the periods 16:00-17:00 was compared on both days to estimate the energy savings. Using an energy meter, a 63% increase in the chiller's energy consumption was measured during faulty operation when compared with normal operation on Monday. As faults were simultaneously introduced in all cooling coil control valves, the measured increase is apportioned in the ratio of airflow through each zone. Using this approach, nearly a 33% increase in the chiller's energy consumption is estimated as attributable to the stuck valve fault in the north zone's cooling coil control valve. Such faults typically go unnoticed until considerable energy has been lost due to traditional facility management practices. The developed tool not just diagnoses such faults, but also recommends clear actions for fault correction making a strong commercial case for deployment.

It should be noted that analytical functions within facility management space need development (ref section 1.2.2). The financial viability of a business working towards development of an AFDD tool is assessed and presented APPENDIX F. The financial plan is generated considering a software-as-a-service (SaaS) business model [121]. Such a business model is considered key to a successful deployment, as then the software provider then becomes a stakeholder in the energy saving process. To estimate revenue potential, an addressable market in the Non-Residential Dutch buildings with large AHU/HVAC installations is considered. Further, the organizational development required on a five-year time horizon to support such a business has also been provided in APPENDIX F. Three scenarios have been forecasted for anticipating the revenue that can be generated through such a business. In each of the three scenarios estimated gross margins are a healthy 80%. Through the financial modelling it is estimated that as the energy savings accrue over time, enough EUR value is unlocked for the building owners to finance such an initiative. Despite the high upfront investment, it is forecasted that a SaaS business providing such services can turn profitable at the turn of fourth year from conception if it achieves nearly 1% of the total addressable market. Notably in the worst-case scenario the business would generate free cashflow only at the turn of sixth year, which can be improved through better capitalization of expenses.

## 5.3 DEPLOYMENT RISK ASSESSMENT

The AFDD tool is successfully deployed for AHUs installed at two case-study buildings. For scaling such a solution to multiple building environments in an efficient manner a consistent taxonomy for acquired data through CMS systems would be required. Although, commonly available sensors have been utilized for modelling purposes, the lack of sensors at other buildings is a noteworthy barrier to overcome. As the lack of sensors would add to the lead-time involved in training the AI models utilized in the tool. Brick schema or Project Haystack provide feasible alternatives that can help overcome challenges associated with taxonomy [122]. For addressing the issues with sensors, studied building examples can be utilized as reference for proposing sensors in the near-

term. In the longer term, a more generalizable approach to feature selection should be explored to provide an economically efficient alternative.

Google sheets has been utilized as the backend database for maintaining fault library and diagnosed outcomes. There are limitations for read and write exceptions imposed by the provider, which would need to be considered in detail when scaling to hundreds of building installations. In such a circumstance, it would be desirable to replace this backend with a comprehensive database based on SQL. Pomegranate (ref section 4.1) has been utilized for realization of Bayesian networks in the tool's backend. Since, the applications of such models in commercial applications is limited, it is difficult to assess the scalability of this package. Although, the package has been utilized upon consultation with specialist in this field, it is recommended to test its ability to support concurrent use. This can be tested with the help of specialized software experts.

For a successful scale up of this project, specialist with skills in software development, machine learning (including Bayesian ML) and knowledge expertise in HVAC domain are required. Such skills are hard to find in a single individual, and hence management and recruiting of right talent are key risk considerations that need to be mitigated for this project.

## 6 CONCLUSIONS AND RECOMMENDATIONS FOR FUTURE DEVELOPMENT

---

An AFDD tool for large Air-Handling Units along with its design architecture is presented, and its integration with an operational CMS is demonstrated for two case study buildings. The business layer of the tool combines state-of-the-art techniques from the AI domain and automates the FDD process. The designed tool is portable, scalable, reliable, and interoperable. To validate its reliability, the tool has been tested under varying scenarios such as different building installations, differing operational environments, different fault conditions. The realized specificity of the diagnosis algorithms measured over a long-term (>30 days) time horizon exceeds 90% for both cooling and heating operation of the Air-Handling Unit. Importantly, the trained diagnosis models not only diagnose fault presence conditions but are able to successfully isolate them. Further, the diagnosis model developed for studied cases with different HVAC configurations exhibited similarities, thereby alluding to generalizability of the 4S3F framework.

The CMS setup at these installations can be augmented with the prototyped tool and energy penalties due to faults can be avoided. At the cooling coil installation at Breda, nearly 33% of energy savings are estimated, and consequent additional emissions are thus preventable. The saved costs make the widespread deployment of such tools very attractive. As a step in this direction a SaaS business model is presented, which indicate that such a business can turn profitable in just four years from deployment making it very viable. In the short-term for the industry partner, the tool enhances its software value proposition and would help with executing service contracts profitably.

Using the developed dashboards, faults can be diagnosed and assessed in a user-friendly manner thereby pushing human-in-the-loop diagnostics to the fore. Inclusion of a fault library, key performance indicators and virtual sensors make the presented prototype comprehensive and extensible.

For further development of the tool following areas have been identified:

1. Applying building metadata management schemes such as Project Haystack or Brick Schema, are highly desirable for addressing large scale deployments.
2. To advance the developed tool's AI prowess, dynamic Bayesian networks and automated development of the initial probabilistic model from P&I are recommended.
3. Upon deployment, the faults diagnosed through the tool can be confirmed by building staff for storing fault labels. A scheme for operationalizing this process and keeping it user and action friendly is strongly recommended for overcoming the challenges regarding unavailability of labeled data.
4. Using the presented framework, generalized features for fault detection can be understood that can help overcome the issue of uncertainty and high-dimensionality of data and shift towards smaller and validated datasets.

## 7 REFERENCES

---

- [1] IEA. Tracking Buildings 2020. Paris: 2020.
- [2] IEA. Gas Market Report, Q1 2022. Paris: 2022.
- [3] Mills E. Building commissioning: A golden opportunity for reducing energy costs and greenhouse gas emissions in the United States. *Energy Efficiency* 2011;4:145–73. <https://doi.org/10.1007/s12053-011-9116-8>.
- [4] Zhao Y, Li T, Zhang X, Zhang C. Artificial intelligence-based fault detection and diagnosis methods for building energy systems: Advantages, challenges and the future. *Renewable and Sustainable Energy Reviews* 2019;109:85–101. <https://doi.org/10.1016/j.rser.2019.04.021>.
- [5] Bruton K, Raftery P, Kennedy B, Keane MM, O'Sullivan DTJ. Review of automated fault detection and diagnostic tools in air handling units. *Energy Efficiency* 2014;7:335–51. <https://doi.org/10.1007/s12053-013-9238-2>.
- [6] Kim W, Katipamula S. A review of fault detection and diagnostics methods for building systems. *Science and Technology for the Built Environment* 2018;24:3–21. <https://doi.org/10.1080/23744731.2017.1318008>.
- [7] Li D, Zhou Y, Hu G, Spanos CJ. Optimal Sensor Configuration and Feature Selection for AHU Fault Detection and Diagnosis. *IEEE Transactions on Industrial Informatics* 2017;13:1369–80. <https://doi.org/10.1109/TII.2016.2644669>.
- [8] Yu Y, Woradechjumnroen D, Yu D. A review of fault detection and diagnosis methodologies on air-handling units. *Energy and Buildings* 2014;82:550–62. <https://doi.org/10.1016/j.enbuild.2014.06.042>.
- [9] Eurovent AISBL / IVZW / INPA. Air Leakages in Air Handling Units : Guidelines for Improving Indoor Air Quality and Correcting Performance. 2021.
- [10] Investigating the Facility Management Professional Shortage - Fmlink n.d. <https://fmlink.com/articles/investigating-the-facility-management-professional-shortage/> (accessed July 27, 2020).
- [11] COMMISSION RECOMMENDATION (EU) 2019/1019 of 7 June 2019 on building modernisation. Official Journal of the European Union 2019.
- [12] Verhelst J, van Ham G, Saelens D, Helsen L. Model selection for continuous commissioning of HVAC-systems in office buildings: A review. *Renewable and Sustainable Energy Reviews* 2017;76:673–86. <https://doi.org/10.1016/j.rser.2017.01.119>.
- [13] Shi Z, O'Brien W. Development and implementation of automated fault detection and diagnostics for building systems: A review. *Automation in Construction* 2019;104:215–29. <https://doi.org/10.1016/j.autcon.2019.04.002>.
- [14] Lin G, Kramer H, Granderson J. Building fault detection and diagnostics: Achieved savings, and methods to evaluate algorithm performance. *Building and Environment* 2020;168:106505. <https://doi.org/10.1016/j.buildenv.2019.106505>.
- [15] Ahmad MW, Mourshed M, Yuce B, Rezgui Y. Computational intelligence techniques for HVAC systems: A review. *Building Simulation* 2016;9:359–98. <https://doi.org/10.1007/s12273-016-0285-4>.
- [16] Deloitte. Continuous monitoring and continuous auditing From idea to implementation. 2021.
- [17] Wen JT, Mishra S. Intelligent Building Control Systems. Cham: Springer International Publishing; 2018. <https://doi.org/10.1007/978-3-319-68462-8>.
- [18] Isermann R. Fault-diagnosis systems: An introduction from fault detection to fault tolerance. Springer Berlin Heidelberg; 2006. <https://doi.org/10.1007/3-540-30368-5>.

- [19] Li Y, O'Neill Z. A critical review of fault modeling of HVAC systems in buildings. *Building Simulation* 2018;11:953–75. <https://doi.org/10.1007/s12273-018-0458-4>.
- [20] Ding SX. Model-based fault diagnosis techniques: Design schemes, algorithms, and tools. *Model-Based Fault Diagnosis Techniques: Design Schemes, Algorithms, and Tools* 2008:1–473. <https://doi.org/10.1007/978-3-540-76304-8>.
- [21] Taal A, Itard L, Zeiler W. A reference architecture for the integration of automated energy performance fault diagnosis into HVAC systems. *Energy and Buildings* 2018;179:144–55. <https://doi.org/10.1016/j.enbuild.2018.08.031>.
- [22] Yan K, Huang J, Shen W, Ji Z. Unsupervised learning for fault detection and diagnosis of air handling units. *Energy and Buildings* 2020;210:109689. <https://doi.org/10.1016/j.enbuild.2019.109689>.
- [23] Li Y, O'Neill Z. An innovative fault impact analysis framework for enhancing building operations. *Energy and Buildings* 2019;199:311–31. <https://doi.org/10.1016/j.enbuild.2019.07.011>.
- [24] Fan C, Liu X, Xue P, Wang J. Statistical characterization of semi-supervised neural networks for fault detection and diagnosis of air handling units. *Energy and Buildings* 2021;234:110733. <https://doi.org/10.1016/J.ENBUILD.2021.110733>.
- [25] Gunay HB, Shen W, Yang C. Text-mining building maintenance work orders for component fault frequency. *Building Research & Information* 2018. <https://doi.org/10.1080/09613218.2018.1459004>.
- [26] Zhang R, Hong T. Modeling of HVAC operational faults in building performance simulation. *Applied Energy* 2017;202:178–88. <https://doi.org/10.1016/j.apenergy.2017.05.153>.
- [27] Chen J, Zhang L, Li Y, Shi Y, Gao X, Hu Y. A review of computing-based automated fault detection and diagnosis of heating, ventilation and air conditioning systems. *Renewable and Sustainable Energy Reviews* 2022;161:112395. <https://doi.org/10.1016/J.RSER.2022.112395>.
- [28] Chakraborty D, Elzarka H. Advanced machine learning techniques for building performance simulation: a comparative analysis. <https://doi.org/10.1080/19401493.2018.1498538> 2018;12:193–207. <https://doi.org/10.1080/19401493.2018.1498538>.
- [29] Walker S, Khan W, Katic K, Maassen W, Zeiler W. Accuracy of different machine learning algorithms and added-value of predicting aggregated-level energy performance of commercial buildings. *Energy and Buildings* 2020;209:109705. <https://doi.org/10.1016/j.enbuild.2019.109705>.
- [30] Najafi M, Auslander DM, Bartlett PL, Haves P, Sohn MD. Application of machine learning in the fault diagnostics of air handling units. *Applied Energy* 2012;96:347–58. <https://doi.org/10.1016/j.apenergy.2012.02.049>.
- [31] Zhao Y, Wen J, Wang S. Diagnostic Bayesian networks for diagnosing air handling units faults – Part II: Faults in coils and sensors. *Applied Thermal Engineering* 2015;90:145–57. <https://doi.org/10.1016/J.APPLTHERMALENG.2015.07.001>.
- [32] Zhao Y, Wen J, Xiao F, Yang X, Wang S. Diagnostic Bayesian networks for diagnosing air handling units faults – part I: Faults in dampers, fans, filters and sensors. *Applied Thermal Engineering* 2017;111:1272–86. <https://doi.org/10.1016/J.APPLTHERMALENG.2015.09.121>.
- [33] Hu M, Chen H, Shen L, Li G, Guo Y, Li H, et al. A machine learning bayesian network for refrigerant charge faults of variable refrigerant flow air conditioning system. *Energy and Buildings* 2018;158:668–76. <https://doi.org/10.1016/J.ENBUILD.2017.10.012>.
- [34] Pradhan O, Wen J, Chen Y, Wu T, O'Neill Z. Dynamic Bayesian Network for Fault Diagnosis 2021.
- [35] Xiao F, Zhao Y, Wen J, Wang S. Bayesian network based FDD strategy for variable air volume terminals. *Automation in Construction* 2014;41:106–18. <https://doi.org/10.1016/j.autcon.2013.10.019>.
- [36] Verbert K, Babuška R, de Schutter B. Combining knowledge and historical data for system-level fault diagnosis of HVAC systems. *Engineering Applications of Artificial Intelligence* 2017;59:260–73. <https://doi.org/10.1016/j.engappai.2016.12.021>.

- [37] Ferretti NM, Choinière D. Annex 47 Extended Project Summary 2006. <https://doi.org/10.6028/NIST.TN.1750>.
- [38] Choinière D, Milesi-Ferretti N. Cost Effective Commissioning of Existing and Low Energy Buildings. 2014.
- [39] Granderson J, Singla R, Mayhorn E, Ehrlich P, Vrabie D, Frank S. Characterization and Survey of Automated Fault Detection and Diagnostics Tools | Energy Technologies Area 2017. <https://eta.lbl.gov/publications/characterization-survey-automated> (accessed March 16, 2021).
- [40] Bruton K, Raftery P, O'Donovan P, Aughney N, Keane MM, O'Sullivan DTJ. Development and alpha testing of a cloud based automated fault detection and diagnosis tool for Air Handling Units. *Automation in Construction* 2014;39:70–83. <https://doi.org/10.1016/j.autcon.2013.12.006>.
- [41] Schein J, Bushby ST, Castro NS, House JM. A rule-based fault detection method for air handling units. *Energy and Buildings* 2006;38:1485–92. <https://doi.org/10.1016/j.enbuild.2006.04.014>.
- [42] Granderson J, Lin G, Singla R, Mayhorn E, Ehrlich P, Vrabie D, et al. Commercial Fault Detection and Diagnostics Tools: What They Offer, How They Differ, and What's Still Needed 2021. <https://doi.org/10.20357/B7V88H>.
- [43] Prouzeau A, Dharshini MB, Balasubramaniam M, Henry J, Hoang N, Dwyer T. Visual Analytics for Energy Monitoring in the Context of Building Management. 2018 International Symposium on Big Data Visual and Immersive Analytics, BDVA 2018 2018. <https://doi.org/10.1109/BDVA.2018.8534026>.
- [44] Hüllermeier E, Waegeman W. Aleatoric and epistemic uncertainty in machine learning: an introduction to concepts and methods. *Machine Learning* 2021;110:457–506. <https://doi.org/10.1007/S10994-021-05946-3/FIGURES/17>.
- [45] Taal A, Itard L. P&ID-based symptom detection for automated energy performance diagnosis in HVAC systems. *Automation in Construction* 2020;119:103344. <https://doi.org/10.1016/j.autcon.2020.103344>.
- [46] Nehasil O, Dobiášová L, Mazanec V, Široký J. Versatile AHU fault detection – Design, field validation and practical application. *Energy and Buildings* 2021;237:110781. <https://doi.org/10.1016/J.ENBUILD.2021.110781>.
- [47] Foster EC, Towle BA. *Software engineering : a methodical approach*. Auerbach Publications; 2021.
- [48] Zeiler W. *Basisboek Ontwerpen*. Noordhoff Publishers; 2014.
- [49] Bruton K, Coakley D, Raftery P, Cusack DO, Keane MM, O'Sullivan DTJ. Comparative analysis of the AHU InFO fault detection and diagnostic expert tool for AHUs with APAR. *Energy Efficiency* 2014 8:2 2014;8:299–322. <https://doi.org/10.1007/S12053-014-9289-Z>.
- [50] Taal A, Itard L. Fault detection and diagnosis for indoor air quality in DCV systems: Application of 4S3F method and effects of DBN probabilities. *Building and Environment* 2020;174:106632. <https://doi.org/10.1016/j.buildenv.2019.106632>.
- [51] Walden DD, Roedler GJ, Forsberg K, Hamelin RD, Shortell TM, International Council on Systems Engineering. *Systems engineering handbook : a guide for system life cycle processes and activities*. 2015.
- [52] National Aeronautics And Space Administration. *NASA systems engineering handbook*. NASA Special Publication 2007:356.
- [53] Huls AJ. Systematic energy performance assessment in operating office buildings Identification and assessment of energy performance gaps in Dutch office buildings, using the Pareto analysis and LEAN Energy Analysis. 2016.
- [54] Wang H, Chen Y. A robust fault detection and diagnosis strategy for multiple faults of VAV air handling units. *Energy and Buildings* 2016;127:442–51. <https://doi.org/10.1016/j.enbuild.2016.06.013>.
- [55] Chen T, Guestrin C. XGBoost: A Scalable Tree Boosting System. *Proceedings of the ACM SIGKDD International Conference on Knowledge Discovery and Data Mining* 2016;13-17-August-2016:785–94. <https://doi.org/10.1145/2939672.2939785>.

- [56] Patel BN, Rosenberg L, Willcox G, Baltaxe D, Lyons M, Irvin J, et al. Human-machine partnership with artificial intelligence for chest radiograph diagnosis. *Npj Digital Medicine* 2019 2:1 2019;2:1–10. <https://doi.org/10.1038/s41746-019-0189-7>.
- [57] Knapp J. *Sprint : How to Solve Big Problems and Test New Ideas in Just Five Days*. Bantam Press; 2016.
- [58] Ameisen E. *Building Machine Learning Powered Applications*. O'Reilly UK Ltd.; 2020.
- [59] Leprince J, Miller C, Zeiler W. Data mining cubes for buildings, a generic framework for multidimensional analytics of building performance data. *Energy and Buildings* 2021;248:111195. <https://doi.org/10.1016/j.enbuild.2021.111195>.
- [60] Chakraborty D, Elzarka H. Early detection of faults in HVAC systems using an XGBoost model with a dynamic threshold. *Energy and Buildings* 2019;185:326–44. <https://doi.org/10.1016/j.enbuild.2018.12.032>.
- [61] McDowall R. *Fundamentals of Air System Design*. ASHRAE; 2010.
- [62] Singhal A, Singhal S, Bhatia A, Garg V. *AUTOMATED FAULT DETECTION AND DIAGNOSIS FOR ENERGY RECOVERY WHEEL UNITS USING STATISTICAL MACHINE LEARNING METHOD*, 2018.
- [63] LAWRENCE W, SCHRECK T. Rotary heat exchangers save energy and prevent a need for recirculation which contributes to the decrease the risk of COVID-19 transfer. *REHVA Journal* 2020.
- [64] Li S, Wen J. Development and validation of a dynamic air handling unit model - Part I ( RP 1312 ) . *ASHRAE Transactions* 2010;116.
- [65] Li S, Wen J, Klaassen CJ. Development and validation of a dynamic air handling unit model - Part II ( RP 1312 ) . *ASHRAE Transactions* 2010;116.
- [66] Wen J, Shun L. *RP-1312 -- TOOLS FOR EVALUATING FAULT DETECTION AND DIAGNOSTIC METHODS FOR AIR-HANDLING UNITS*. Atlanta, G.A.: 2012.
- [67] Deru M, Field K, Studer D, Benne K, Griffith B, Torcellini P, et al. *U.S. Department of Energy Commercial Reference Building Models of the National Building Stock*. 2011.
- [68] EnergyPlus 2021. <https://energyplus.net/> (accessed May 4, 2021).
- [69] Zhang L. Simulation analysis of built environment based on design builder software. *Applied Mechanics and Materials* 2014;580–583:3134–7. <https://doi.org/10.4028/WWW.SCIENTIFIC.NET/AMM.580-583.3134>.
- [70] Wetter M, Benne KS, Gautier A, Nouidui TS, Ramle A, Roth A, et al. *LIFTING THE GARAGE DOOR ON SPAWN, AN OPEN-SOURCE BEM- CONTROLS ENGINE*, 2020.
- [71] Roth K, Westphalen D, Llana P, Feng M. The Energy Impact of Faults in U.S. Commercial Buildings. *International Refrigeration and Air Conditioning Conference* 2004.
- [72] Lee SH, Yik FWH. A study on the energy penalty of various air-side system faults in buildings. *Energy and Buildings* 2010;42:2–10. <https://doi.org/10.1016/j.enbuild.2009.07.004>.
- [73] Kim J, Frank S, Braun JE, Goldwasser D. Representing Small Commercial Building Faults in EnergyPlus, Part I: Model Development. *Buildings* 2019;9:233. <https://doi.org/10.3390/buildings9110233>.
- [74] Lu X, Fu Y, O'Neill Z, Wen J. A holistic fault impact analysis of the high-performance sequences of operation for HVAC systems: Modelica-based case study in a medium-office building. *Energy and Buildings* 2021;252:111448. <https://doi.org/10.1016/j.enbuild.2021.111448>.
- [75] Gunay B, Shen W, Yang C. Characterization of a Building's operation using automation data: A review and case study. *Building and Environment* 2017;118:196–210. <https://doi.org/10.1016/j.buildenv.2017.03.035>.

- [76] Carpenter J. Project Management in Libraries, Archives and Museums | ScienceDirect 2011. <https://www.sciencedirect.com/book/9781843345664/project-management-in-libraries-archives-and-museums#book-description> (accessed March 16, 2021).
- [77] Zhang L, Leach M, Bae Y, Cui B, Bhattacharya S, Lee S, et al. Sensor impact evaluation and verification for fault detection and diagnostics in building energy systems: A review. *Advances in Applied Energy* 2021;3:100055. <https://doi.org/10.1016/J.ADAPEN.2021.100055>.
- [78] Li, Shun. A Model-Based Fault Detection and Diagnostic Methodology for Secondary HVAC Systems. 2009.
- [79] Lu X, O'Neill Z, Li Y, Niu F. A novel simulation-based framework for sensor error impact analysis in smart building systems: A case study for a demand-controlled ventilation system. *Applied Energy* 2020;263:114638. <https://doi.org/10.1016/J.APENERGY.2020.114638>.
- [80] Comstock MC, Braun JE, Groll EA. The sensitivity of chiller performance to common faults. *HVAC and R Research* 2001;7:263–79. <https://doi.org/10.1080/10789669.2001.10391274>.
- [81] Afram A, Janabi-Sharifi F. Review of modeling methods for HVAC systems. *Applied Thermal Engineering* 2014;67:507–19. <https://doi.org/10.1016/j.applthermaleng.2014.03.055>.
- [82] Miller C, Arjunan P, Kathirgamanathan A, Fu C, Roth J, Park JY, et al. The ASHRAE Great Energy Predictor III competition: Overview and results. *Science and Technology for the Built Environment* 2020;26:1427–47. <https://doi.org/10.1080/23744731.2020.1795514>.
- [83] XGBoost Parameters 2021. <https://xgboost.readthedocs.io/en/latest/parameter.html> (accessed August 25, 2021).
- [84] Shi R, Xu X, Li J, Li Y. Prediction and analysis of train arrival delay based on XGBoost and Bayesian optimization. *Applied Soft Computing* 2021;109:107538. <https://doi.org/10.1016/J.ASOC.2021.107538>.
- [85] Zhang L, Frank S, Kim J, Jin X, Leach M. A systematic feature extraction and selection framework for data-driven whole-building automated fault detection and diagnostics in commercial buildings. *Building and Environment* 2020;186:107338. <https://doi.org/10.1016/j.buildenv.2020.107338>.
- [86] Pedregosa F, Varoquaux G, Gramfort A, Michel V, Thirion B, Grisel O, et al. Scikit-learn: Machine Learning in Python. *Journal of Machine Learning Research* 2011;12:2825–30.
- [87] Lundberg SM, Lee S-I. A Unified Approach to Interpreting Model Predictions. In: I. Guyon, U. V. Luxburg, S. Bengio, H. Wallach, R. Fergus, S. Vishwanathan, et al., editors. *Advances in Neural Information Processing Systems 30*, Curran Associates, Inc.; 2017, p. 4765–74.
- [88] Wen J. Development and Validation of a Dynamic Air Handling Unit Model, Part 1 (RP-1312)(OR-10-007) Human Behavior and Low Energy Architecture: Linking Environmental Adaptation, Personal Comfort, and Energy Use in the Built Environment View project Tools for Evaluating Fault Detection and Diagnostic Methods for HVAC Secondary Systems of a Net Zero Building View project. 2010.
- [89] Wen J. Development and validation of a dynamic air handling unit model, Part 2 Human Behavior and Low Energy Architecture: Linking Environmental Adaptation, Personal Comfort, and Energy Use in the Built Environment View project Tools for Evaluating Fault Detection and Diagnostic Methods for HVAC Secondary Systems of a Net Zero Building View project Shun Li. 2010.
- [90] Tu R, Liu XH, Jiang Y. Performance comparison between enthalpy recovery wheels and dehumidification wheels. *International Journal of Refrigeration* 2013;36:2308–22. <https://doi.org/10.1016/J.IJREFRIG.2013.07.014>.
- [91] Güllüce H, Özdemir K. Design and operational condition optimization of a rotary regenerative heat exchanger. *Applied Thermal Engineering* 2020;177:115341. <https://doi.org/10.1016/J.APPLTHERMALENG.2020.115341>.
- [92] Hung YW, Travis Horton W. Semi-empirical mapping method for energy recovery wheel performance simulation. *International Journal of Refrigeration* 2021;123:102–10. <https://doi.org/10.1016/J.IJREFRIG.2020.10.018>.

- [93] de Antonellis S, Intini M, Joppolo CM, Leone C. Design Optimization of Heat Wheels for Energy Recovery in HVAC Systems. *Energies* 2014, Vol 7, Pages 7348-7367 2014;7:7348–67. <https://doi.org/10.3390/EN7117348>.
- [94] Jani DB, Mishra M, Sahoo PK. Performance prediction of rotary solid desiccant dehumidifier in hybrid air-conditioning system using artificial neural network. *Applied Thermal Engineering* 2016;98:1091–103. <https://doi.org/10.1016/J.APPLTHERMALENG.2015.12.112>.
- [95] Khanmohammadi S, Shahsavar A. Energy analysis and multi-objective optimization of a novel exhaust air heat recovery system consisting of an air-based building integrated photovoltaic/thermal system and a thermal wheel. *Energy Conversion and Management* 2018;172:595–610. <https://doi.org/10.1016/J.ENCONMAN.2018.07.057>.
- [96] Panaras G, Mathioulakis E, Belessiotis V, Kyriakis N. Experimental validation of a simplified approach for a desiccant wheel model. *Energy and Buildings* 2010;42:1719–25. <https://doi.org/10.1016/J.ENBUILD.2010.05.006>.
- [97] de Antonellis S, Intini M, Joppolo CM. Desiccant wheels effectiveness parameters: Correlations based on experimental data. *Energy and Buildings* 2015;103:296–306. <https://doi.org/10.1016/J.ENBUILD.2015.06.041>.
- [98] Zhang LZ, Niu JL. Performance comparisons of desiccant wheels for air dehumidification and enthalpy recovery. *Applied Thermal Engineering* 2002;22:1347–67. [https://doi.org/10.1016/S1359-4311\(02\)00050-9](https://doi.org/10.1016/S1359-4311(02)00050-9).
- [99] Nóbrega CEL, Brum NCL. Modeling and simulation of heat and enthalpy recovery wheels. *Energy* 2009;34:2063–8. <https://doi.org/10.1016/J.ENERGY.2008.08.016>.
- [100] Wang P, Gao RX. Automated Performance Tracking for Heat Exchangers in HVAC. *IEEE Transactions on Automation Science and Engineering* 2017;14:634–45. <https://doi.org/10.1109/TASE.2017.2666184>.
- [101] Bilodeau S, Brousseau P, Lacroix M, Mercadier Y. Frost formation in rotary heat and moisture exchangers. *International Journal of Heat and Mass Transfer* 1999;42:2605–19. [https://doi.org/10.1016/S0017-9310\(98\)00323-8](https://doi.org/10.1016/S0017-9310(98)00323-8).
- [102] Comino F, Guijo-Rubio D, Ruiz de Adana M, Hervás-Martínez C. Validation of multitask artificial neural networks to model desiccant wheels activated at low temperature. *International Journal of Refrigeration* 2019;100:434–42. <https://doi.org/10.1016/J.IJREFRIG.2019.02.002>.
- [103] Madhikermi M, Malhi AK, Främling K. Explainable artificial intelligence based heat recycler fault detection in air handling unit. *Lecture Notes in Computer Science (Including Subseries Lecture Notes in Artificial Intelligence and Lecture Notes in Bioinformatics)* 2019;11763 LNAI:110–25. [https://doi.org/10.1007/978-3-030-30391-4\\_7](https://doi.org/10.1007/978-3-030-30391-4_7).
- [104] Zhao Y, Wang S, Xiao F. A statistical fault detection and diagnosis method for centrifugal chillers based on exponentially-weighted moving average control charts and support vector regression. *Applied Thermal Engineering* 2013;51:560–72. <https://doi.org/10.1016/J.APPLTHERMALENG.2012.09.030>.
- [105] Frank S, Lin G, Jin X, Singla R, Farthing A, Zhang L, et al. Metrics and Methods to Assess Building Fault Detection and Diagnosis Tools 2019.
- [106] Altman DG, Bland JM. Diagnostic tests. 1: Sensitivity and specificity. *BMJ: British Medical Journal* 1994;308:1552. <https://doi.org/10.1136/BMJ.308.6943.1552>.
- [107] Kull TM, Mikola A, Tukka A, Köse A, Petlenkov E, Thalfeldt M. Continuous automated ventilation heat recovery efficiency performance assessment using building monitoring system. *E3S Web of Conferences* 2021;246:10006. <https://doi.org/10.1051/E3SCONF/202124610006>.
- [108] Hoogsteen G. A Cyber-Physical Systems Perspective on Decentralized Energy Management 2017. <https://doi.org/10.3990/1.9789036544320>.
- [109] The pandas development team. pandas-dev/pandas: Pandas 2020.

- [110] Harris CR, Millman KJ, van der Walt SJ, Gommers R, Virtanen P, Cournapeau D, et al. Array programming with NumPy. *Nature* 2020;585:357–62. <https://doi.org/10.1038/s41586-020-2649-2>.
- [111] Buitinck L, Louppe G, Blondel M, Pedregosa F, Mueller A, Grisel O, et al. API design for machine learning software: experiences from the scikit-learn project 2013.
- [112] Schreiber J. Pomegranate: fast and flexible probabilistic modeling in python 2017.
- [113] Hossain S. Visualization of Bioinformatics Data with Dash Bio. *Proceedings of the 18th Python in Science Conference* 2019:126–33. <https://doi.org/10.25080/MAJORA-7DDC1DD1-012>.
- [114] al Dakheel J, del Pero C, Aste N, Leonforte F. Smart buildings features and key performance indicators: A review. *Sustainable Cities and Society* 2020;61:102328. <https://doi.org/10.1016/J.SCS.2020.102328>.
- [115] Li H, Hong T, Lee SH, Sofos M. System-level key performance indicators for building performance evaluation. *Energy and Buildings* 2020;209:109703. <https://doi.org/10.1016/J.ENBUILD.2019.109703>.
- [116] Darwazeh D, Gunay B, Duquette J. Development of Inverse Greybox Model-Based Virtual Meters for Air Handling Units. *IEEE Transactions on Automation Science and Engineering* 2021;18:323–36. <https://doi.org/10.1109/TASE.2020.3005888>.
- [117] Horyna V, Hanuš O, Smid R. Virtual Mass Flow Rate Sensor Using a Fixed-Plate Recuperator. *IEEE Sensors Journal* 2019;19:5760–8. <https://doi.org/10.1109/JSEN.2019.2894526>.
- [118] Choi Y, Yoon S. Virtual sensor-assisted in situ sensor calibration in operational HVAC systems. *Building and Environment* 2020;181:107079. <https://doi.org/10.1016/J.BUILDENV.2020.107079>.
- [119] Gomes HM, Read J, Bifet A, Barddal JP, Ao Gama J. Machine learning for streaming data. *ACM SIGKDD Explorations Newsletter* 2019;21:6–22. <https://doi.org/10.1145/3373464.3373470>.
- [120] Merkel D. Docker: lightweight Linux containers for consistent development and deployment. *Linux Journal* 2014;2014.
- [121] Clinton L, Whisnant R. 20 Business Model Innovations for Sustainability. 2014.
- [122] Li J, Li N, Yan R, Farruh K, Li A, Li K. Research on Brick Schema Representation for Building Operation with Variable Refrigerant Flow Systems 2021. <https://doi.org/10.48550/arxiv.2108.07037>.
- [123] Zender-świercz E. A Review of Heat Recovery in Ventilation. *Energies* 2021, Vol 14, Page 1759 2021;14:1759. <https://doi.org/10.3390/EN14061759>.
- [124] Justo Alonso M, Liu P, Mathisen HM, Ge G, Simonson C. Review of heat/energy recovery exchangers for use in ZEBs in cold climate countries. *Building and Environment* 2015;84:228–37. <https://doi.org/10.1016/J.BUILDENV.2014.11.014>.
- [125] Hoval. Design handbook: Rotary heat exchangers. 2021.
- [126] Kim R, Hong Y, Choi Y, Yoon S. System-level fouling detection of district heating substations using virtual-sensor-assisted building automation system. *Energy* 2021;227:120515. <https://doi.org/10.1016/J.ENERGY.2021.120515>.
- [127] Zhou Z, Chen H, Xing L, Li G, Gou W. An experimental study of the behavior of a model variable refrigerant flow system with common faults. *Applied Thermal Engineering* 2022;202:117852. <https://doi.org/10.1016/J.APPLTHERMALENG.2021.117852>.
- [128] Buffa S, Fouladfar MH, Franchini G, Gabarre IL, Chicote MA. Advanced Control and Fault Detection Strategies for District Heating and Cooling Systems—A Review. *Applied Sciences* 2021, Vol 11, Page 455 2021;11:455. <https://doi.org/10.3390/APP11010455>.
- [129] Roulet CA, Heidt FD, Foradini F, Pibiri MC. Real heat recovery with air handling units. *Energy and Buildings* 2001;33:495–502. [https://doi.org/10.1016/S0378-7788\(00\)00104-3](https://doi.org/10.1016/S0378-7788(00)00104-3).
- [130] Holmberg RB. Prediction of condensation and frosting limits in rotary wheels for heat recovery in buildings. *ASHRAE Transactions* 1989:64–9.

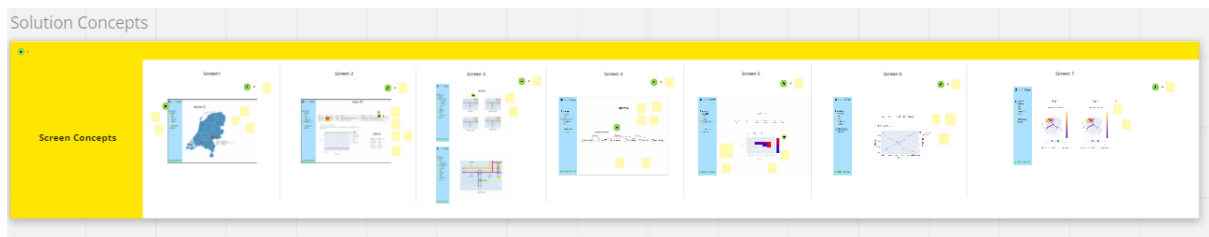
- [131] Montgomery R, McDowall R. Fundamentals of HVAC Control Systems. ASHRAE; 2007.
- [132] Dai M, Lu X, Xu P. Causes of low delta-T syndrome for chilled water systems in buildings. *Journal of Building Engineering* 2021;33:101499. <https://doi.org/10.1016/j.jobbe.2020.101499>.
- [133] van der Horst SAM (Stijn). Economically optimizing maintenance of air handling units. University of Technology Eindhoven, 2019.
- [134] Cui J, Wang S. A model-based online fault detection and diagnosis strategy for centrifugal chiller systems. *International Journal of Thermal Sciences* 2005;44:986–99. <https://doi.org/10.1016/J.IJTHERMALSCI.2005.03.004>.
- [135] Akbari A, Kouravand S, Chegini G. Experimental analysis of a rotary heat exchanger for waste heat recovery from the exhaust gas of dryer. *Applied Thermal Engineering* 2018;138:668–74. <https://doi.org/10.1016/J.APPLTHERMALENG.2018.04.103>.
- [136] Liu Z, Huang Z, Wang J, Yue C, Yoon S. A novel fault diagnosis and self-calibration method for air-handling units using Bayesian Inference and virtual sensing. *Energy and Buildings* 2021;250:111293. <https://doi.org/10.1016/J.ENBUILD.2021.111293>.
- [137] Deshmukh S, Glicksman L, Norford L. Case study results: fault detection in air-handling units in buildings. <https://doi.org/10.1080/1751254920181545143> 2018;14:305–21. <https://doi.org/10.1080/17512549.2018.1545143>.
- [138] Beccali M, Butera F, Guanella R, Adhikari R. PERFORMANCE EVALUATION OF ROTARY DESICCANT WHEELS USING A SIMPLIFIED PSYCHOMETRIC MODEL AS DESIGN TOOL, 2002.
- [139] Zendehboudi A. Implementation of GA-LSSVM modelling approach for estimating the performance of solid desiccant wheels. *Energy Conversion and Management* 2016;127:245–55. <https://doi.org/10.1016/J.ENCONMAN.2016.08.070>.
- [140] Zendehboudi A, Li X. Desiccant-wheel optimization via response surface methodology and multi-objective genetic algorithm. *Energy Conversion and Management* 2018;174:649–60. <https://doi.org/10.1016/J.ENCONMAN.2018.07.078>.
- [141] Parmar H, Hindoliya DA. Artificial neural network based modelling of desiccant wheel. *Energy and Buildings* 2011;43:3505–13. <https://doi.org/10.1016/J.ENBUILD.2011.09.016>.
- [142] Jani DB, Mishra M, Sahoo PK. Performance prediction of rotary solid desiccant dehumidifier in hybrid air-conditioning system using artificial neural network. *Applied Thermal Engineering* 2016;98:1091–103. <https://doi.org/10.1016/J.APPLTHERMALENG.2015.12.112>.
- [143] Angrisani G, Roselli C, Sasso M. Effect of rotational speed on the performances of a desiccant wheel. *Applied Energy* 2013;104:268–75. <https://doi.org/10.1016/J.APENERGY.2012.10.051>.
- [144] Ruivo CR, Costa JJ, Figueiredo AR, Kodama A. Effectiveness parameters for the prediction of the global performance of desiccant wheels – An assessment based on experimental data. *Renewable Energy* 2012;38:181–7. <https://doi.org/10.1016/J.RENENE.2011.07.023>.
- [145] Nasif MS, Morrison GL, Behnia M, Behnia M. Heat and Mass Transfer in Air to Air Enthalpy Heat Exchangers n.d.
- [146] Zhang Z, Jiang C, Zhang Y, Zhou W, Bai B. Virtual entropy generation (VEG) method in experiment reliability control: Implications for heat exchanger measurement. *Applied Thermal Engineering* 2017;110:1476–82. <https://doi.org/10.1016/J.APPLTHERMALENG.2016.09.051>.
- [147] Netherlands: Building Market Brief - Climate-KIC 2018. <https://www.climate-kic.org/insights/netherlands-building-market-brief/> (accessed March 30, 2021).

## 8 APPENDIX

---

### APPENDIX A. DESIGN AND METHODOLOGY

Storyboards prepared using Miro for collecting feedback from stakeholders.



Wall of Justice summarizing the feedback collected from various stakeholders.



The presented initial concepts are tested with stakeholders to develop an initial prototype that is iteratively improved to develop the final product presented in Chapter 4.

## APPENDIX B. SYSTEMS DESCRIPTION, CASE STUDIES,

### Addendum to System Description discussed in section 2.3.1

In the process airstream side (ref. Figure 11), airflow is controlled through the outside air damper. In the Netherlands, to maintain higher ventilation rates AHUs operate with 100% outdoor air control strategy. The supply air contaminants are filtered using an air filter selected to meet constraints such as purchase cost, operational cost, and effectiveness [61]. The effectiveness of a filtered can be measured on a Minimum Efficiency Reporting Values (MERV) scale, which is a 20-point scale where MERV 1 is the least efficient filter whilst MERV 20 is the most efficient type. AHUs being studied in this research are typically employ MERV 5 and above, whilst superior designs of such installations employ Bag type filters that are rated MERV 13 and above.

The inlet stream is then pre-heated or pre-cooled by recovering heat from the extract stream using a heat exchanger such as run-around coil, plate heat exchanger, or rotary heat-exchanger [123]. They are an essential component of the deployed ventilation system, that aid its efficient energetic performance. Rotary heat exchangers recover heat more efficiently than its alternatives such as a plate or run-around coil [124] and are also a common feature of the AHUs deployed at considered case-studies (ref section 3.2). In rotary heat exchangers besides sensible heat, latent heat is also exchanged, which is majorly influenced by material and/or surface of the storage mass[125]. The efficiency of temperature and humidity exchange is measured using (2) and (3) respectively. The reference factor for humidity efficiency is termed as condensation potential, that implies difference between humidity of warm-air and saturation humidity of cold-air [125]. Rotary heat exchangers or heat recovery wheels are manufactured in three designs namely a) Condensation wheel; b) Enthalpy wheel (hygroscopic wheel); c) Sorption wheel [125][125]. The storage mass used for the construction differentiates these three-wheel types. High humidity efficiencies (more than 80%) can be achieved with Condensation wheels that are suited for winter operation. Sorption wheels on the other hand are more suited for summer operation as they helpful in reducing cooling load by drying the fresh air. Moisture transfer happens through pure sorption and no condensation. Enthalpy wheels transmit humidity through both sorption and condensation; however, the sorption component is low and so is the humidity transmission in summer operation.

$$\eta_t = \frac{t_{22} - t_{21}}{t_{11} - t_{21}} \quad (2)$$

$$\eta_x = \frac{x_{22} - x_{21}}{x_{11} - x_{21}} \quad (3)$$

#### Key:

**t** - Temperature (K; °C), **x** - Absolute humidity [g/kg]

11 - Extract air, 21 - Fresh air, 12 - Exhaust air, 22 - Supply air

Commonly studied faults in literature pertaining to HRWs are summarized in Table 23. To this end Madhikermi et al. in [103] point out that fault detection within HRW is cumbersome as failure modes are typically unknown and are mostly unique. However, early diagnosis of such faults is key to economic and energetically efficient operation of AHU.

Table 23: Possible faults in Heat Recovery Wheel

#	Fault	Fault classification	Reference
1	Fouling/Scaling	Component fault	[19,126–128]
2	Leakage/ Air-Short Circuiting/Cross-Contamination	Component fault	[124,129]
3	Frosting	Control fault	[101,124,130]
4	Improper rotational control (stuck, wrong speed etc.)	Control fault	[103]

Post heat recovery, the supply air is heated or cooled to maintain supply air temperature setpoint by regulating the fluid flow through the heating or cooling coil via a control valve. The heat exchange process through the coils is characterized by the material properties of the coil, its geometry and the temperature differences on both air and fluid side [61]. There are primarily two types of configurations for control valves 2-way and 3-way and further three-valve styles namely: globe, butterfly, and ball [131]. These valves are remotely operated via BMS through actuators and modulate the position of its stem against the flow of fluid from Normally Open (NO) or Normally Closed (NC) positions. The flow through the coils is mixed or diverted for 3-Way valves configurations or throttled in case of 2-Way Valves configurations. Flow modulation through the valves can either be quick opening, linear, parabolic, and equal percentage adjustments (see Figure 44), which serves as one of the key characteristics when selecting the valves[132]Valve flow characteristic observed at the 3-way control valve deployed at Breda (see section 2.3.2) is also shown in Figure 44. Any faults within heating and/or cooling coils often would reduce the system efficiency [19]. The most encountered faults within these coils are fouling, scaling, leaking and/or stuck valve [19].

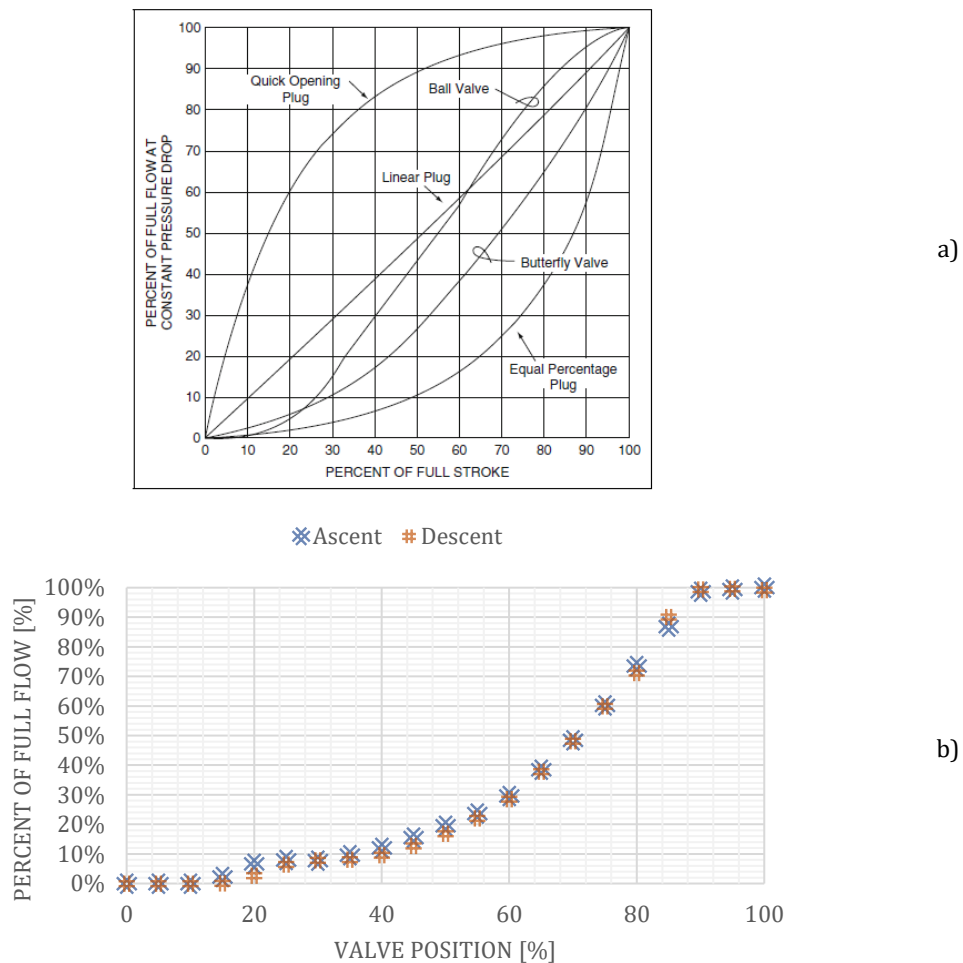


Figure 44: a) General valve characteristics at constant pressure drop [131]; b) valve characteristics of the three-way valve deployed at Breda office

Downstream of coils, air-handling systems typically employ centrifugal or axial fans to control the flow of air [61]. The fan speed is regulated using a variable frequency drive (VFD) connected to the fan motor, which regulates it to maintain a static pressure setpoint. The coupling mechanism between the fan motor and drive can either be direct or using a belt-drive. At the two validation cases considered (ref. section 2.3.2), although fans are equipped with VFDs, they are operated at a constant speed for employing a CAV strategy. For characterizing fans in performance curves provided by their OEM are typically studied [133]. Most common failure modes within fans are burning-out of motor, loose, or broken fan belt, out-of-balance impeller, power control issues [23].

In BMS systems, controllers are operated on a series of pulses based on control logics [131]. These digital controls are often referred to as Direct Digital controls or simply DDC. Often proportional, integral, and differential (PID) and closed loop control strategy is deployed for cooling or heating control valves. DDC-based temperature controller for cooling and heating coil valve control is shown in Figure 45. Typically, the feedback for the valve control is a combination of outdoor air, return and supply air conditions. Control sequence for operation of cooling and heating valves installed at case study discussed in section 2.3 is shown in Figure 45. This sequential operation of AHU is often referred to cooling and heating mode operation.

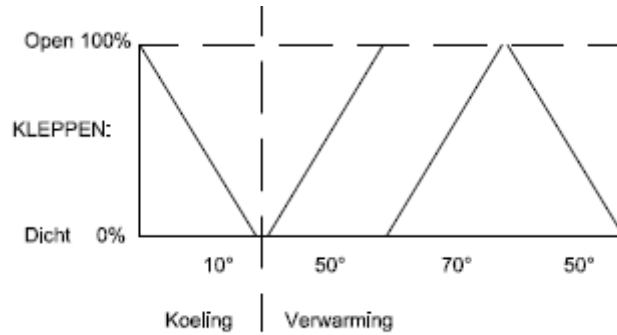


Figure 45: Control sequence of AHU operation – Nijmegen school

On the return side, the extract or return air is filtered before undergoing regeneration process within the heat exchanger. The filter employed in this case is typically rated at the same or lower MERV levels than the supply filter. The air of the heat recovery process is exhausted using an exhaust fan, that typically operates at a slightly lower speed than supply fan. This strategy of slightly imbalanced flow is deployed to prevent the risk of leakage from return to supply by maintaining a constant positive pressure between the two. Although, in field deployments the static pressure difference  $\Delta p_{22-11}$  (see Figure 46) is often negative, which leads to contamination of supply air stream necessitating additional measures [9]. The fraction of extract air in supply air, is termed as exhaust air transfer ratio (EATR).

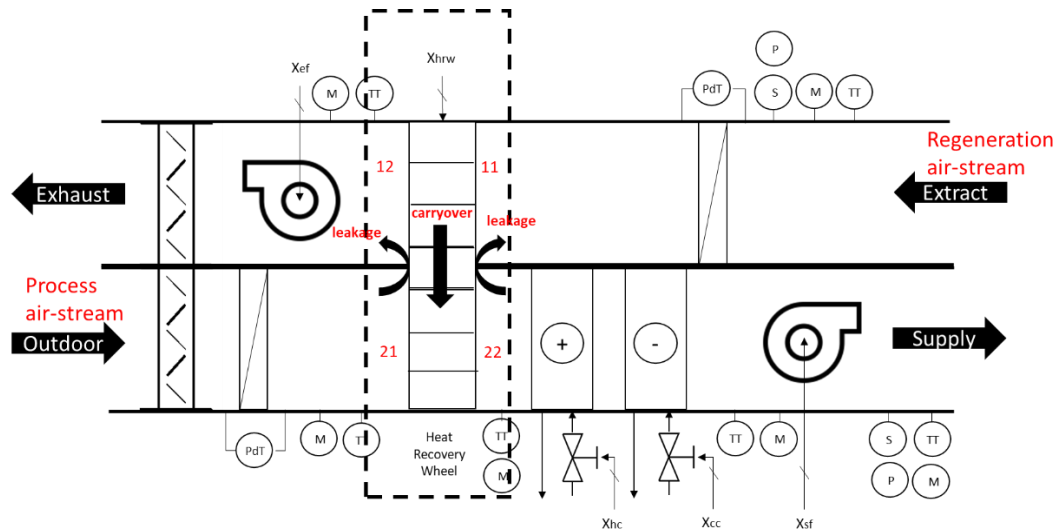


Figure 46: General AHU schematic showing leakage of air around heat recovery wheels (HRWs)

### Energy resource station (ASHRAE RP1312A)

The schematic of the AHU installed at the building is provided below. For me details on introduced faults refer to [66,88,89] and for detailed description of the building refer to [74]

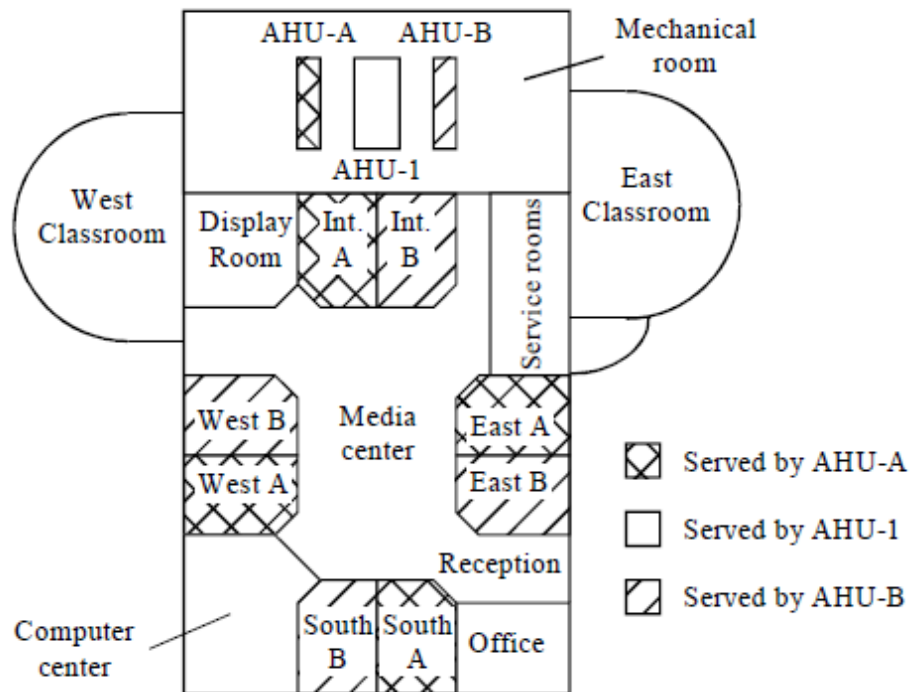


Figure 47: AHUs installed at Energy Resource Station building

### Hoofddorp office

The chosen building is an office building located in Hoofddorp close to Schipol airport. Four Air-Handling Units (AHUs) are installed on its roof. Further, data from these AHUs collected between January 2011 and November 2019, is utilized for this analysis. Furthermore, the list of available measurements on the AHUs along with its design parameters are provided in [133]

## Breda office

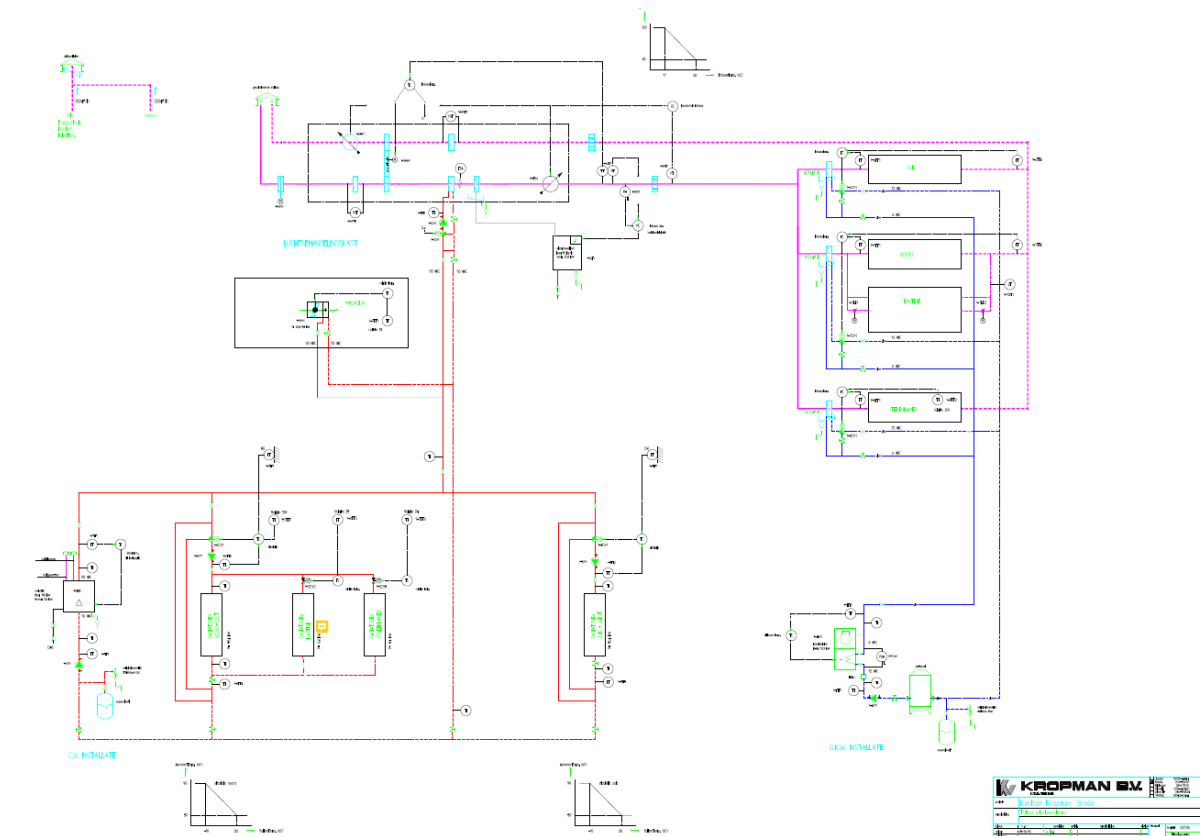


Figure 48: P&ID Breda office

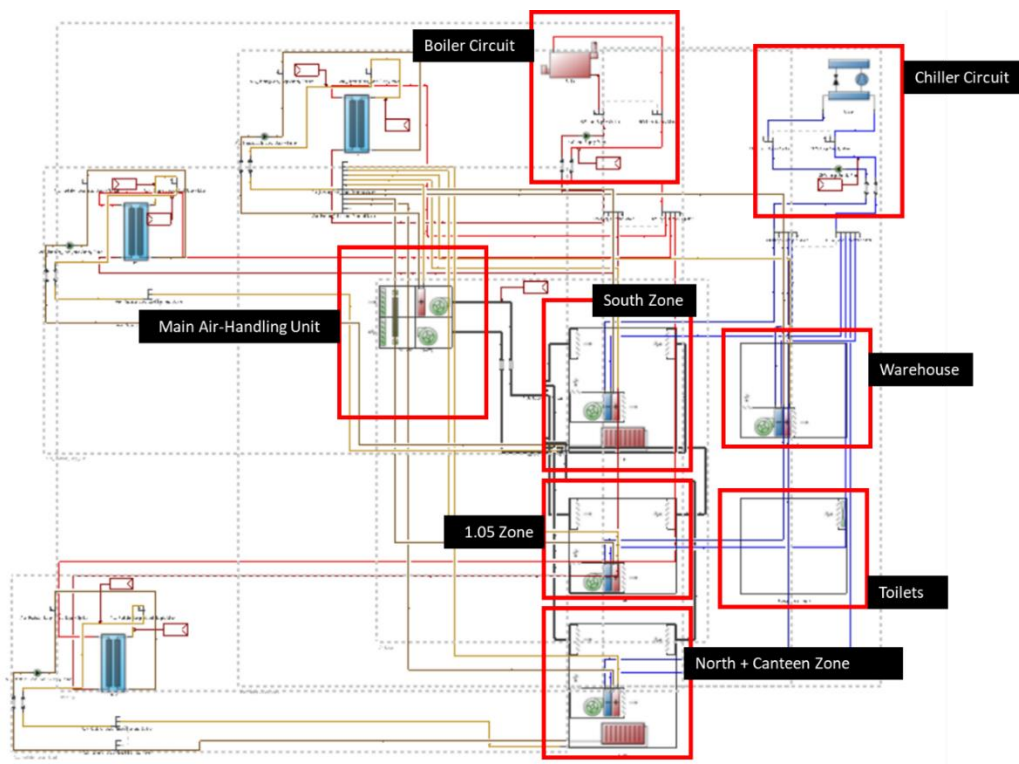


Figure 49: Breda simulation model - HVAC layout - heating operation

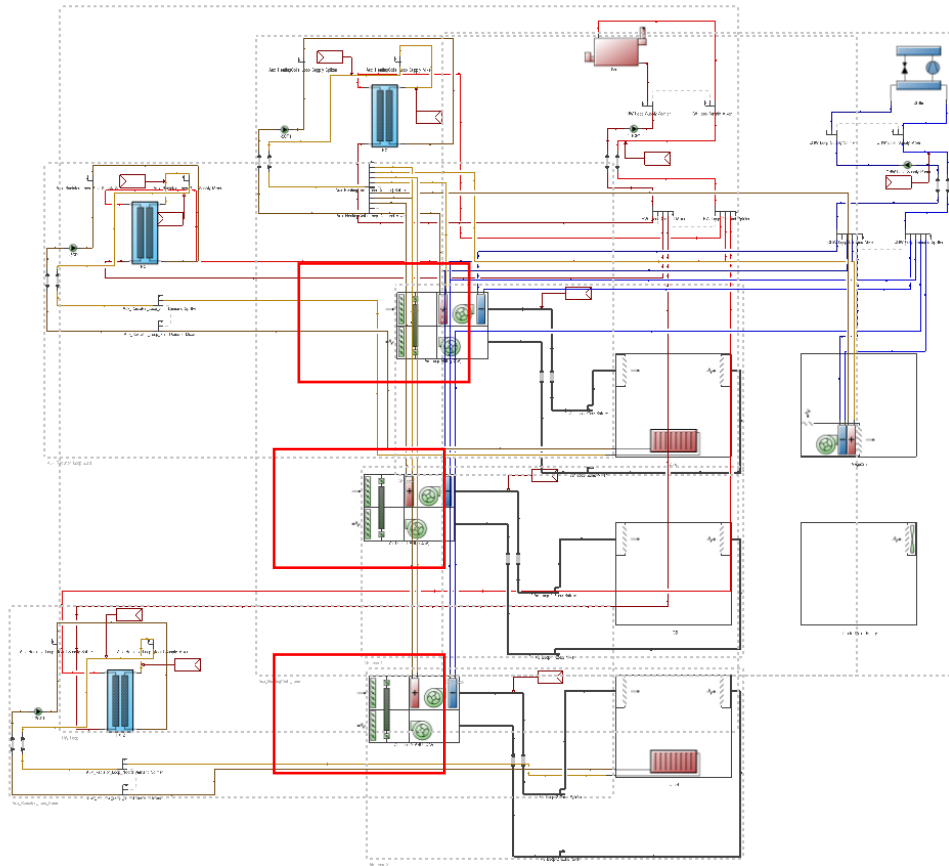


Figure 50: Breda simulation model - HVAC layout - cooling operation

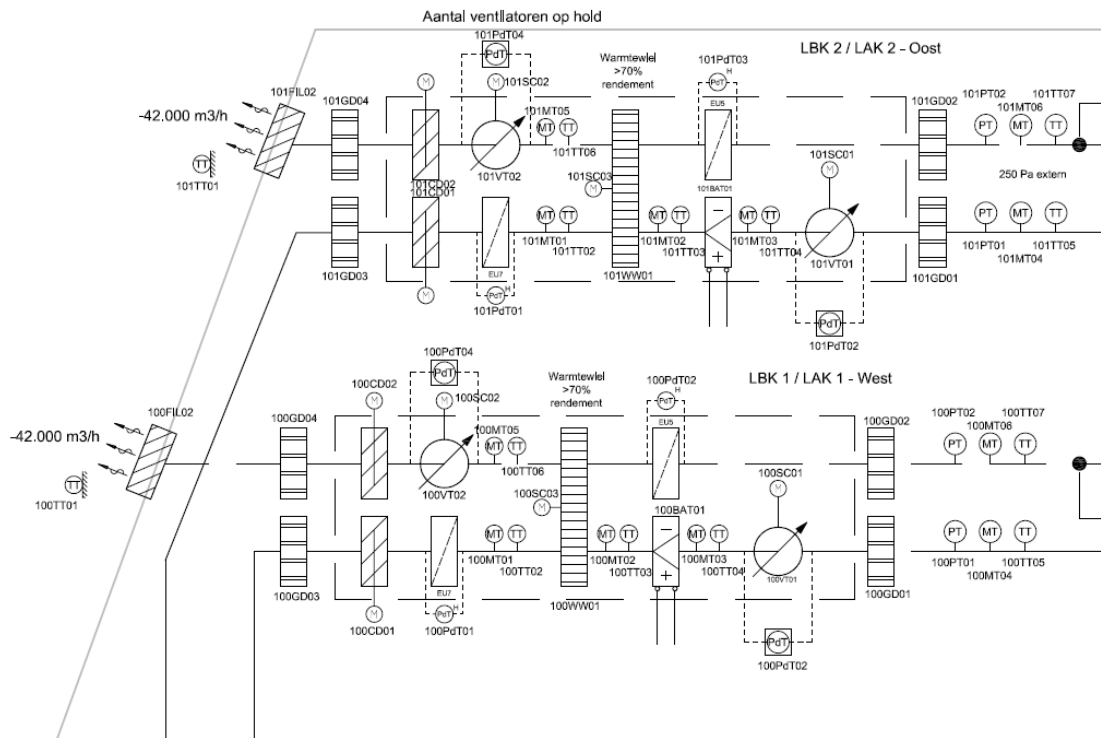


Figure 51: P&ID subsection Nijmegen school

## APPENDIX C. FAULT IMPACT ANALYSIS AND SENSOR IMPACT ANALYSIS

### Fault Modelling with EnergyPlus

Table 24: Fault Modelling Strategy

Fault No.	System Function	System Element	Fault	Fault Group	Method fault introduction in EnergyPlus Model	Corresponding Object in EnergyPlus	Observed Model Weaknesses or Identified from Literature
F1	Cooling	Valve	Valve stuck open	Stuck Fault	Set the minimum chilled water flow to its maximum value using EnergyPlus Energy Management System (EMS). Studied by setting minimum chilled water flow through the coil to 99% of Maximum Actuated Value.	Controller:WaterCoil	Difficult or impossible to emulate complete Valve characteristic without external interfacing. Valve control only limited to flow rate variation
F2	Cooling	Valve	Valve stuck closed	Stuck Fault	Set the minimum and maximum actuated values of chilled water flow as close to zero as possible.	Controller:WaterCoil	
F3	Cooling	Valve	Valve stuck partially open	Stuck Fault	Set the minimum and maximum actuated values of chilled water flow to value corresponding to the position valve is stuck using EnergyPlus EMS.	Controller:WaterCoil	
F4	Cooling	Valve	Leaky valve	Performance Degradation	Using EnergyPlus EMS set the minimum value to a percentage value of the maximum actuated flow, to emulate a percentage equivalent to the leak.	Controller:WaterCoil	
F5	Cooling	Valve	Unstable valve control	Control Fault	EnergyPlus does not currently support dynamic control	NA	Dynamic Valve actuation such as PID type controls cannot be simulated without external interfacing

F6	Cooling	Coil	Coil fouling	Fouling Fault	Vary FouledUARated or FoulingFactor to apply severity.	FaultModel:Fouling:Coil	Pressure drop across the coil is ignored
F7	Heating	Valve	Valve stuck open	Stuck Fault	Set the minimum hot water flow to its maximum value using EnergyPlus Energy Management System (EMS).	Controller:WaterCoil	Difficult or impossible to emulate complete Valve characteristic without external interfacing. Valve control only limited to flow rate variation
F8	Heating	Valve	Valve stuck closed	Stuck Fault	Set the minimum and maximum actuated values of hot water flow close to zero	Controller:WaterCoil	
F9	Heating	Valve	Valve stuck partially open	Stuck Fault	Set the minimum and maximum actuated values of hot water flow to value corresponding to the position valve is stuck using EnergyPlus Energy Management System (EMS).	Controller:WaterCoil	
F10	Heating	Valve	Leaky valve	Performance Degradation	Set the minimum value to a percentage value of the maximum actuated flow, to emulate a percentage equivalent to the leak using EnergyPlus Energy Management System (EMS).	Controller:WaterCoil	
F11	Heating	Valve	Unstable valve control	Control Fault	EnergyPlus does not currently support dynamic control	NA	Dynamic Valve actuation such as PID type controls cannot be simulated without external interfacing
F12	Heating	Coil	Coil fouling	Fouling Fault	Vary FouledUARated method or FoulingFactor method to apply severity. For the studied case fault was modelled with 40% severity.	FaultModel:Fouling:Coil	Pressure drop across the coil is ignored
F13	Ventilation	Damper	Outdoor air intake	Stuck Fault	The general methodology for introduction of this fault is by changing the amount of minimum air	Controller:Outdoor Air	Detailed Controller response

			damper stuck		introduced to be introduced into the system. Although, it comes with a pre-requisite being that economizer should be operational (Y. Li & O'Neill, 2016) or a demand control ventilation strategy be utilized. However, since both cases are not true for the studied case, hence the strategies for modelling procedure do not yield any impact. Hence it was ignored from final fault impact analysis.		modelling possibilities are insufficient and hence require external interfacing
F14	Ventilation	Damper	Return air damper stuck	Stuck Fault	The studied case study building does not carry a return side damper and hence the fault modelling for the fault has not been pursued further.		-
F15	Ventilation	Damper	Exhaust air damper stuck	Stuck Fault	The studied case study building does not carry a exhaust side damper and hence the fault modelling for the fault has not been pursued further.		-
F16	Ventilation	Fan	Fan Motor Efficiency degradation	Performance Degradation	The fault was applied by changing the efficiency value of the fan motor. The fault was studied to emulate a 20% degradation than nominal value.	Fan:VariableVolume> Fan Total Efficiency	The fan power equation, does not explicitly take Fan Motor efficiency into account
F17	Ventilation	Fan	Supply fan stuck at constant rate	Stuck Fault	Set the Fan Power Minimum Flow Fraction or Fan Power Minimum Flow Rate to higher value than default. A fan stuck at 50% of maximum supply flow rate situation was emulated.	Fan:VariableVolume>FanPowerMinimumFlowFraction	Detailed pressure drop characteristics cannot be emulated in a dynamic fashion using the utilized Fan object. Further, can be extended to incorporate

							te VFD control characteristics.
F18	Ventilation	Fan	Return Fan stuck at constant rate	Stuck Fault	The modelling methodology is the same as demonstrated for Supply Fan fault modelling. Since, the current baseline model doesn't contain a supply fan, this fault is ignored for this study.	Fan:VariableVolume>Maximum Flow Rate	-
F19	Ventilation	Fan	Return fan complete failure	Abrupt Fault	Set the maximum flow rate for the fan to a value close to zero. In the studied case study AHU, there is no fan on the return side hence it was not modelled.	Fan:VariableVolume>Maximum Flow Rate	-
F20	Ventilation	Fan	Supply fan complete failure	Abrupt Fault	Set the maximum flow rate for the fan to a value close to zero	Fan:VariableVolume>Maximum Flow Rate	-
F21	Ventilation	Duct	Duct fouling	Fouling Fault	Duct fouling is caused due to the dust that accumulates in the various components along the supply path, thereby causing a reduction in the air flow. This fault in effect can be modelled in the same way as fouling filter fault. From the relation between pressure drop and mass flow rate at maximum fan speed condition, the pressure drop can be estimated at reduced air flow condition. This increased pressure drop can then be specified in the FoulingFilter object to emulate the fouling duct scenario and explained in detailed in this report with the explanation for Fouling Filter. Fault was modelled with a severity of 10%, which emulates a 10% increase in pressure	FaultModel:Fouling:AirFilter	Separate Native Fault object should be introduced for this.

					drop over the nominal value.		
F2 2	Ventilation	Duct	Duct leakage	Performance Degradation	<p>The duct leakage in EnergyPlus is modeled using the EnergyPlus Simplified Duct Leakage Model (SDLM). Here the supply or return duct leakage can be easily modeled by specifying the nominal upstream and constant downstream leakage fraction values. The nominal upstream leakage fraction is the fraction of leaked air upstream of the terminal unit and similarly downstream leakage fraction implies leakage downstream of the terminal unit. The leakage fraction can be varied up to 30%. For the studied scenario a higher side 10% leak upstream of the terminal unit was applied in the fault model.</p>	ZoneHVAC:AirDistributionUnit > Nominal Upstream Leakage Fraction, Constant Downstream Leakage Fraction	-
F2 3	Ventilation	Filter	Fouling Air Filter	Fouling Fault	<p>The fault is applied by understanding the system curve for dirty filter condition and tracing it on the fan curve. Three particular conditions are possible a) where a variable speed fan is able to meet the required airflow, b) The variable speed fan cannot increase the speed any further to meet the air flow requirements, and c) constant speed fan cannot meet the increased flow. The increased resistance due to fouling filter causes excess pressure drop which is larger than design pressure drop. This increased pressure drop proportional to resistance is utilized to introduce severity. In the studied case faults with 20% severities were introduced. For the solver</p>	FaultModel:FoulingAirFilter	-

					to identify the system curve for the fouled filter, a fan curve corresponding to its maximum speed was provided.		
F24	Ventilation	Filter	Broken Air filter	Abrupt Fault	In effect broken filter would lead to a reduction in pressure drop across the filter and would produce an effect opposite to observed whilst modeling a fouling filter fault. The fault is applied by understanding the system curve for broken filter condition and tracing it on the fan curve. The decreased pressure drops which is smaller than design pressure drop, would lead to a higher air mass flowrate being introduced. The pressure drop proportional to leak is utilized to introduce severity. In the studied case 20% severity were introduced, which is in line with similar study carried out by (Zhao et. al., 2014). For the solver to identify the system curve for the fouled filter, a fan curve corresponding to its maximum speed was provided.	FaultModel:Fouling:AirFilter	-
F25	Sensing	Sensor	Cooling Coil Supply air temperature bias	Sensor Fault	Fault is applied by providing a schedule, severity, and offset value for the bias by specifying these values using the Native Fault Objects.	FaultModel:TemperatureSensorOffset:CoilSupplyAir	The chosen sensor fault model can be extended to include other fault characteristics such as transient nature or development time etc if a deeper
F26	Sensing	Sensor	Heating Coil Supply air temperature bias	Sensor Fault	Fault is applied by providing a schedule, severity and offset value for the bias by specifying these values using the Native Fault Objects.	FaultModel:TemperatureSensorOffset:CoilSupplyAir	
F27	Sensing	Sensor	Return air temperature	Sensor Fault	Fault is applied by providing a schedule, severity and offset value for the bias by specifying	FaultModel:TemperatureSen	

			ature bias		these values using the Native Fault Objects. The fault model was tested, however as the return side fan was not modelled, hence introduction of any faulty condition didn't yield impact the energy performance. Also, the control of the modelled Heat Recovery unit was assumed to be static in nature.	sorOffset: ReturnAir	analysis is required
F28	Sensing	Sensor	Mixed air temperature bias	Sensor Fault			
F29	Sensing	Sensor	<a href="#">Supply air pressure sensor</a>	Sensor Fault	EnergyPlus does not currently support dynamic control. More specifically, in EnergyPlus fan are modelled with simple polynomial curve fit models. Detailed fan modelling such as duct-static-pressure reset strategies are possible, however again only through specific performance curves and not sensor based dynamic control strategies.		
F30	Sensing	Sensor	Other sensors that may be available -Rh	Sensor Fault	Relative Humidity Sensor faults are supported by EnergyPlus through native fault objects called <i>FaultModel:HumidistatOffset</i> that can possibly affect humidity control strategy if applied at cooling coil level. However, since the boundary of this study is limited to AHU, this fault is ignored for further consideration.		
F31	Sensing	Sensor	Other sensors that may be available -CO2	Sensor Fault			
F32	Control	Controller	Min. outdoor airflow setpoint inappropriate	Control Fault	The fault does not apply to the studied HVAC configuration and is applicable for Air-Handling Units with an Air Side Economizer.		
F33	Control Control	Controller	Max. airflow setpoint inappropriate	Control Fault	The fault does not apply to the studied HVAC configuration and is applicable for Air-Handling Units with an Air Side Economizer.		

F3 4	Control Control	Controller	Max. outdoor airflow setpoint inappropriate	Control Fault	The fault does not apply to the studied HVAC configuration and is applicable for Air-Handling Units with an Air Side Economizer.		
F3 5	Control	Controller	Cooling Supply air temperature setpoint too low	Control Fault	Setpoints in Energy+ are controlled by a specialized object called Setpoint Manager. The same can be utilized to change the setpoint to higher or lower value to emulate the fault effect. A 9°C temperature set point was defined to emulate an approximate 20% deviation from baseline scenario.	Setpoint Manager: Scheduled	-
F3 6	Control	Controller	Heating Supply air temperature setpoint too low	Control Fault	Setpoints in Energy+ are controlled by a specialized object called Setpoint Manager. The same can be utilized to change the setpoint to higher or lower value to emulate the fault effect. A 9°C temperature set point was defined to emulate an approximate 20% deviation from baseline scenario.	Setpoint Manager: Scheduled	-
F3 7	Control	Controller	Cooling Supply air temperature setpoint too high	Control Fault	Setpoints in Energy+ are controlled by a specialized object called Setpoint Manager. The same can be utilized to change the setpoint to higher or lower value to emulate the fault effect. A 17°C temperature set point was defined to emulate an approximate 20% deviation from baseline scenario.	Setpoint Manager: Scheduled	-
F3 8	Control	Controller	Heating Supply air temperature setpoint	Control Fault	Setpoints in Energy+ are controlled by a specialized object called Setpoint Manager. The same can be utilized to change the setpoint to higher or lower value to emulate the fault effect. A	Setpoint Manager: Scheduled	-

			t too high		17°C temperature set point was defined to emulate an approximate 20% deviation from baseline scenario.		
F39	Control	Controller	Inappropriate scheduling of fans and coils	Control Fault	The stated fault deals with dynamic occupancy-based schedules as opposed to constant schedules assumed in the baseline model used for this study. Hence, this fault is not studied further. In theory, to study this fault accurately EnergyPlus would require to be interfaced with other software to emulate a dynamic response model over multiple simulations.	-	

## Sensor Impact Analysis

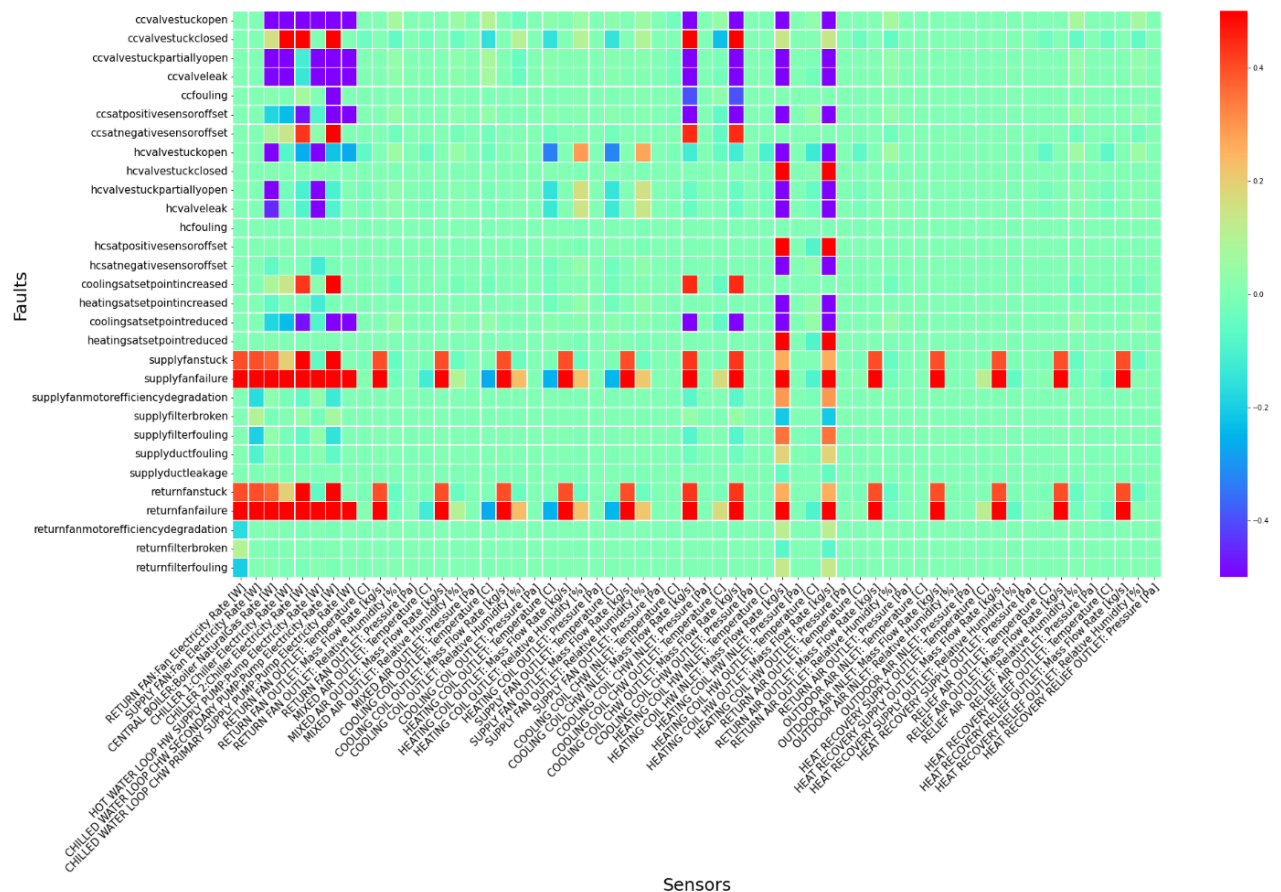


Figure 52: Sensor impact analysis: 5-zone building - Peak weather

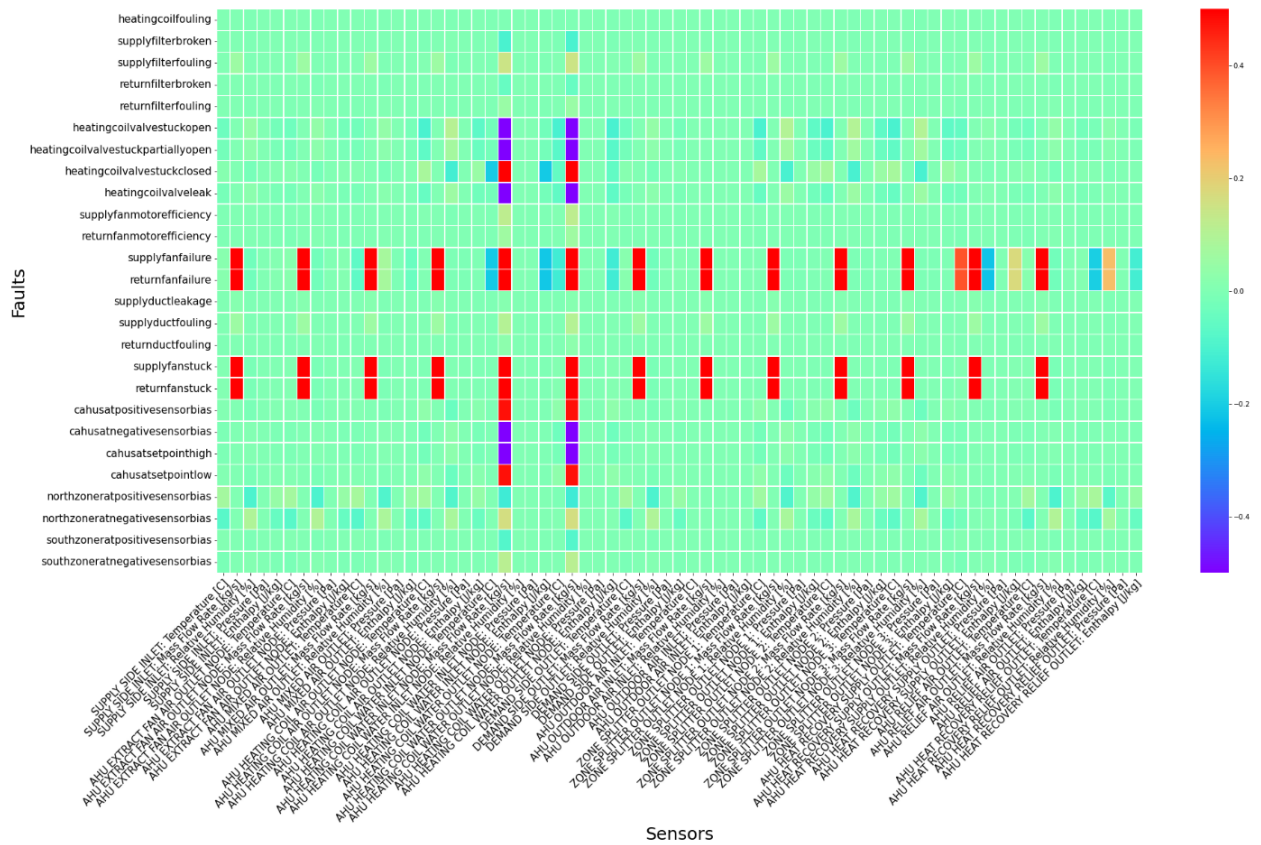


Figure 53: Sensor impact analysis - Breda office - Peak winter period

## Fault Impact analysis

Figure 54 and Figure 55 show deviation from energy baseline.

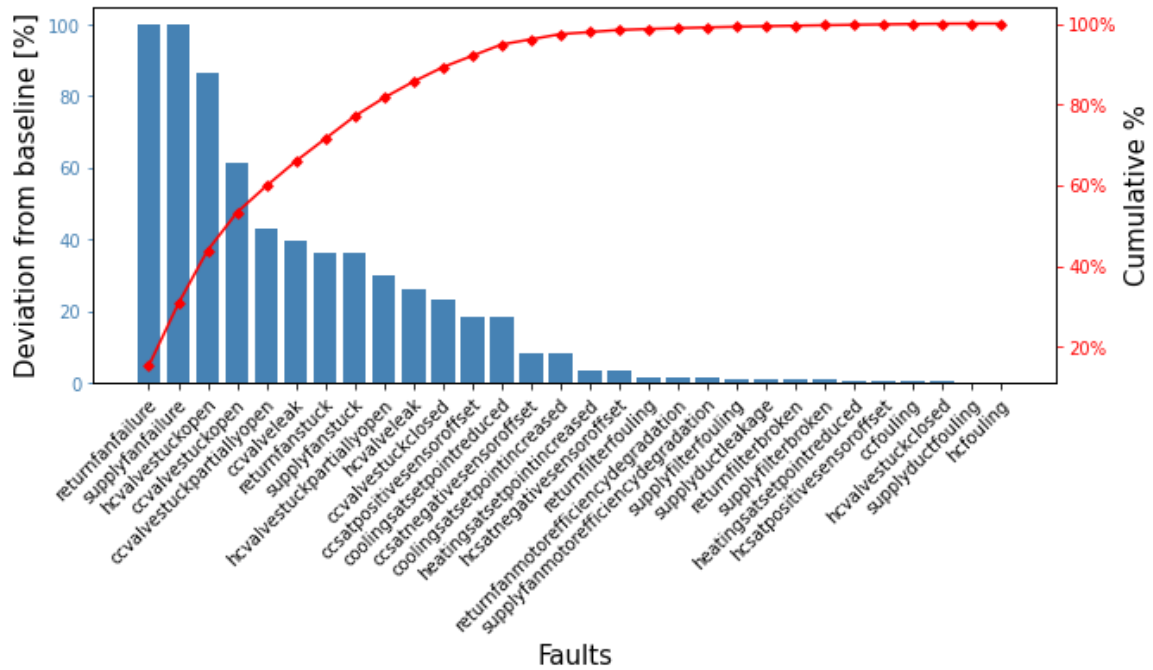


Figure 54: Fault impact analysis: 5-zone building - Peak weather period

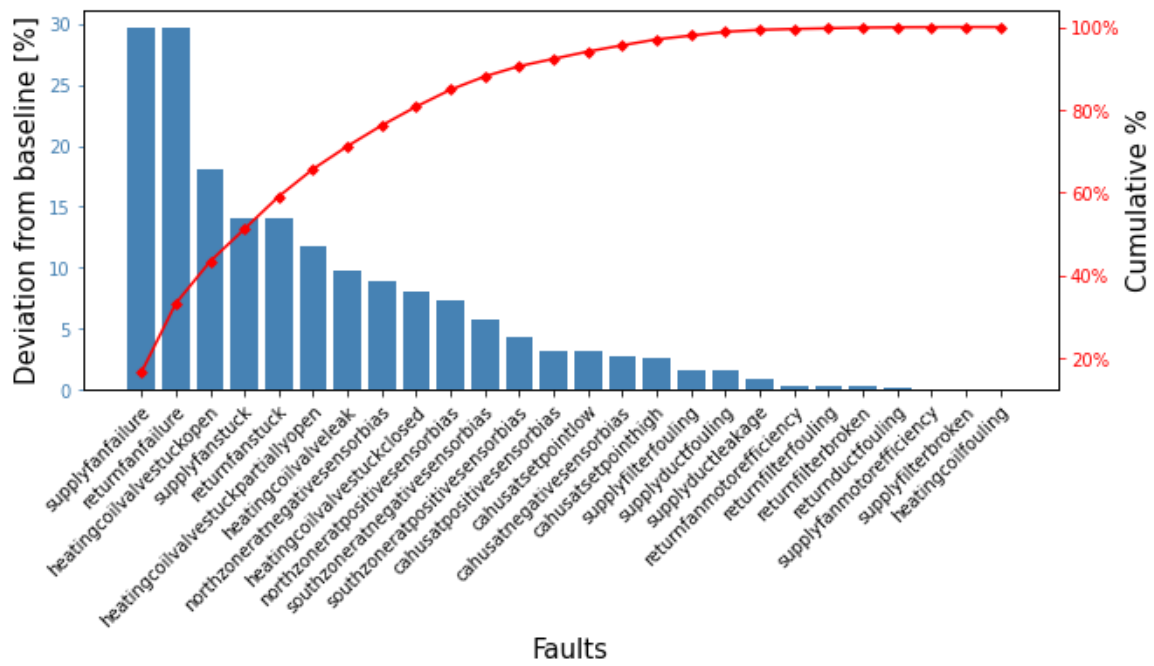


Figure 55: Fault impact analysis - Breda office - Peak winter period

## APPENDIX D. FDD BUSINESS LAYER – FAULT DETECTION AND FAULT DIAGNOSIS

Table 25: Features Utilized for training Cooling and Heating Valve Prediction Models at Energy Resource Station and Hoofddorp office

Case-Study Building Name	Energy resource station	Hoofddorp office	Energy resource station	Hoofddorp office
Cooling/Heating Valve Position Prediction Model	Cooling Valve Position Prediction	Heating Valve Position Prediction	Heating Valve Position Prediction	Heating Valve Position Prediction
AHU Reference	AHU B	AHU 2	AHU B	AHU 2
Features used for prediction	Exhaust Air Damper, Chilled Water Pump CHWP-A Water Flow Rate, Sum of Room Supply Air Flow Rates, Return Air Flow Rate, Outside Air Flow Rate, AHU Supply Air Temperature, Mixed Air Temperature, Return Air Temperature, Heating Water Coil, Discharge Air Temperature, Supply Air Duct Static Pressure, Supply Fan VFD Speed, Return Fan VFD Speed, Supply Air Humidity, Return Air Humidity, Outside Air Temperature, OA Duct Temperature, Heating, Water Coil Leaving Water Temperature, Heating Water Coil, Mixed Water Temperature, Chilled Water Coil Entering Water Temperature, Chilled Water Coil Leaving Water Temperature, Chilled Water Coil Mixed Water Temperature	Supply ventilator [rpm], Supply ventilator [kW], Exhaust ventilator [rpm], Exhaust ventilator [kW], Control wtw [%], PdT supply filter [Pa], Supply water temp. [°C], Retour water Temp. [°C], PT Supply [Pa], Supply air Temp. [°C], Supply air Hum. [%], Exhaust air Temp. [°C], Exhaust air Hum. [%], PT Exhaust [Pa], PdT Exhaust Filter [Pa], Control Exhaust Vent. [%], Outside Temp. [°C], Outside Hum. [%], Inlet Temp LBK2 [°C]	MA-TEMP SA-TEMP HWC-DAT HWP-GPM OAD-TEMP HWC-LWT RMT-CFM dayofweek hour RA-TEMP	Supply water temp. [°C] Exhaust air Temp. [°C] Retour water Temp. [°C] Outside Temp. [°C] PdT supply filter [Pa] PdT Exhaust Filter [Pa] Supply air Hum. [%] hour Supply air Temp. [°C] Control Exhaust Vent. [%] Supply ventilator [rpm] dayofyear week dayofweek PT Exhaust [Pa] Exhaust air Hum. [%] month Outside Hum. [%] Exhaust ventilator [kW] PT Supply [Pa]

The list of faults along with respective date on which the fault was introduced are summarized in the Table 26 shown below. For all day's fault is applied for the entire occupancy period i.e., between 06:00-18:00. More information on how these faults were introduced can be found in [66]

Table 26: List of faults introduced at Energy resource station building [66]

Fault description	Date
EA Damper Stuck (Fully Open)	20/8/2007
EA Damper Stuck (Fully Close)	21/8/2007
Return Fan at fixed speed (30% speed)	22/8/2007
Return Fan complete failure	23/8/2007
Cooling Coil Valve Control unstable (Reduce PID PB by half)	24/8/2007
Cooling Coil Valve Reverse Action	3/9/2007
OA Damper Stuck (Fully Closed)	26/8/2007
Cooling Coil Valve Stuck (Fully Closed)	27/8/2007
Cooling Coil Valve Stuck (Fully Open)	31/8/2007
Cooling Coil Valve Stuck (Partially Open - 15%)	1/9/2007
Cooling Coil Valve Stuck (Partially Open - 65%)	2/9/2007
Heating Coil Valve Leaking (Stage 1 - 0.4GPM)	28/8/2007
Heating Coil Valve Leaking (Stage 2 - 1.0GPM)	29/8/2007
Heating Coil Valve Leaking (Stage 3 - 2.0GPM)	30/8/2007
OA Damper Leak (45% Open)	5/9/2007
OA Damper Leak (55% Open)	6/9/2007
AHU Duct Leaking (after Supply Fan)	7/9/2007
AHU Duct Leaking (before Supply Fan)	8/9/2007

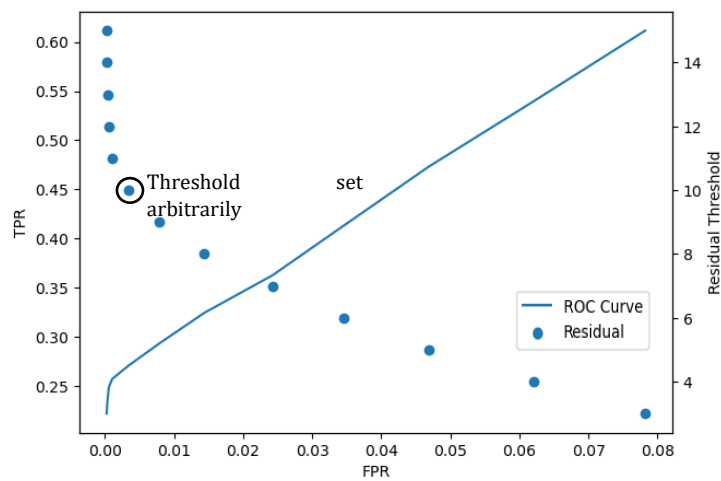
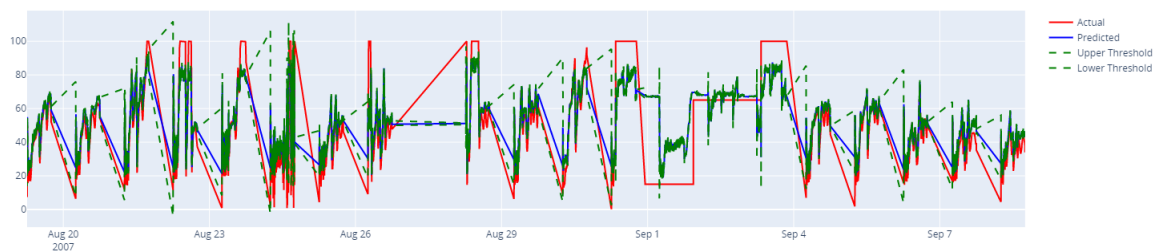


Figure 56: ROC curve for tuning the residual threshold of the developed cooling coil valve prediction model

### Dynamic Threshold method for generating residuals

As was discussed in Section 2.3 and Section 2.4, the usefulness of the model can be improved by determining the right threshold on the residual utilized determining the boundary between faulty and normal behaviour. An appropriate threshold setting is important for both early and robust fault detection [134]. The uncertainty of the residual is characterized by uncertainty due to both model fitting and measurement errors. To overcome this uncertainty, the confidence of the prediction can be improved further by dynamic threshold setting and moving this process online wherein the threshold can be determined in real-time [134]. [13] surveyed various articles and found that moving average and exponentially weighted moved average (EWMA) that utilize time series modelling approaches are quite popular. Besides, [60] also surveyed literature on this topic and identified the popularity of statistical modelling techniques. [60] proposed a dynamic threshold setting method that emanates from Chebyshev's inequality that can handle a wide range of probability distributions. They propose a moving window approach wherein mean and standard deviation of a predicted variable are computed on a rolling window basis. A dynamic threshold can be computed by varying the hyperparameters of this model. The two hyperparameters moving window width and number of standard deviations can be set to improve fault classification accuracy.

This method is tested to understand the possibility for inclusion in the fault detection process discussed in section 3.4. The following Figure 57 showcases the results from testing this approach for Energy resource station building case study. To ascertain its efficacy the classification accuracy of the model which incorporates correctly classifying both normal and faulty behaviour is compared with fixed threshold method. The hyperparameters window size and no. of standard deviations were set to 10 and 3 respectively. Since, the data is sampled at every minute a value of 10 implies a window size of 10 minutes, whilst 3 implies the equivalent standard deviations away from the computed mean within the moving window. Using this approach, an upper and lower threshold are determined. Here, both thresholds are important since an upper threshold controls the energy cost whilst lower threshold controls the comfort cost.



*Figure 57: Fault detection with dynamic threshold*

For comparison, a fixed threshold with a magnitude of  $\pm 8\%$  was utilized. This was the inflection point observed on plot shown in Figure 56. Comparing the two, with the fixed threshold method a classification accuracy of 44% was observed whilst it improved to 68% when threshold was determined dynamically. This gain of over 50% points to the effectiveness of the approach.

## Feature selection using SHAP

Features selected using RFECV and PCC and iterated in Table 12 are analysed and their contribution is shown in Figure 58a). The graph shows rank ordered contribution of features based upon their mean absolute impact on the model's prediction. Further, these features are iteratively selected in the order of highest absolute impact. Least impactful features are dropped, and model's performance is tested on key performance indicators (KPIs): R2 score, and root mean squared error (RMSE). It can be observed from Figure 58b) that after selecting the top seven features, the performance on the model on the KPIs doesn't improve significantly. Hence, these top seven features are finalized, and the model trained using these features was proceeded with for fault detection.

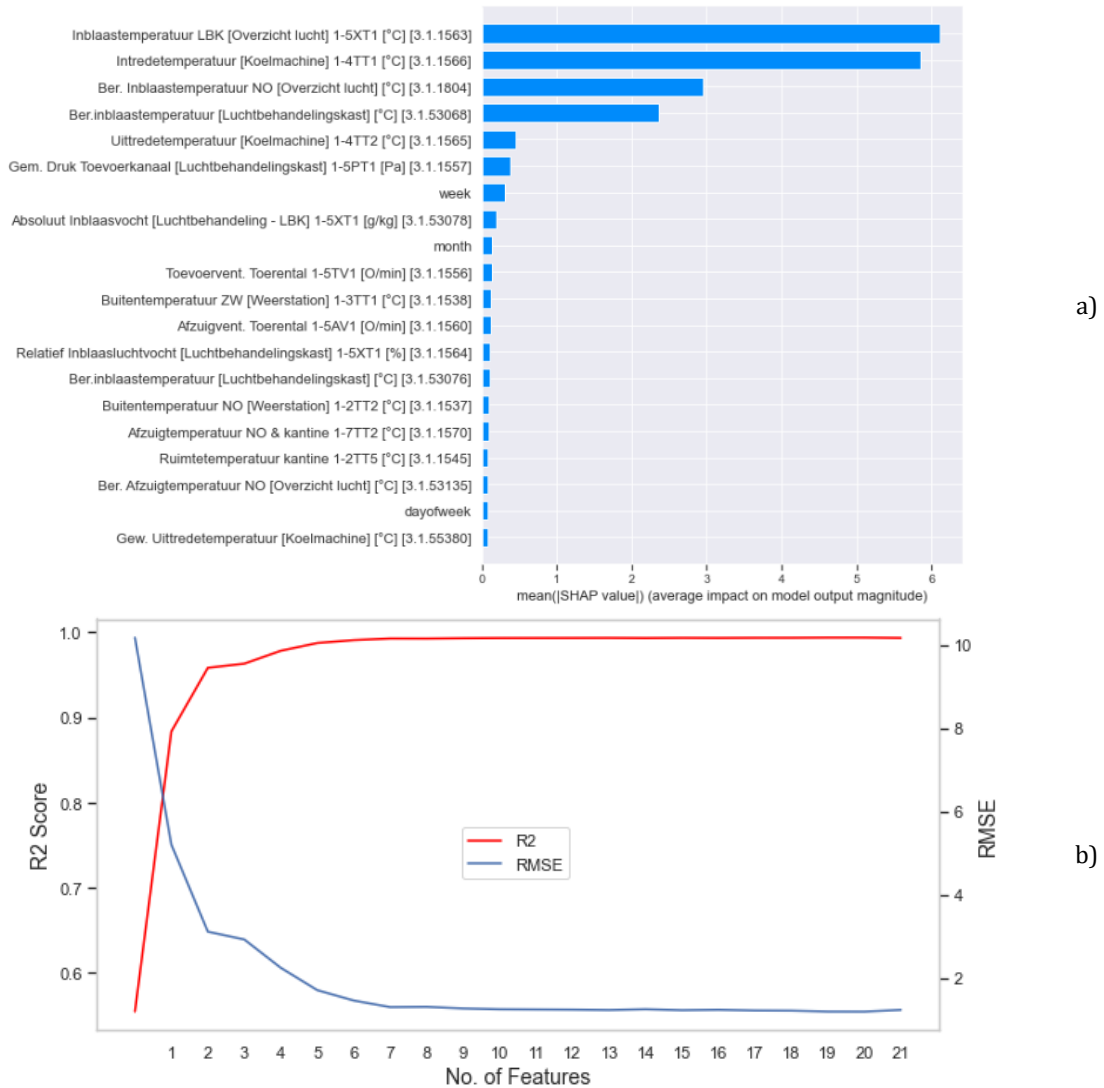


Figure 58: Feature contribution evaluation using SHAP

## Experiments to evaluate lead-time of trained ML models

In general limitation of a tree-based models such as XGBoost with decision trees used earlier is their inability to extrapolate beyond the data observed in the training set. Therefore, it's important to further explore the generalization character of trained models presented earlier. The model performance is explored at Hoofddorp office and Breda office by training data from a cooling season of an year using the approach discussed in section 3.4 and is summarized in plots shown in Figure 59.

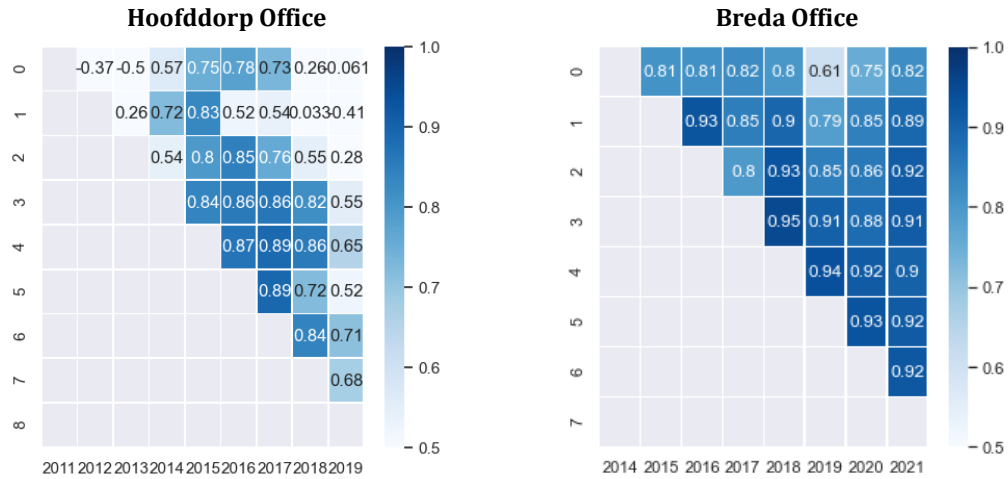


Figure 59: Experiments to evaluate lead-time for black-box models with datasets from Hoofddorp office and Breda office

At Nijmegen school for the experiments, the available dataset from 2020 until 2021 was utilized. This dataset was first filtered for when the AHU operated in cooling mode and data from the period when fault experiments are carried out in 2020 was removed. This final dataset from nearly 52 weeks spread over 2020 and 2021 was partitioned on a weekly basis hence resulting in 52 smaller datasets. Thereafter, each of the smaller datasets were iteratively added to compose a training and test set (split in a ratio of 80:20 respectively). On each iteration model performance was measured on KPIs: R2 score, RMSE, and cross-validation RMSE were measured on the test set and the unutilized dataset. Measuring the performance of the model over the unutilized dataset is indicative of the generalizability of the trained model. It can be observed from Figure 60 that data recorded from at least 20 weeks is required on a minimum to train an acceptable model ( $CV-RMSE < 0.3$ ). For this case, it is also observed that an accurate enough model (uncertainty  $< 10\%$ ) is realized only upon training the model with at least 34 weeks of data. Although, an accurate model is realized using the approach, its performance unexpectedly dips post 47<sup>th</sup> iteration. This is a consequence of the change in building supply air setpoint as observable from Figure 60. To this end if significant changes in control/operations strategy are implemented model retraining is recommended. Therefore, keeping a track of critical features of the model is important and is proposed to be considered in the overall FDD strategy.

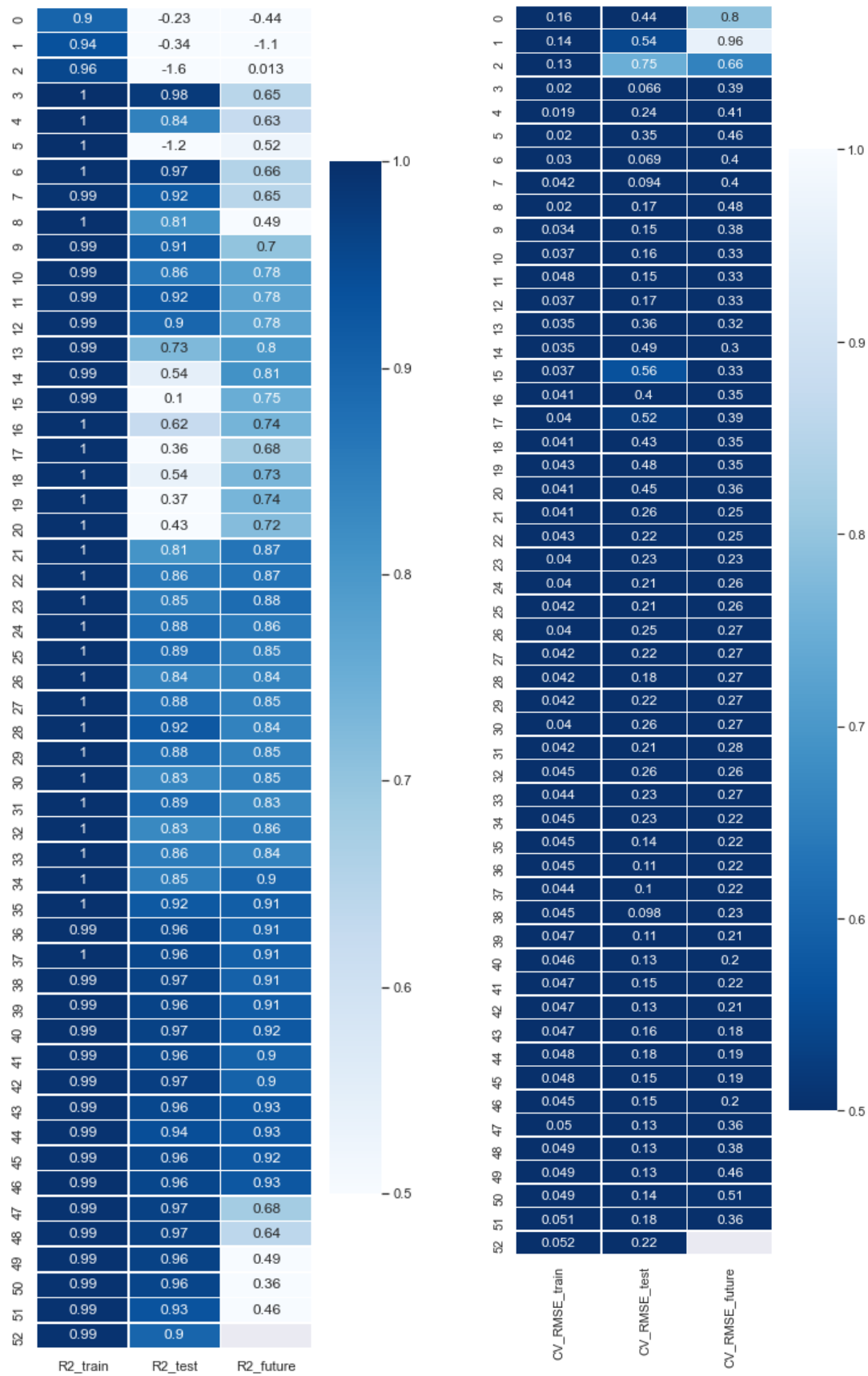


Figure 60: R2 Score and RMSE with weekly tests – ROC Nijmegen

**List of fault experiments carried out at Breda office and Nijmegen school for experimental validation of developed diagnosis model for cooling mode operation**

*Table 27: Chronology of faults introduced at Breda office in 2021*

<b>Fault Name</b>	<b>Fault description</b>	<b>Fault Introduction Method – Brief Description</b>	<b>P&amp;ID Ref</b>	<b>Severity / Setting</b>	<b>Period</b>
Valve Leak	Valve cannot close fully	Minimum valve position was hard set to a fixed value equivalent to severity of fault	1-6CV1	30%	23/06/2021-24/06/2021
Valve Leak	Valve cannot close fully	Minimum valve position was hard set to a fixed value equivalent to severity of fault	1-7CV1	20%	23/06/2021-24/06/2021
Valve Leak	Valve cannot close fully	Minimum valve position was hard set to a fixed value equivalent to severity of fault	1-8CV1	20%	23/06/2021-24/06/2021
Valve Leak	Valve cannot close fully	Minimum valve position was hard set to a fixed value equivalent to severity of fault	1-6CV1	30%	25/06/2021
Valve Leak	Valve cannot close fully	Minimum valve position was hard set to a fixed value equivalent to severity of fault	1-7CV1	20%	25/06/2021
Valve Leak	Valve cannot close fully	Minimum valve position was hard set to a fixed value equivalent to severity of fault	1-8CV1	20%	25/06/2021
Valve Leak	Valve cannot close fully	Minimum valve position was hard set to a fixed value equivalent to severity of fault	1-6CV1	20%	30/06/2021-02/07/2021
Valve Leak	Valve cannot close fully	Minimum valve position was hard set to a fixed value equivalent to severity of fault	1-7CV1	30%	30/06/2021-02/07/2021
Valve Leak	Valve cannot close fully	Minimum valve position was hard set to a fixed value equivalent to severity of fault	1-8CV1	30%	30/06/2021-02/07/2021
Stuck Valve	Valve stuck at fixed position	Minimum and Maximum valve positions were hard set to severity of the fault	1-6CV1	50%	02/07/2021-05/07/2021
Stuck Valve	Valve stuck at fixed position	Minimum and Maximum valve positions were hard set to severity of the fault	1-7CV1	50%	02/07/2021-05/07/2021
Stuck Valve	Valve stuck at fixed position	Minimum and Maximum valve positions were hard set to severity of the fault	1-8CV1	50%	02/07/2021-05/07/2021
Reduced Setpoint	Supply air set point reduced to value less than desired	Supply air setpoint control logic was reset, and its value was fixed to a set value	3.1.1806	16°C	07/07/2021-12/07/2021

<b>Fault Name</b>	<b>Fault description</b>	<b>Fault Introduction Method - Brief Description</b>	<b>P&amp;ID Ref</b>	<b>Severity / Setting</b>	<b>Period</b>
Reduced Setpoint	Supply air set point reduced to value less than desired	Supply air setpoint control logic was reset, and its value was fixed to a set value	3.1.1804	16°C	07/07/2021-12/07/2021
Reduced Setpoint	Supply air set point reduced to value less than desired	Supply air setpoint control logic was reset, and its value was fixed to a set value	3.1.1808	16°C	07/07/2021-12/07/2021
Reduced Setpoint	Supply air set point reduced to value less than desired	Supply air setpoint control logic was reset, and its value was fixed to a set value	3.1.1806	17°C	14/07/2021-16/07/2021
Reduced Setpoint	Supply air set point reduced to value less than desired	Supply air setpoint control logic was reset, and its value was fixed to a set value	3.1.1804	17°C	14/07/2021-16/07/2021
Reduced Setpoint	Supply air set point reduced to value less than desired	Supply air setpoint control logic was reset, and its value was fixed to a set value	3.1.1808	17°C	14/07/2021-16/07/2021
Stuck Valve	Valve stuck at fixed position	Minimum and Maximum valve positions were hard set to severity of the fault	1-6CV1	75%	16/07/2021-19/07/2021
Stuck Valve	Valve stuck at fixed position	Minimum and Maximum valve positions were hard set to severity of the fault	1-7CV1	75%	16/07/2021-19/07/2021
Stuck Valve	Valve stuck at fixed position	Minimum and Maximum valve positions were hard set to severity of the fault	1-8CV1	75%	16/07/2021-19/07/2021
Reduced Setpoint	Supply air set point reduced to value less than desired	Supply air setpoint control logic was reset, and its value was fixed to a set value	3.1.1806	17°C	22/07/2021
Reduced Setpoint	Supply air set point reduced to value less than desired	Supply air setpoint control logic was reset, and its value was fixed to a set value	3.1.1804	17°C	22/07/2021
Reduced Setpoint	Supply air set point reduced to value less than desired	Supply air setpoint control logic was reset, and its value was fixed to a set value	3.1.1808	17°C	22/07/2021
Lower Air Flow	Supply Air flow rate was reduced and maintained a fixed value	Fan speed was reduced from its usual setting ~80%	1-5TV2	60%	22/07/2021-23/07/2021
Valve Experiments	No Fault	Valve Position was adjusted from 0-100 and then back from 100-0. Other cooling valve positions were manually fixed to 0 and pump was manually switched ON.	1-7CV1	NA	29/07/2021

<b>Fault Name</b>	<b>Fault description</b>	<b>Fault Introduction Method – Brief Description</b>	<b>P&amp;ID Ref</b>	<b>Severity / Setting</b>	<b>Period</b>
Valve Experiments	No Fault	Valve Position was adjusted from 0-100 and then back from 100-0. Other cooling valve positions were manually fixed to 100 and pump was manually switched ON.	1-6CV1	NA	29/07/2021
Valve Experiments	No Fault	Valve Position was adjusted from 0-100 and then back from 100-0. Other cooling valve positions were manually fixed to 100 and pump was manually switched ON.	1-7CV1	NA	12/08/2021
Lower Air Flow	Supply Air flow rate was reduced and maintained a fixed value	Fan speed was reduced from its usual setting ~80%	1-5TV2	60%	12/08/2021-16/08/2021
Valve Experiments	No Fault	Valve Position was adjusted from 0-100 and then back from 100-0. Other cooling valve positions were manually fixed to 100 and pump was manually switched ON.	1-8CV1	NA	18/08/2021
Higher Air Flow	Supply Air flow rate was increased and maintained a fixed value	Fan speed was increased from its usual setting ~80%	1-5TV2	100%	18/08/2021-20/08/2021
Lower Air Flow	Supply Air flow rate was reduced and maintained a fixed value	Fan speed was reduced from its usual setting ~80%	1-5TV2	70%	20/08/2021

Table 28: Chronology of faults introduced at Nijmegen school in 2020

<b>Fault Name</b>	<b>Fault description</b>	<b>Fault Introduction Method – Brief Description</b>	<b>AHU</b>	<b>P&amp;ID Ref</b>	<b>Severity / Setting</b>	<b>Start Date</b>	<b>End Date</b>
Reduced Setpoint	Supply air set point reduced to value less than desired	Supply air setpoint control logic was reset, and its value was fixed to a set value	1	100TT04	18	25/Jul	26/Jul
Reduced Setpoint	Supply air set point reduced to value less than desired	Supply air setpoint control logic was reset, and its value was fixed to a set value	1	100TT04	18	25/Jul	26/Jul
Reduced Setpoint	Supply air set point reduced to value less than desired	Supply air setpoint control logic was reset, and its value was fixed to a set value	1	100TT04	18	25/Jul	26/Jul
Reduced Setpoint	Supply air set point reduced to value less than desired	Supply air setpoint control logic was reset, and its value	1	100TT04	17	26/Jul	26/Jul

<b>Fault Name</b>	<b>Fault description</b>	<b>Fault Introduction Method – Brief Description</b>	<b>AHU</b>	<b>P&amp;ID Ref</b>	<b>Severity / Setting</b>	<b>Start Date</b>	<b>End Date</b>
		was fixed to a set value					
Reduced Setpoint	Supply air set point reduced to value less than desired	Supply air setpoint control logic was reset, and its value was fixed to a set value	1	100TT04	17	26/Jul	26/Jul
Reduced Setpoint	Supply air set point reduced to value less than desired	Supply air setpoint control logic was reset, and its value was fixed to a set value	1	100TT04	17	26/Jul	26/Jul
Reduced Setpoint	Supply air set point reduced to value less than desired	Supply air setpoint control logic was reset, and its value was fixed to a set value	1	100TT04	17	26/Jul	26/Jul
Reduced Setpoint	Supply air set point reduced to value less than desired	Supply air setpoint control logic was reset, and its value was fixed to a set value	1	100TT04	16	26/Jul	26/Jul
Reduced Setpoint	Supply air set point reduced to value less than desired	Supply air setpoint control logic was reset, and its value was fixed to a set value	1	100TT04	16	26/Jul	26/Jul
Reduced Setpoint	Supply air set point reduced to value less than desired	Supply air setpoint control logic was reset, and its value was fixed to a set value	1	100TT04	16	26/Jul	26/Jul
Reduced Setpoint	Supply air set point reduced to value less than desired	Supply air setpoint control logic was reset, and its value was fixed to a set value	1	100TT04	16	26/Jul	26/Jul
Reduced Setpoint	Supply air set point reduced to value less than desired	Supply air setpoint control logic was reset, and its value was fixed to a set value	1	100TT04	16	26/Jul	26/Jul
Reduced Setpoint	Supply air set point reduced to value less than desired	Supply air setpoint control logic was reset, and its value was fixed to a set value	1	100TT04	15	26/Jul	26/Jul
Reduced Setpoint	Supply air set point reduced to value less than desired	Supply air setpoint control logic was reset, and its value was fixed to a set value	1	100TT04	15	26/Jul	26/Jul

<b>Fault Name</b>	<b>Fault description</b>	<b>Fault Introduction Method – Brief Description</b>	<b>AHU</b>	<b>P&amp;ID Ref</b>	<b>Severity / Setting</b>	<b>Start Date</b>	<b>End Date</b>
Reduced Setpoint	Supply air set point reduced to value less than desired	Supply air setpoint control logic was reset, and its value was fixed to a set value	1	100TT04	15	26/Jul	26/Jul
Reduced Setpoint	Supply air set point reduced to value less than desired	Supply air setpoint control logic was reset, and its value was fixed to a set value	1	100TT04	15	26/Jul	26/Jul
Reduced Setpoint	Supply air set point reduced to value less than desired	Supply air setpoint control logic was reset, and its value was fixed to a set value	1	100TT04	15	26/Jul	26/Jul
Reduced Setpoint	Supply air set point reduced to value less than desired	Supply air setpoint control logic was reset, and its value was fixed to a set value	1	100TT04		26/Jul	
Reduced Setpoint	Supply air set point reduced to value less than desired	Supply air setpoint control logic was reset, and its value was fixed to a set value	1	100TT04	22	31/Jul	
Reduced Setpoint	Supply air set point reduced to value less than desired	Supply air setpoint control logic was reset, and its value was fixed to a set value	1	100TT04	17	03/Aug	09/Aug
Reduced Setpoint	Supply air set point reduced to value less than desired	Supply air setpoint control logic was reset, and its value was fixed to a set value	1	100TT04	17	03/Aug	09/Aug
Reduced Setpoint	Supply air set point reduced to value less than desired	Supply air setpoint control logic was reset, and its value was fixed to a set value	1	100TT04	17	03/Aug	09/Aug
Reduced Setpoint	Supply air set point reduced to value less than desired	Supply air setpoint control logic was reset, and its value was fixed to a set value	1	100TT04	17	03/Aug	09/Aug
Reduced Setpoint	Supply air set point reduced to value less than desired	Supply air setpoint control logic was reset, and its value was fixed to a set value	1	100TT04	17	03/Aug	09/Aug
Reduced Setpoint	Supply air set point reduced to value less than desired	Supply air setpoint control logic was reset, and its value was fixed to a set value	1	100TT04	17	03/Aug	09/Aug

<b>Fault Name</b>	<b>Fault description</b>	<b>Fault Introduction Method – Brief Description</b>	<b>AHU</b>	<b>P&amp;ID Ref</b>	<b>Severity / Setting</b>	<b>Start Date</b>	<b>End Date</b>
		was fixed to a set value					
Reduced Setpoint	Supply air set point reduced to value less than desired	Supply air setpoint control logic was reset, and its value was fixed to a set value	1	100TT04	17	07/Aug	07/Aug
Reduced Setpoint	Supply air set point reduced to value less than desired	Supply air setpoint control logic was reset, and its value was fixed to a set value	1	100TT04	22	09/Aug	09/Aug

## Results from experimental validation of cooling mode operation faults introduced at Breda office

On 2<sup>nd</sup> July 2021 at 17:20, a stuck valve fault experiment was carried out. Herein, the three-way cooling coil control valve position installed at north zone was fixed at 50% open. This fault was introduced until 10:48 on 5<sup>th</sup> July 2021. Zooming into the behaviour of our diagnosis strategy on the 3<sup>rd</sup> July 2021 as shown in Figure 61, it can be observed a that a large residual exceeding +20% is observable between actual and predicted valve positions, thereby activating the CCV Prediction node (see Table 16). Thereby, the computed posterior probability of positive stuck valve state is computed higher than 65% indicating fault presence with a high confidence.

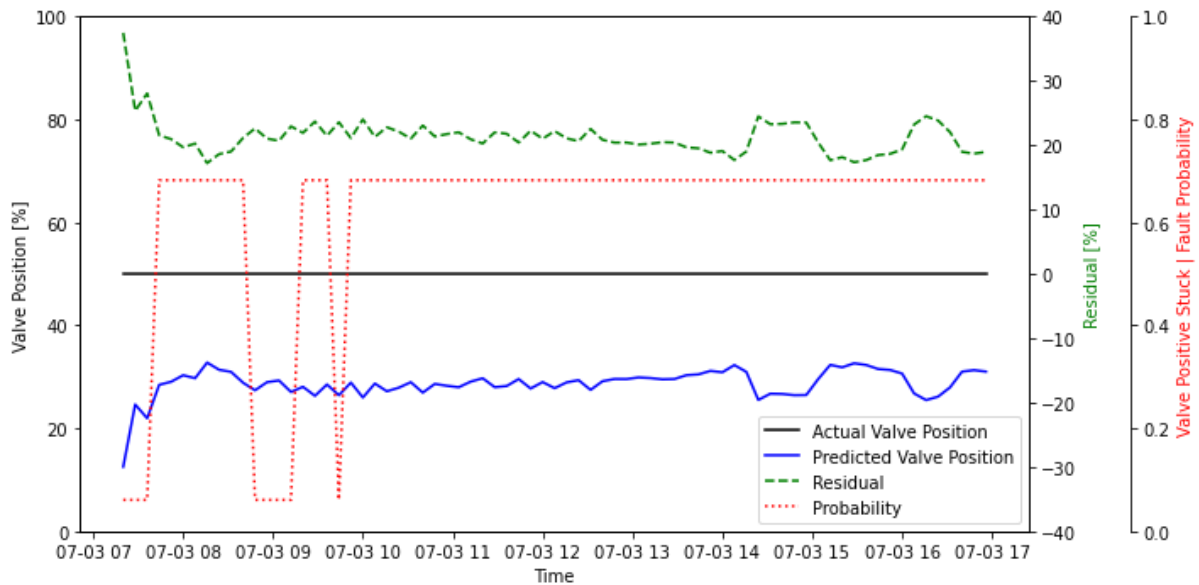


Figure 61: Stuck valve fault experiment

On 07<sup>th</sup> July 2021 at 17:20, a reduced supply air temperature setpoint experiment was carried out. Herein, the supplied air temperature setpoint that is cascaded control using the prevalent outdoor and return air conditions was reduced to 16°C. Nominally this value is set at 18°C, hence introducing a fault with 2K severity. This fault was manually induced until 08:24 on 12<sup>th</sup> July 2021. Zooming into the behaviour of our diagnosis strategy on the 08<sup>th</sup> of July 2021 as shown in Figure 62, it can be observed a that a residual exceeding +5% is observable between actual and predicted valve positions and 1°C between actual and desired supply air setpoint conditions. The CCV Prediction node and SAT Desired Comparison node (see Table 16) are activated given these values exceed the set thresholds. However, the RAT Setpoint Comparison symptom node is not activated as the fault severity is not too high. Despite, the computed posterior probability of Reduced Supply Air Temperature (SAT) fault is computed higher than 85% indicating fault presence with a very high confidence.

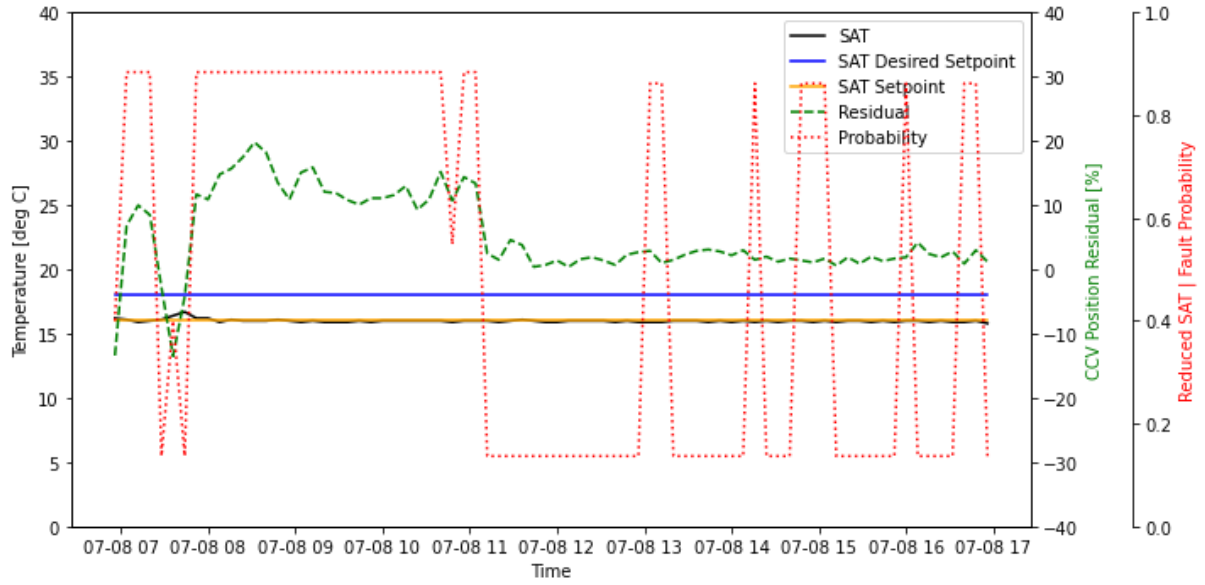


Figure 62: Reduced supply air set point experiment

On 22<sup>nd</sup> July 2021 at 16:30, a lower airflow experiment was carried out. Herein, the supplied airflow was reduced using the variable frequency drive installed on the supply fan from its nominal 85% to 60%. It meant that the supplied air pressure dropped from nominal 300Pa to 150Pa. This fault was introduced until 17:12 on 23<sup>rd</sup> July 2021. Zooming into the behaviour of our diagnosis strategy on the 23<sup>rd</sup> July 2021 as shown in Figure 63, it can be observed a that a residual exceeding +5% is observable between actual and predicted valve positions and 0.5m/s between actual and predicted airspeed conditions. The CCV Prediction node and Airflow Comparison node (see Table 16) are activated given these values exceed the set thresholds. Thereby, the computed posterior probability of lower airflow fault is computed higher than 90% indicating fault presence with a very high confidence.

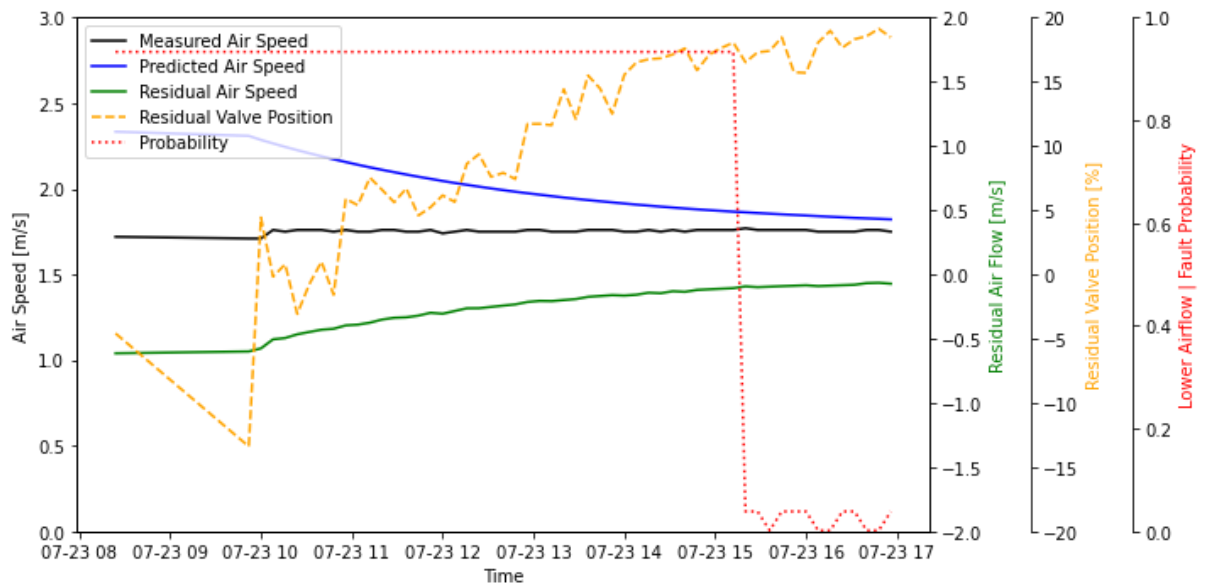


Figure 63: Lower airflow fault experiment

#### KPIs for experimental validation

$$precision = \frac{TP}{TP + FP}$$

(4)

$$recall/sensitivity = \frac{TP}{TP + FN} \quad (5)$$

$$specificity = \frac{TN}{TN + FP} \quad (6)$$

### DBN for cooling mode operation at Nijmegen school and its experimental validation

As with Breda, the layout of the DBN network emanates from the P&ID of the installed HVAC system. The P&I diagram for the AHU one is shown in APPENDIX A. For the first prototype of the FDD tool, this AHU is considered. The component fault nodes are depicted in purple in the DBN are shown in Figure 64. For the studied sub-system, Air flow fault node is an abstraction for any air side faults in components such as ducts, fans, or filters that can abruptly alter the supplied airflow. Red SAT and cooling coil valve (CCV) Stuck nodes depict reduced setpoint and cooling coil control valve stuck faults respectively.

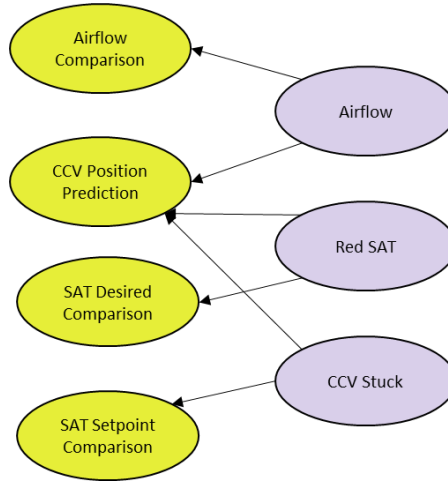


Figure 64: DBN for cooling mode operation – Nijmegen school

Despite there being differences, in HVAC configuration network structure did not differ besides the Red SAT node as can be observed upon comparing Figure 24 and Figure 64. The alteration had to be made since at Nijmegen the supply air temperature control strategy is directly correlated with the prevailing outdoor air temperature. In contrast, at Breda the supply air temperature is controlled using two variables return air and outdoor air temperatures. The symptom nodes were thus adjusted to account for this change.

Table 29: DBN model - Symptom Nodes description -Cooling mode operation at Nijmegen school

#	Symptom Node	Symptom State	Rules for setting the state
1	Airflow Comparison	High	$F_{act} - F_{pred} > \theta$
		Low	$F_{act} - F_{pred} < -\theta$
		Fault-free	$F_{act} - F_{pred} \leq \theta$
2	SAT Desired Comparison	Negative	$T_{set} - T_{set,des} < -\theta$
		Fault-free	$T_{set} - T_{set,des} \leq \theta$
3	CCV Prediction	Positive	$X_{ccv} - X_{ccv,pred} > \theta$
		Negative	$X_{ccv} - X_{ccv,pred} < -\theta$
		Fault-free	$X_{ccv} - X_{ccv,pred} \leq \theta$
4	SAT Setpoint Comparison	Positive	$T_{sa} - T_{sa,set} > \theta$
		Negative	$T_{sa} - T_{sa,set} < -\theta$
		Fault-free	$T_{sa} - T_{sa,set} \leq \theta$

Key:

**F** - Flow Rate in m<sup>3</sup>/s, **T** - Temperature in °C, **X** - Control Position in %, **Θ** - Threshold, **act** - Actual, **pred** - Predicted, **ccv** - Cooling coil valve, **des** - Desired, **sa** - Supply air, **set** - Setpoint

For experimental validation of the developed diagnosis model, fault experiments carried out in 2020 are utilized. Reduced SAT fault shown in DBN (see Figure 64) was introduced over periods in July and August 2020. The chronology of these experiments is listed in Table 28.

On 03<sup>rd</sup> August 2020 at 11:03, a reduced supply air temperature setpoint experiment was carried out. Herein, the supplied air temperature setpoint that is feedforward control using the prevalent outdoor air condition was reduced to 17°C. Nominally this value is set at 21°C, hence introducing a fault with a 4K severity. This fault was manually induced until 22:07 on 09<sup>th</sup> August 2020.

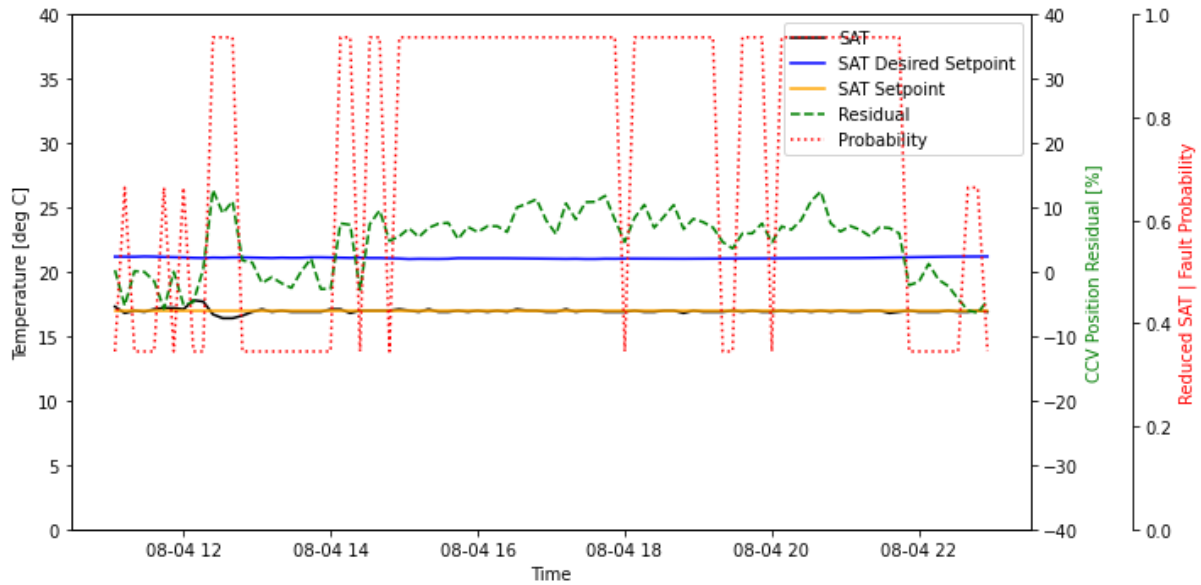


Figure 65: Reduced supply air temperature setpoint experiment on 4<sup>th</sup> August

Zooming into the behaviour of our diagnosis strategy on the 04<sup>th</sup> August 2020 as shown in Figure 65, it can be observed a that a residual exceeding +5% is observable between actual and predicted valve positions and 4K between actual and desired supply air setpoint conditions. The CCV Prediction node and SAT Desired Comparison node (see Table 29) are activated given these values exceed the set thresholds. Thereby, the computed posterior probability of Reduced Supply Air Temperature (SAT) fault is computed higher than 95% indicating fault presence with a very high confidence.

To observe the ability of the prototyped FDD to rule out a fault condition, computed posterior fault probabilities are plotted in Figure 66. It is clearly observable that once fault is corrected as was done in the late evening of 09<sup>th</sup> August 2020, fault probability reduces to its set prior probability indicating fault absence on 10<sup>th</sup> August 2020.

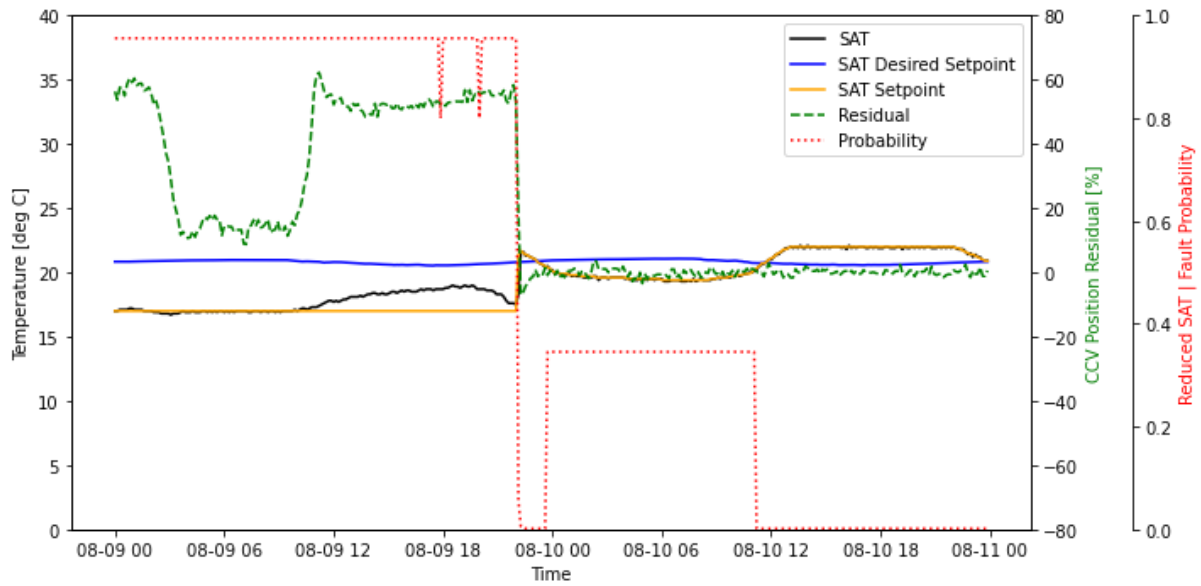


Figure 66: Reduced supply air temperature setpoint experiment on 9<sup>th</sup> August and corrected on 10<sup>th</sup>

The long-term operational performance of the DBN (see Figure 65) for cooling mode operation of the AHU at Nijmegen school was tested. The test was carried out using data collected over the summer experimental period between 01<sup>st</sup> July 2020 and 31<sup>st</sup> August 2020. During this period a mix of fault and fault-free days (on days no fault experiment was carried out) were considered. The confusion matrix in Figure 67 is indicative of the performance of the adopted fault diagnosis strategy. The KPIs shown in Table 18, indicates a very good diagnosis ability of the prototyped FDD tool.

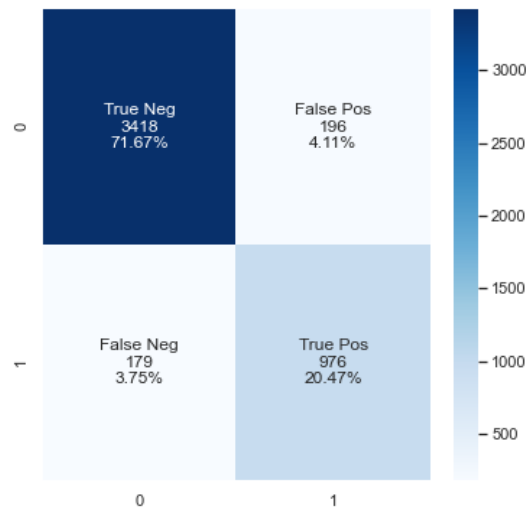


Figure 67: Experimental validation - Confusion Matrix - Nijmegen school – Cooling mode operation

## Rules for separating sequence of operation of the various Air-Handling Units

Table 30: Operation mode detection rules for Breda office and Nijmegen school

Site	AHU	Mode of Operation	Rule
Breda office	Central AHU	Heating Mode	Supply Hot water temperature > 25, Heating Coil Valve Open, Cooling Coil Valves closed
Breda office	North Zone, South Zone	Cooling Mode	Chilled water temperature < 8, Heating Coil Valve Closed, Cooling Coil Valves Open
Nijmegen school	AHU One, AHU Two	Heating Mode	Supply water temperature > 33, Heating Coil Valve Open, Cooling Coil Valves closed
Nijmegen school	AHU One, AHU Two	Cooling Mode	Supply water temperature < 16, Cooling Valve Open, Fan Switched On

## List of fault experiments carried out at Breda office and Nijmegen school for experimental validation of developed diagnosis model for heating mode operation

Table 31: Chronology of faults introduced at Breda office

Fault Name	Fault description	Fault Introduction Method - Brief Description	P&ID Ref No. and	Severity / Setting	Start Date	Stop Date
Stuck Valve	Valve stuck at fixed position	Valve position was hard set to a fixed value equivalent to severity of fault	1-5CV1	40%	20/10/2021	22/10/2021
Increased setpoint	Supply air setpoint control logic was reset, and its value was fixed to a set value	North-East zone fixed at 27 deg C, South-West zones at 25 deg C	3.1.1804, 3.1.1806	2°C	28/10/2021	28/10/2021
Increased setpoint	Supply air setpoint control logic was reset, and its value was fixed to a set value	North-East zone fixed at 27 deg C	3.1.1804	2°C	12/11/2021	12/11/2021
Stuck Valve	Valve stuck at fixed position	Valve position was hard set to a fixed value equivalent to severity of fault	1-5CV1	60%	23/11/2021	23/11/2021
Increased setpoint	Supply air setpoint control logic was reset, and its value was fixed to a set value	North-East zone fixed at 26 deg C	3.1.1804	1°C	30/11/2021	30/11/2021
Air flow	Higher Air Flow	Supply Air flow rate was increased and maintained a fixed value	1-5TV2	100%	14/12/2021	14/12/2021
Sensor offset	Supply air temperature sensor in main AHU	Add an offset in the corresponding sensor in BAS	3.1.1563	-2	08/10/2021	08/10/2021

Sensor offset	Supply air temperature sensor in zone north	Add an offset in the corresponding sensor in BAS	3.1.1569	-2	18/10/2021	20/10/2021
Sensor offset	Outdoor air temperature sensor	Add an offset in the corresponding sensor in BAS	3.1.53320	-2	25/10/2021	27/10/2021
Sensor offset	Return air temperature sensor in zone north	Add an offset in the corresponding sensor in BAS	3.1.1570	-2	02/11/2021	03/11/2021
Sensor offset	Supply heating water temperature sensor in main AHU	Add an offset in the corresponding sensor in BAS	3.1.1552	5	09/11/2021	10/11/2021
Sensor offset	Supply heating water temperature sensor in main AHU	Add an offset in the corresponding sensor in BAS	3.1.1552	-5	08/12/2021	09/12/2021

Table 32: Chronology of faults introduced at Nijmegen school

<b>Fault Name</b>	<b>Fault description</b>	<b>Fault Introduction Method – Brief Description</b>	<b>P&amp;ID Ref No. and</b>	<b>Severity / Setting</b>	<b>Start Date</b>	<b>Stop Date</b>
Increased setpoint	Supply air setpoint control logic was reset, and its value was fixed to a set value	Supply air temperature is determined using a feedforward control strategy based on outdoor air temperature. To introduce the fault, the heating curve is shifted by value equivalent to fault severity.	100TT04	2K	01/03/2022	01/03/2022
Stuck Valve	Valve stuck at fixed position	Valve position was hard set to a fixed value equivalent to severity of fault	07CV03	10%	03/03/2022	03/03/2022
Increased setpoint	Supply air setpoint control logic was reset, and its value was fixed to a set value	Supply air temperature is determined using a feedforward control strategy based on outdoor air temperature. To introduce the fault, the heating curve is shifted by value equivalent to fault severity.	100TT04	2K	24/03/2022	25/03/2022

## DBN for heating mode operation at Nijmegen school and its experimental validation

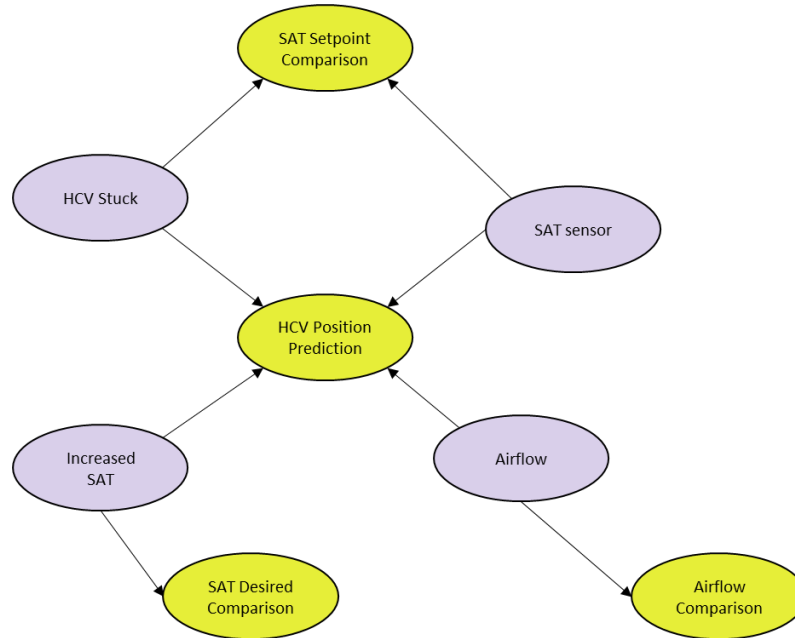


Figure 68: DBN for heating mode operation – AHU one at Nijmegen school

The supply air temperature setpoint is set at the outlet of fan, which is typically higher than the supply temperature at the air outlet of the heating coil due to fan heat. To generate a residual under fault scenario the SAT setpoint is compared with a predicted supply temperature using an XGBoost model. This model estimates supply temperature at the fan outlet using the supply air temperature at the heating coil outlet. This way an accurate residual is generated for fault detection purpose on the SAT Setpoint Comparison node.

Table 33: Symptom Nodes description for heating mode DBN – Breda office

#	Symptom Node	Symptom State	Rules for setting the state
1	Airflow Comparison	High	$F_{act} - F_{pred} > \Theta$
		Low	$F_{act} - F_{pred} < -\Theta$
		Fault-free	$F_{act} - F_{pred} \leq \Theta$
2	SAT Desired Comparison	Positive	$T_{set} - T_{set,des} > \Theta$
		Negative	$T_{set} - T_{set,des} < -\Theta$
		Fault-free	$T_{set} - T_{set,des} \leq \Theta$
3	HCV Position Prediction	Positive	$X_{hcv} - X_{hcv,pred} > \Theta$
		Negative	$X_{hcv} - X_{hcv,pred} < -\Theta$
		Fault-free	$X_{hcv} - X_{hcv,pred} \leq \Theta$
4	SAT Setpoint Comparison	Positive	$T_{sa} - T_{sa,set} > \Theta$
		Negative	$T_{sa} - T_{sa,set} < -\Theta$
		Fault-free	$T_{sa} - T_{sa,set} \leq \Theta$

**Key:** **F** - Flow Rate in m<sup>3</sup>/s, **T** - Temperature in °C, **X** - Control Position in %, **Θ** - Threshold, **act** - Actual, **pred** - Predicted, **hcv** - Heating coil valve, **des** - Desired, **sa** - Supply air, **set** - Setpoint

## Surveyed Literature for modelling heat recovery wheels

The following table summarizes approaches utilized in literature for modelling heat recovery wheels.

Table 34: Literature summary for modelling heat recovery wheels

#	Ref	Title	Approach	Comments
1	[126]	System-level fouling detection of district heating substations using virtual-sensor-assisted building automation system	Data-driven	Neural network model to predict FDI that can be utilized for
2	[100]	Automated Performance Tracking for Heat Exchangers in HVAC	Data-driven	a total variation (TV) filter integrated with an enhanced PF, termed local search PF (LSPF), is developed. Residual generation, control parameters. Tracking gradual perf degradation through exp function and sudden through step function. Sim model utilized to test the approach and RP1043 data utilized to validate experimentally.
3	[135]	Experimental analysis of a rotary heat exchanger for waste heat recovery from the exhaust gas of dryer	Experimental approach	Measuring the impact of key variables such as temp, flow, rotational speed etc. on key KPIs
4	[136]	A novel fault diagnosis and self-calibration method for air-handling units using Bayesian Inference and virtual sensing	Data Driven	Propose a virtual sensor for tracking fouling in heat exchangers using the UA and LMTD. Validate the proposed approach using a TRNSYS model.
5	[129]	Real heat recovery with air handling units	Experimental	Tracer gas introduction for leakage detection
6	[137]	Case study results: fault detection in air-handling units in buildings	Data Driven	Optimal operation of hear recovery pump
7	[130]	Prediction of condensation and frosting limits in rotary wheels for heat recovery in buildings	Physical/Heuristic Model	Specific to Frosting: Tracking the moisture carrying capacity (using mollier diagram) of supply air at sub zero temperatures. Simultaneously, understanding the excess water in exhaust stream.
8	[101]	Frost formation in rotary heat and moisture exchangers	Experimental/Mathematical	$T_s < 0$ and $\Delta\omega = \omega_\gamma - \omega_s > 0$ . absolute humidity is the prevailing parameter for characterizing the frosting phenomenon. A frost mass fraction chart was established in terms of the relative humidity of the warm exhaust stream and of the temperature of the cold supply stream
9	[138]	PERFORMANCE EVALUATION OF ROTARY DESICCANT WHEELS USING A SIMPLIFIED PSYCHOMETRIC MODEL AS DESIGN TOOL	Numerical	Method to solve for enthalpy of different desiccant wheels using a grey-box approach – <b>Model 54</b>
10	[97]	Desiccant wheels effectiveness parameters: Correlations based on experimental data	Data Driven	Developed Efficiency Factors for measuring enthalpy and Rh effectiveness. Explores the dependence of effectiveness parameters on inlet air and rotational speed of the wheel. Further, generalization of the previously utilized

				effectiveness parameters over a wide boundary condition is proposed. Considered measurement points such as T and Rh on all four locations around desiccant wheel and a delta P across the wheel.
11	[96]	Experimental validation of a simplified approach for a desiccant wheel model	Data Driven	efficiency factors with fewer measurements as opposed to [17]. Utilizes an analogy method, wherein performance of desiccant wheel is approximated using a simple heat transfer process as experienced in an heat exchanger. Two variables F1 (approximates adiabatic lines) and F2 (approximates Rh lines) referred to as combined potentials are introduced. Method enables prediction of outlet states of wheel on basis of calculated values of the combined potentials efficiencies $\eta F1$ , $\eta F2$ . Considered regeneration side temperatures are quite high in comparison to the typically experienced in building conditions in Netherlands.
12	[139]	Implementation of GA-LSSVM modelling approach for estimating the performance of solid desiccant wheels	Data Driven	Using LSSVM and GA, predict $T_{pro,out}$ , $\omega_{pro,out}$ , $T_{reg,out}$ , $\omega_{reg,out}$ , $\eta_{deh}$ , MRC, and SER for both WSG and LT3 type desiccant wheels.
13	[140]	Optimization - Desiccant-wheel optimization via response surface methodology and multi-objective genetic algorithm	Data Driven	Central Idea - outlet temperature and humidity ratio of process air are not independent of each other; a desiccant wheel must be optimized by considering state conditions of outlet air in the process stream to allow the desiccant wheels to work in a high-efficiency mode. Response surface method proposed to optimize both parameters together. Finally, equation for $T_{out,process}$ is written in terms of humidity ratio that explains the interaction effect for silica gel and molecular sieve based desiccant wheels. Surface area ratio is found to be the most dominant independent variable. Nonetheless, not all physical dimensions or operating conditions of a wheel (e.g. wheel depth or rotational speed) were considered in this approach.
14	[141]	Artificial neural network-based modelling of desiccant wheel	Data Driven	Predict DBT and specific humidity of air at outlet of desiccant wheel in the operation range of 60-150 deg C regeneration temperature. For optimization MRC considered as an objective. Multiple objective functions evaluated. However, the approach is dated since ANN modelling has significantly advanced since then.
15	[142]	Performance prediction of rotary solid desiccant dehumidifier in hybrid air-conditioning system using artificial neural network	Data Driven	Solid desiccant system. 7 predictors and 6 predicted variables using a multi-output ANN based regressor. Moisture removal rate and effectiveness of the dehumidifier are considered as key performance indicators.
16	[102]	Optimization - Validation of multitask artificial neural networks to model desiccant wheels activated at low temperature	Data Driven	Data-driven approach followed to overcome the limitations of complexity associated with physical modelling approaches discussed previously. Multi-task learning ANN model (predicted variables: Temp and Humidity Ratio at output of HRW). Predictors used: Return Air Temp & Humidity condition, Suction Air Temp & Humidity Condition, Supply air flow rate and speed of rotation.

17	[92]	Semi-empirical mapping method for energy recovery wheel performance simulation	Numerical	Algebraic Equations utilized to developed an Energy Recovery Wheel model. Equations determining effectiveness of wheel as a function of speed of rotation, air face velocity, and wheel depth are derived.
18	[93]	Optimization – Design Optimization of Heat Wheels for Energy Recovery in HVAC Systems	Numerical	Explores the effects of various design aspects on the performance of HRW, considering parameters such as revs, dimensions, velocity etc. Effect is measured on sensible effectiveness and pressure drop.
19	[143]	Effect of rotational speed on the performances of a desiccant wheel	Experimental	KPIs such as DCOP, SER and effectiveness are analysed to study their dependence on rotational speed of silica gel based desiccant wheel for low temperature regenerators (60–70 °C). SER is found to be monotonically increasing function of rotational speed, whilst effectiveness (dehumidification) increases and starts decreasing after a certain threshold. Op conditions that maximize DCOP are opposite to those that maximize effectiveness (dehumidification)
20	[144]	Effectiveness parameters for the prediction of the global performance of desiccant wheels – An assessment based on experimental data	Experimental	Compares a set of performance indicators proposed in previous research such as by [96]. Enthalpy and moisture absorption content (at equilibrium) were found to be the most suitable indicators. However, only in the scenario that sorption isotherms are known. Correlations for effectiveness parameters that can be directly derived from manufacturers data would be effective.
21	[98]	Performance comparisons of desiccant wheels for air dehumidification and enthalpy recovery	Numerical	Numerical equations proposed to study the effect of rotational speed, number of transfer units and specific area on performance indicators for wheel are investigated. Performance indices looked at are sensible effectiveness, latent effectiveness, dehumidification effectiveness, specific dehumidification power are considered. Key observations: 1. Air dehumidification is more sensitive to rotary speed than enthalpy recovery is. 2. latent effectiveness is usually smaller than the sensible effectiveness, because the moisture transfer resistance is usually larger than the heat transfer resistance. In other words, mass diffusion in the solid is far less than the thermal diffusion. 3. NTU increases with specific area
22	[145]	Heat and Mass Transfer in Air-to-Air Enthalpy Heat Exchangers	Numerical	Numerical model for counter flow heat exchanger (membrane based)
23	[146]	Virtual entropy generation (VEG) method in experiment reliability control: Implications for heat exchanger measurement	Numerical	Utilize first and second law of thermodynamics to deal with measurement uncertainty in heat exchangers.
24	[99]	Modeling and simulation of heat and enthalpy recovery wheels	Numerical	Developed a mathematical model for heat and mass transfer for rotary heat exchangers and are further validated using independent observations. Key Finding: Heat wheels are far less efficient than enthalpy recovery wheels.

### Fault experiments for validation of HRW models discussed in section 3.5.3

Table 35: Chronology of fault experiments carried out at Breda office and Nijmegen school

Location	Fault Name	Fault description	Fault Introduction Method – Brief Description	P&ID Ref No.	Severity / Setting	Start Date	Stop Date
AHU One Nijmegen school	Control failure	Heat recovery wheel isn't rotating	Heat recovery wheel control position is manually overridden and set to a fixed speed	100SC03	0%	14/03/2022	14/03/2022
AHU One Nijmegen school	VFD bypass	Control of heat recovery wheel is bypassed, and the heat recovery wheel rotates at a fixed 100% speed	Heat recovery wheel control position is manually overridden and set to a fixed speed	100SC03	100%	23/03/2022	23/03/2022
Central AHU Breda office	Control failure	Heat recovery wheel isn't rotating	Heat recovery wheel control position is manually overridden and set to a fixed speed	1-5WW1	0%	17/03/2022	17/03/2022

In the following figure, faulty vs fault free operations are compared for Breda office. The fault introduced at Breda office is shown in Table 35. It can be observed upon comparing the figures that during fault operation the heat recovered is a lot less than predicted through the model. Hence, the developed model is found useful for distinguishing between such faults.

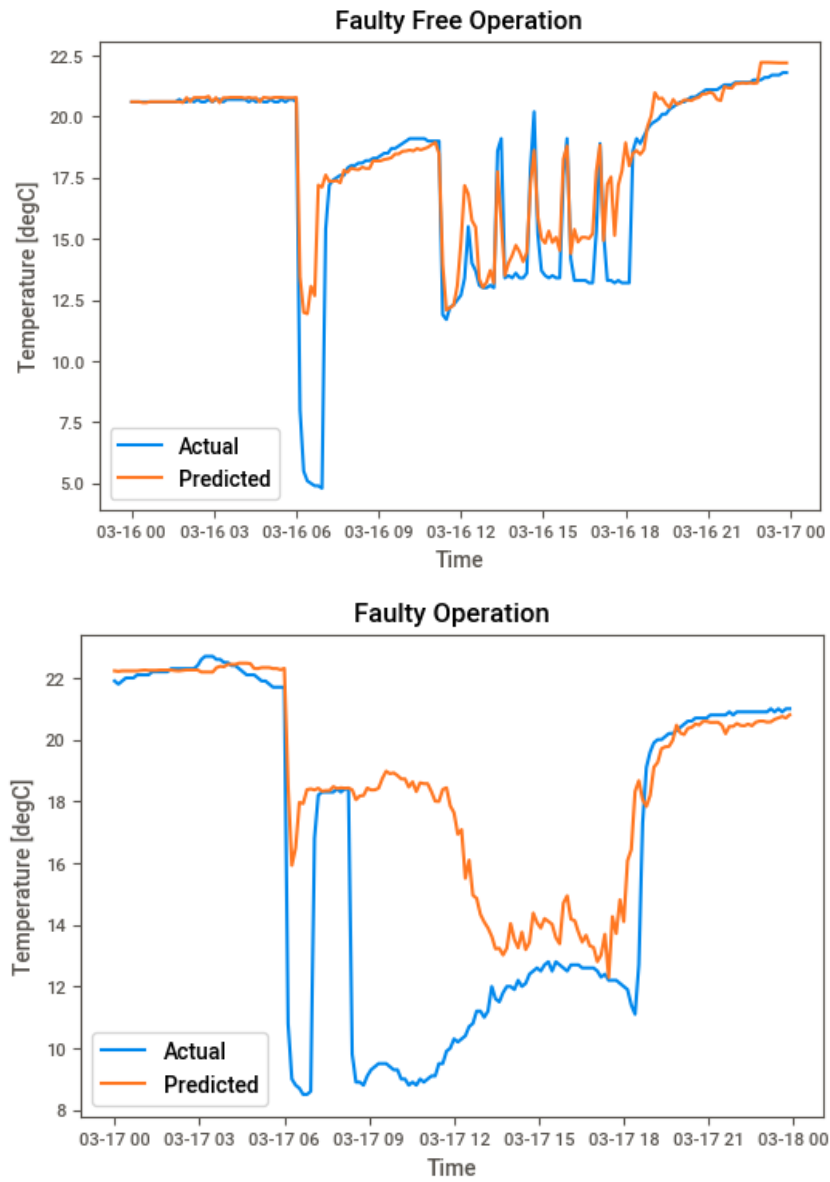


Figure 69: Comparison of predicted vs actual temperatures post heat recovery wheel during faulty and free operation for Breda office

APPENDIX E. FDD APPLICATION

Model Management

The model management framework can be envisaged as a ledger, wherein performance of models trained with data is recorded. In the current implementation, its conception is simplified to initiate and inspire steps required in this direction. A database of models is maintained. In Figure 70, model performance tracking page for Breda office is shown. Here, the trained models are listed along with their latest performance evaluation on indicators such as R2 score (see c on Figure 70), and RMSE (see d on Figure 70) discussed in section 3.4. The model performance over these indicators, is tracked in time and compared with the baseline performance (performance realized in the offline training process) to detect a model performance anomaly. An alert (see e on Figure 70) is generated in case the tracked performance drops, which can also be observed using the check performance button displayed alongside (see f on Figure 70).

To explore the features for their importance and contributions to the trained model a button is provided. Clicking on the button (see b on Figure 70) opens a pop-up where such information is provided. Further, on the pop-up, a drift detection algorithm is setup for tracking drift of the most important features. It is envisaged that alerts generated through drift detection and combined with model KPIs would be shown in the Alerts bar (see e on Figure 70). They are further proposed to be integrated as model faults in the developed DBNs.

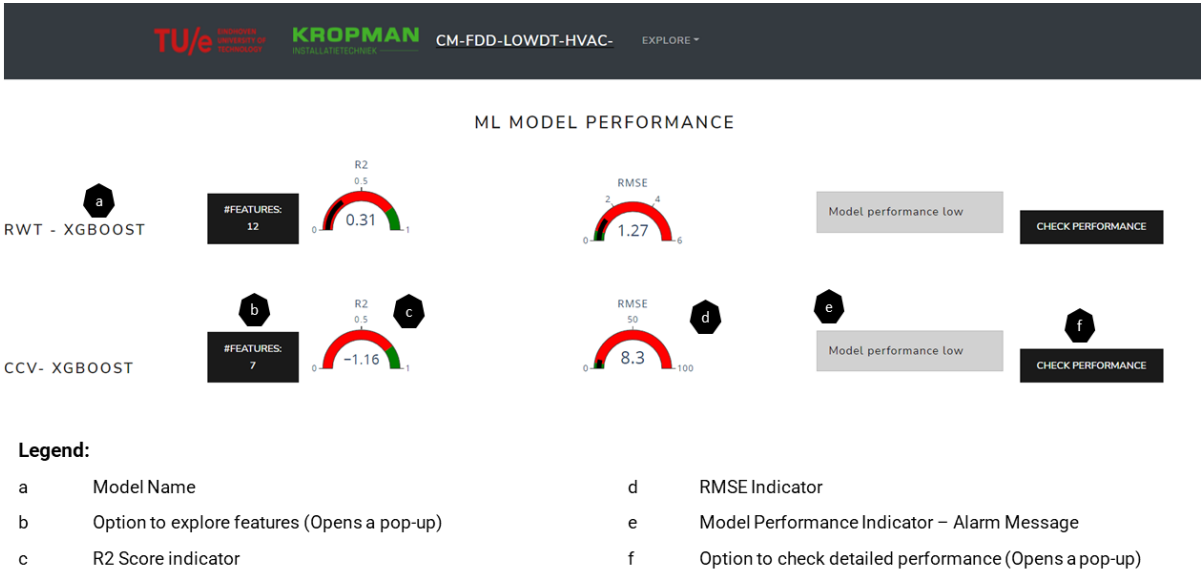


Figure 70: FDD Application - Machine Learning models tracking page for Breda office

## APPENDIX F. DISCUSSION

### Compliance against prioritized requirements:

Table 36: Compliance matrix of the developed AFDD tool towards various domain, functional and non-functional requirements identified for their verification

Requirement	Priority	Compliance
Select and show key performance indicators that can track system performance	High	
Select and prioritize key faults that cause the largest energy performance gap	High	
Express clear linkages between developed diagnosis strategy and HVAC system	High	
Explain predictions of deployed machine learning models	High	
Isolability, Evaluation and decision support capabilities: Utilize Bayesian methods that can deal with uncertain information. Further, embed features to evaluate outcomes and support decision making.	High	
No. of Sensors/Measurement Requirements: For modelling utilize as less sensors as possible to avoid sensor uncertainty	Medium	
Ease and Automation of training and tuning, Limited need for handcrafting of algorithms: Model training and tuning procedure to be completely automated	Low	
Detection Time: Detection time for detecting abrupt faults needs to be less than or equal to 3 hours	Low	
Computational requirements (Memory): Model deployment for a single building should be supported on a standard PC with 16GB memory	Low	
Provide support for training, testing, evaluating, and deploying Bayesian networks	High	
Visualize diagnostic Bayesian networks including symptom states and fault probabilities	High	
Provide support for training, testing, evaluating, and deploying machine learning models	High	
Validate datasets before utilizing them for serving predictions	High	
Software should be able to interface with CMS (InsiteSuite) over API	High	
Store meta information about the underlying HVAC system	Medium	
Visualize diagnosed faults in a clear manner	Medium	
Provide supporting evidence and information on diagnosed faults	Medium	
Develop a fault library that can store fault and meta information on faults	Medium	
Provide support for tracking performance of deployed machine learning models and raise flags for retraining	Medium	
Software should support date, time and text filter and sort functionalities wherever applicable	Medium	
Provide support for utilizing state-of-the-art feature selection techniques	Low	
Feature to compare results from multiple regression modelling frameworks such as gradient boosting, decision tress	Low	
Software should support dynamic Bayesian networks	Low	
Software should be able to interface directly with BMS deployed on site for data ingestion	Low	
Software should support APIs for data export from developed application	Low	
Software should carry a mechanism to input expert information that can be further utilized for labelling or correction purposes	Low	
<b>Security:</b> Only designated and authorized use of client data	High	
<b>Maintainability:</b> Software should be free of poor coding practices and should carry ample documentation and annotations for easy maintainability Data tags utilized in the software should be human understandable	High	
<b>Interoperability:</b> Should be designed in a manner that it can support open interfaces for connectivity with external applications	High	
<b>Scalability:</b> Should be deployed and tested over multiple building use-cases Should be able to handle multiple data sources	High	

Requirement	Priority	Compliance
Should be able to accommodate newer algorithms		
<b>Portability:</b> Software should be agnostic to operating system environment. It can be deployed on any local or cloud environment that carries sufficient memory and support Python Software visualization layer should support standard browser interfaces	Medium	
<b>Performance:</b> Should be able infer and generate results by processing real-time data streams Should be able to validate inputs and clearly indicate errors	Low	
<b>Reusability:</b> Software dependencies should be clearly expressed Machine learning and Bayesian network modeling blocks should be reusable	Low	

## Financial Plan

### 1. Market

The Dutch Non-Residential buildings market which is the target market for the product is approximately 38% of the total buildings stock, which is equivalent to circa 550 million sq. mts [147]. Of this, a total serviceable market is estimated at 47% of the total Non-Residential buildings stock or 258.5 million sq. mts. This building stock is proposed to be sorted further based on large, medium, and small building types. **In the sales strategy, large, and medium building types with centralized/large AHU systems would be targeted first as the product market fit is best realized.**

### 2. Competition

The technology providers for the Non-residential Intelligent Buildings can be fragmented into 3 different categories. Smart Hardware or Software providers and Building Management System (BMS) systems providers. There are also service providers that offer bundled solutions (Hardware and Software), however are limited in number, and can be perceived like the BMS systems providers. The proposed solution has been benchmarked against these providers and the results of which are summarized in Table 37.

Table 37: Competitive benchmarking

Competitor Type	Market Opportunity Focus	Strategic Intent	Market Share Objective	Competitive Position	Strategic Posture	Competitive Strategy
Legacy BMS solution providers	New Construction and Automation	Maintain Current Position	Expansion via upselling	Very Strong	Mostly defensive	Striving for low-cost leadership
Smart Hardware solution providers	Automation	Be dominant leader	Aggressive Expansion	Stuck in the middle	Mostly offensive	Focus on volumes business
Smart Software solution providers	Operation and Maintenance	Move into top 5	Expansion via acquisition	Direct Competition	Mostly offensive	Focus on land-grab

### 3. Revenue Forecast

The business model is reliant on the value generated (energy savings and operational efficiency realized) for the customer. Therefore, the pricing strategy has been linked to the value delivered. Three scenarios namely worst, nominal, and best have been projected. In each of the scenarios the realized revenue would be 45%,55%,65% of the available wallet share or in other words value delivered. Figure 71 shows forecasted Annual recurring revenue (ARR) position in each of these scenarios. Under a nominal case, 116% CAGR is estimated over Y2 revenue. The CAC in this scenario is projected to go down from a high of 2.11 Euros/sq. mt. to 0.52 Euros/sq. mt. thereby leaving a healthy margin for growth and investments into our R&D. Further it is anticipated that the business would generate a revenue/employee of EUR 270k in 5 years.

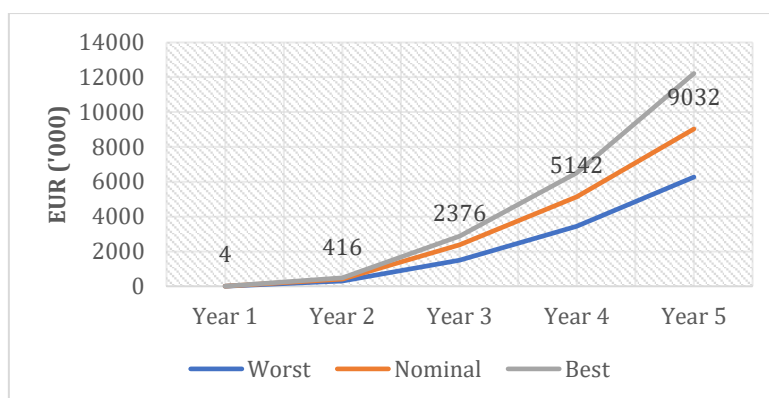


Figure 71: Revenue Generation

#### 4. Financial Model

The financial model for the nominal case is shown in Table 38 and whilst others are excluded from this report. Considering the worst and nominal scenarios, anticipated financing requirements for the first two years are pegged between EUR 1.5-1.6 million. In the best case, to fund additional growth a 20% higher financing need over nominal case is estimated. In year 1 the business would require a runway of nearly EUR 400k.

Table 38: Profit and Loss Statement

Profit & Loss		Year 1	Year 2	Year 3	Year 4	Year 5
Sales		3,754	415,800	2,375,912	5,141,662	9,031,917
Cost of goods sold	(-/-)	(26,000)	(89,840)	(297,273)	(483,316)	(630,021)
<b>Gross Margin</b>		<b>(22,246)</b>	<b>325,960</b>	<b>2,078,639</b>	<b>4,658,346</b>	<b>8,401,896</b>
Personnel cost	(-/-)	(34,800)	(84,600)	(346,400)	(436,000)	(498,000)
Sales & Marketing	(-/-)	(36,000)	(295,400)	(442,550)	(618,962)	(716,668)
General Administration	(-/-)	(105,000)	(246,960)	(429,975)	(451,474)	(474,047)
Research & development	(-/-)	(305,000)	(511,150)	(655,398)	(881,328)	(936,294)
Other costs	(-/-)	(61,480)	(134,960)	(223,390)	(267,600)	(272,300)
<b>Total cost</b>		<b>(542,280)</b>	<b>(1,273,070)</b>	<b>(2,097,713)</b>	<b>(2,655,364)</b>	<b>(2,897,310)</b>
<b>Earnings before interest tax depreciation and amortisation (EBITDA)</b>		<b>(564,526)</b>	<b>(947,110)</b>	<b>(19,074)</b>	<b>2,002,981</b>	<b>5,504,585</b>
Depreciation and amortisation	(-/-)	(4,640)	(12,092)	(22,144)	(30,315)	(35,152)
<b>Earnings before interest and tax (EBIT)</b>		<b>(569,166)</b>	<b>(959,202)</b>	<b>(41,217)</b>	<b>1,972,666</b>	<b>5,469,434</b>
Interest	6%	-	(24,028)	(68,385)	(80,988)	(8,407)
<b>Financial cost</b>		<b>-</b>	<b>(24,028)</b>	<b>(68,385)</b>	<b>(80,988)</b>	<b>(8,407)</b>
<b>Earnings before tax (EBT)</b>		<b>(569,166)</b>	<b>(983,230)</b>	<b>(109,602)</b>	<b>1,891,679</b>	<b>5,461,027</b>
Tax	25%	142,292	245,807	27,400	(472,920)	(1,365,257)
<b>Net result</b>		<b>(426,875)</b>	<b>(737,422)</b>	<b>(82,201)</b>	<b>1,418,759</b>	<b>4,095,770</b>

## 5. Assumptions for business model

The assumptions utilized for preparing the financial model are summarized in Table 39 and Figure 72. In the table the business model assumptions are provided whilst in figure, the proposed organizational development required to sustain such a business are provided.

Table 39: Business Model assumptions

Description	EUR	UOM
Price Per KWh	0.14	EUR/KWh
EUR Saved per KWh (@20% Savings Rate)	0.03	EUR/KWh
Avg. Non Residential Energy Consumption	200	KWh/m2
Savings Rate	5.6	KWh/m2
Price for customer @ 45% Savings	3.08	EUR/m2

The proposed business model can be termed software as a service (SaaS). Therefore, a lot of emphasis is laid on the strategic value of employees. The details of estimated year-on-year team size are provided in Figure 72.

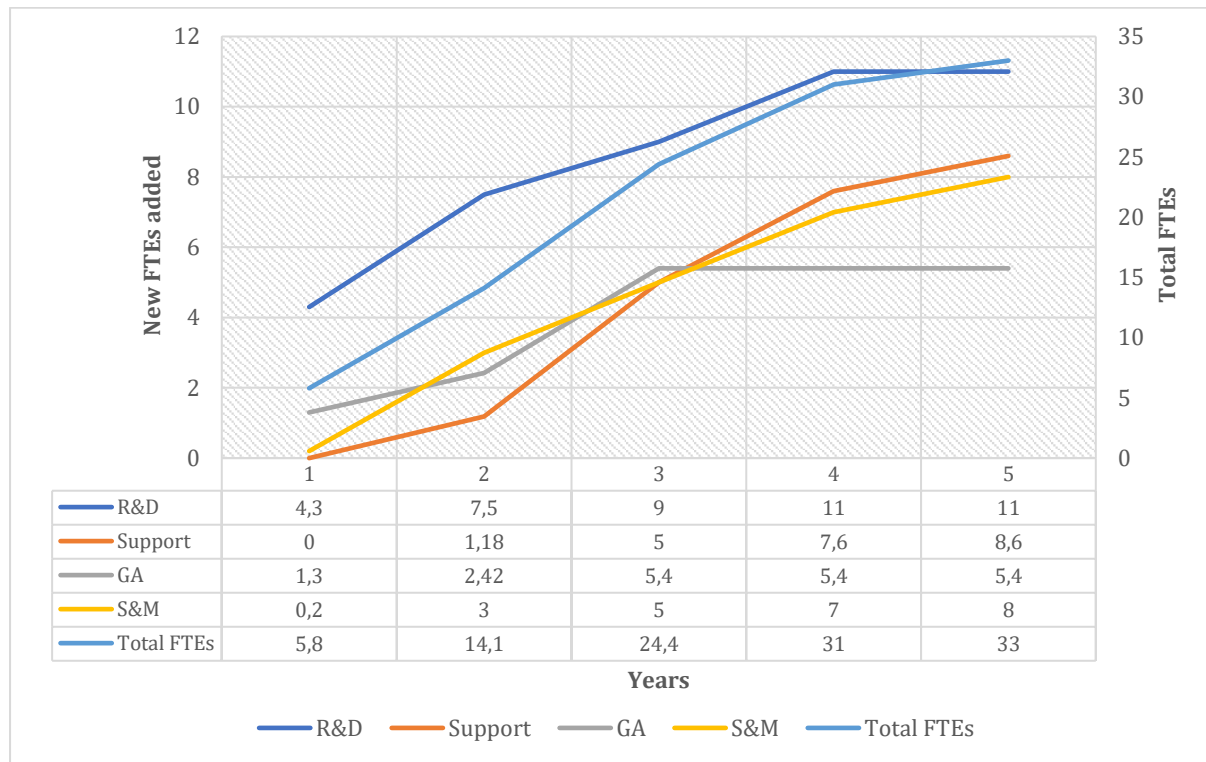


Figure 72: Number of FTEs year on year